UNESP - Universidade Estadual Paulista
"Júlio de Mesquita Filho"
Faculdade de Odontologia de Araraquara

Evelin Carine Alves Silva

Reação tecidual e potencial bioativo de cimentos biocerâmicos reparadores e endodônticos em associação ou não a substâncias antimicrobianas

Araraquara

2024

UNESP - Universidade Estadual Paulista

“Júlio de Mesquita Filho”

Faculdade de Odontologia de Araraquara

Evelin Carine Alves Silva

Reação tecidual e potencial bioativo de cimentos biocerâmicos reparadores e endodônticos em associação ou não a substâncias antimicrobianas

Tese de Doutorado apresentado ao Programa de Pós-Graduação em Odontologia, Área de Endodontia, da Faculdade de Odontologia de Araraquara da Universidade Estadual Paulista “Júlio de Mesquita Filho” como requisito para obtenção do título de Doutora em Odontologia.

Orientadora: Profª. Drª. Juliane Maria Guerreiro Tanomaru

Coorientador: Paulo Sérgio Cerri

Araraquara

2024

S586r

Silva, Evelin Carine Alves
Reação tecidual e potencial bioativo de cimentos biocerâmicos reparadores e endodônticos em associação ou não a substâncias antimicrobianas / Evelin Carine Alves Silva. -- Araraquara, 2024
121 p. : il., tabs., fotos

Tese (doutorado) - Universidade Estadual Paulista (UNESP), Faculdade de Odontologia, Araraquara
Orientadora: Juliane Maria Guerreiro Tanomaru
Coorientador: Paulo Sergio Cerri

1. Teste de materiais. 2. Endodontia. 3. Imuno-histoquímica. I. Título.

Sistema de geração automática de fichas catalográficas da Unesp. Biblioteca do Universidade Estadual Paulista (UNESP), Faculdade de Odontologia, Araraquara. Dados fornecidos pelo autor(a).

Essa ficha não pode ser modificada.

Evelin Carine Alves Silva

Reação tecidual e potencial bioativo de cimentos biocerâmicos reparadores e endodônticos em associação ou não a substâncias antimicrobianas

Comissão Julgadora

Defesa de Tese para obtenção do grau de Doutor em Odontologia

Presidente e orientadora: Profª. Drª. Juliane Maria Guerreiro Tanomaru

2ª Examinadora: Profª. Drª. Gisele Faria

3ª Examinadora: Profª. Drª. Raquel Assed Bezerra Segato

4º Examinador: Pro. Dr. Gustavo Sivieri de Araujo

Araraquara, 27 de março de 2024.

DADOS CURRICULARES

Evelin Carine Alves Silva

NASCIMENTO: 01 de maio de 1991-Porto Velho-Rondônia

FILIAÇÃO: Izabel Cristina Alves Pereira
Eduardo Romagna Pereira

2009-2013

Graduação em Odontologia pela Faculdade de Macapá-FAMA, Macapá-AP.

2014-2015

Especialização em Endodontia pela Faculdade Avantis-GOE, Macapá-AP.

2018-2020

Mestre em Odontologia, área de concentração em Endodontia, pela Universidade Estadual Paulista "Júlio de Mesquita Filho", Faculdade de Odontologia de Araraquara – FOAr/UNESP, Araraquara-SP.

2020-2024

Doutoranda em Odontologia, área de concentração em Endodontia, pela Universidade Estadual Paulista "Júlio de Mesquita Filho", Faculdade de Odontologia de Araraquara – FOAr/UNESP, Araraquara-SP.

ASSOCIAÇÕES SBPqO – Sociedade Brasileira de Pesquisa em Odontologia.

Dedico esta tese de doutorado à memória eterna de minha mãe Izabel Cristina Bastos Alves, seus ensinamentos, encorajamentos e amor infinito moldaram não apenas quem sou como pessoa, mas também me guiaram através dos desafios e triunfos desta jornada acadêmica.

À minha irmã Êmilie Cristine Alves Pereira, cujo apoio e companheirismo têm sido uma fonte constante de inspiração e conforto, agradeço por sua presença constante e por compartilhar comigo cada passo dessa jornada da vida, sendo meu coração fora do peito. Ao meu querido paidrasto, cujo amor, orientação e apoio inabaláveis têm sido uma bênção em minha vida, fazendo inúmeros sacrifícios por mim ao longo dos anos.

Ao meu amado esposo Gabriel de Oliveira Silva, que tornou tudo isso possível, seu apoio e amor incondicional foram a âncora que me sustentou em meio às tempestades e me impulsionou em direção aos meus objetivos mais elevados. Cada passo deste caminho foi iluminado pela sua presença amorosa e pelo seu encorajamento constante. Nos longos dias em que me vi mergulhada em livros e pesquisas, você estava lá para me confortar e me motivar. Nas horas de dúvida e incerteza, foi a sua fé em mim que me deu forças para continuar avançando. Suas palavras de incentivo, companheirismo e gestos de carinho foram a inspiração que alimentou minha determinação e perseverança.

AGRADECIMENTOS

“As pessoas felizes lembram o passado com gratidão, alegram-se com o presente e encaram o futuro sem medo”, e é dessa maneira que agradeço por mais uma etapa alcançada.

Agradeço ao meu Deus, autor da vida, que me possibilitou chegar até aqui, pela proteção diária, cuidado e todas as bênçãos incontáveis.

Ao meu amado esposo, companheiro e parceiro de vida. Obrigada pelo apoio incondicional, pelos sacrifícios, pela compreensão, ajuda e torcida em todos os momentos. A jornada se tornou mais leve com você ao meu lado. Obrigada por me lembrar todos os dias do que eu sou capaz e por ser meu porto seguro.

À minha mãe (*in memoriam*) por toda educação, amor e dedicação devotada a mim ao longo dos meus 24 anos. Mesmo não estando presente, você é parte de mim e minha eterna saudade.

À minha irmã (minha eterna companheira) Êmilie por todo amor, apoio, paciência e incentivo e ao meu paidrasto Regi (Muito mais que padrasto, meu pai), pelo apoio, amor, pelas orações, compreensão, torcida, muitos investimentos. Se cheguei até aqui, é porque tive vocês durante o caminho, vocês são parte de mim e me acompanham em todo lugar e todos os dias.

Ao meu sogro pelo apoio e ao meu cunhado Leandro por me ouvir falar dia e noite sobre os meus ratos, ler meus artigos, apoiar e torcer por mim.

A Ne que me acompanhou na primeira prova para o processo seletivo dessa Faculdade, e sempre foi parceira nas viagens, lutas e muita oração.

A Faculdade de Odontologia de Araraquara da Universidade Júlio de Mesquita Filho e à Coordenação do Curso de Pós-Graduação.

À Prof. Drª Juliane Maria Guerreiro-Tanomaru, minha orientadora, o meu muito obrigada pela confiança devotada em mim ao longo desses anos, pela carta de orientação concedida lá no início, por todas as cirurgias, ensinamentos, apoio, risadas e paciência. Este trabalho não teria sido possível sem sua orientação e apoio contínuo. Sou imensamente grata por ter tido o privilégio de tê-la como minha orientadora. Obrigada pelo exemplo de conduta profissional e por generosamente compartilhar seu conhecimento.

Ao Prof. Dr. Mário Tanomaru-Filho, pela oportunidade, confiança, pelos ensinamentos, correções, conselhos e apoio durante todo o decorrer do trabalho.

À Prof. Estela Sasso-Cerri por todas as brincadeiras, conselhos e apoio ao longo deste trabalho.

Ao Prof. Dr. Paulo Sérgio Cerri, obrigada por todos os ensinamentos, pela paciência, pelas correções, por me ensinar a desvendar a Histologia, por todos os conselhos e apoio em todas as fases dessa minha trajetória. Um exemplo de profissional.

Aos meus amigos de Pós-Graduação que foram companhia, apoio e alegria. Em especial a Camila, Jéssica, Luiza que foram companheiras de alegrias, tristezas, trabalhos e vitórias. Presentes que a pós me deu.

Aos amigos da Histologia e Embriologia que me receberam como agregada com tanto carinho e foram companhias ao longo do dia. Obrigada Camila, Renata, André, Salmo, Lucas, Lays e Gabi. Vocês foram apoio, ouvintes de alegrias e tristeza, levo vocês para a vida.

Ao técnico Pedro Simões, muito obrigada por toda ajuda, todo ensinamento e paciência nas atividades do laboratório.

Ao CNPq: o presente trabalho foi realizado com o apoio do Conselho Nacional de Desenvolvimento Científico e Tecnológico.

“If we know what we're doing it wouldn't be called research.”

Albert Einstein[*]

[*] Einstein, A. The collected papers of Albert Einstein. Princeton University Press.1987

Silva ECA. Reação tecidual e potencial bioativo de cimentos biocerâmicos reparadores e endodônticos em associação ou não a substâncias antimicrobianas [tese de doutorado]. Araraquara: Faculdade de Odontologia da UNESP; 2024.

RESUMO

Materiais biocerâmicos são desenvolvidos em função do potencial biológico e bioativo. O controle da infecção endodôntica nos canais radiculares é essencial para o êxito do tratamento endodôntico. A associação de cimentos endodônticos com agentes antimicrobianos e óleos essenciais pode potencializar a ação antimicrobiana. ***Artigo 1:*** Análise da reação inflamatória e potencial bioativo do novo cimento endodôntico biocerâmico NeoSealer Flo em comparação ao Bio-C Sealer e AH Plus. ***Artigo 2:*** Avaliação da reação tecidual de biocerâmico reparador recentemente desenvolvido (Neoputty) em comparação ao Bio-C Repair e MTA Repair HP. ***Artigo 3:*** Análise da biocompatibilidade e potencial bioativo dos biocerâmicos endodônticos (NeoSealer Flo) e BioRoot ™ RCS com ou sem adição de cetramida a 1%. ***Artigo 4:*** Avaliação da reação tecidual e potencial bioativo provocada pelos materiais: MTA HP Repair e Bio-C Repair com ou sem adição do *Thime Essential Oil* (TEO). A reação tecidual foi avaliada após implantação de tubos de polietilenos preenchidos com os respectivos materiais no subcutâneo de ratos. A análise incluiu contagem de células inflamatória e de fibroblastos, estimativa do conteúdo de colágeno e imunoexpressão de osteocalcina após 7, 15, 30 e 60 dias. O método de von Kossa e luz polarizada foram realizados. Os dados foram avaliados por ANOVA two-way seguido do teste de Tukey, com nível de significância de 5%. Os dados da OCN foram submetidos ao teste de Kruskal-Wallis e ao teste post hoc de Dunn e Friedman e Nemenyi. ***Artigo 1:*** NeoFlo mostrou menor biocompatibilidade do que Bio-C Sealer e maior recrutamento de células inflamatórias quando comparado ao AH Plus. Além disso, tanto o NeoFlo quanto o BC foram capazes de estimular a imunoexpressão de OCN nas cápsulas, bem como permitir a deposição de calcita amorfa, sugerindo um potencial bioativo. ***Artigo 2****:* NeoPutty é biocompatível, embora o potencial irritante deste material biocerâmico no tecido conjuntivo seja maior do que o do Bio C Repair e do MTA HP. Além disso, a imunoexpressão da osteocalcina pelas células do tecido conjuntivo, assim como as estruturas positivas para von Kossa e os depósitos birefringentes, são parâmetros sugestivos de que o NeoPutty apresenta potencial bioativo. ***Artigo 3****:* A adição de cetrimida aos cimentos biocerâmicos NeoSealer e BioRoot RCS induziu um maior recrutamento de células inflamatórias. No entanto, a redução na reação inflamatória foi acompanhada por um aumento gradual nos fibroblastos e no teor de colágeno ao longo do tempo, indicando, portanto, que esses materiais são biocompatíveis. Estruturas birrefringentes e imunoexpressão de OCN sugerem o potencial bioativo do NeoFlo puro e do BROOT, bem como desses cimentos com adição de 1% de cetrimida. ***Artigo 4****:* A adição de *Thime Essential Oil* ao cimento Bio-C reduziu o recrutamento de células inflamatórias, indicando que este óleo atenuou a reação inflamatória causada pelo Bio-C Repair. A significativa redução na reação inflamatória, associada ao aumento evidente no número de fibroblastos e no teor de colágeno nas cápsulas ao redor dos materiais apoia a ideia de que esses materiais são biocompatíveis. Além da biocompatibilidade, os resultados também sugeriram que os materiais biocerâmicos experimentais apresentam potencial bioativo. Em conclusão, NeoFlo e NeoPutty inicialmente mostraram potencial inflamatório superior, porém essa resposta diminuiu com o tempo, revelando também potencial bioativo. A inclusão de cetramida levou a um maior recrutamento de células

inflamatórias, enquanto a adição de *Thime Essential Oil* em cimentos reparadores teve o efeito oposto, reduzindo a resposta inflamatória.

Palavras Chaves: Teste de materiais. Endodontia. Imuno-histoquímica.

Silva ECA Tissue reaction and bioactive potential of repair and endodontic bioceramic cements in association or not with antimicrobial substances [tese de doutorado]. Araraquara: Faculdade de Odontologia da UNESP; 2024.

ABSTRACT

Bioceramic materials are created considering their biological potential. Controlling endodontic infection in root canals is crucial to the success of endodontic treatment. Although mechanical instrumentation of root canals significantly reduces endodontic microbiota, complete eradication of microorganisms is not always possible. Thus, the combination of endodontic cements with antimicrobial agents and essential oils can enhance the antimicrobial action. **Article 1:** Analysis of the inflammatory reaction and bioactive potential of the new bioceramic endodontic sealer NeoSealer Flo compared to Bio-C Sealer and AH Plus. **Article 2:** Evaluation of tissue reaction of recently developed repair bioceramic (Neoputty) in comparison to Bio-C Repair and MTA Repair HP. **Article 3:** Analysis of the biocompatibility and bioactive potential of endodontic bioceramics (NeoSealer Flo) and BioRoot™ RCS with or without addition of 1% cetramide. **Article 4:** Assessment of the tissue reaction and bioactive potential caused by the materials: MTA HP Repair and Bio-C Repair with or without the addition of Thime Essential Oil (TEO). The tissue reaction was evaluated after implanting polyethylene tubes filled with the respective materials into the subcutaneous tissue of rats for 7, 15, 30 and 60 days. The following parameters were analysed in the capsules: thickness of the capsules, number of inflammatory cells (IC) and of fibroblasts (Fb), content of birefringent collagen, immunohistochemistry for detection of osteocalcin (OCN), von Kossa method and analysis of unstained sections under polarized light. Data were evaluated by two-way ANOVA followed by Tukey's test, with a significance level of 5%. The OCN data were subjected to the Kruskal-Wallis test and the Dunn and Friedman and Nemenyi post hoc test. **Article 1:** NeoFlo showed lower biocompatibility than Bio-C Sealer and greater recruitment of inflammatory cells when compared to AH Plus. Additionally, both NeoFlo and BC were able to stimulate OCN immunoexpression in the capsules, as well as allow deposition of amorphous calcite, suggesting bioactive potential. **Article 2:** NeoPutty is biocompatible, although the irritant potential of this bioceramic material in connective tissue is higher than that of Bio C Repair and MTA HP. Additionally, osteocalcin immunoexpression by connective tissue cells, as well as positive von Kossa structures and birefringent deposits, are suggestive parameters that NeoPutty exhibits bioactive potential. **Article 3:** The addition of cetrimide to the bioceramic sealers NeoSealer and BioRoot RCS induced greater recruitment of inflammatory cells. However, the reduction in inflammatory reaction was accompanied by a gradual increase in fibroblasts and collagen content over time, indicating that these materials are biocompatible. Birefringent structures and OCN immunoexpression suggest bioactive potential of pure NeoFlo and BROOT, as well as these sealers with the addition of 1% cetrimide. **Article 4:** The addition of thyme oil to Bio-C cement reduced recruitment of inflammatory cells, indicating that this oil alleviated the inflammatory reaction caused by Bio-C Repair. The significant reduction in inflammatory reaction, associated with a noticeable increase in the number of fibroblasts and collagen content in capsules around the materials, supports the idea that these materials are biocompatible. Besides biocompatibility, the results also suggest that the experimental bioceramic materials present bioactive potential. In conclusion, NeoFlo and NeoPutty initially exhibited superior inflammatory potential, however, this response decreased over time, also revealing a bioactive potential. The

inclusion of cetrimide led to a higher recruitment of inflammatory cells, while the addition of thyme oil in reparative cements had the opposite effect, reducing the inflammatory response.

Keywords: Materials testing. Endodontics. Immunohistochemistry.

SUMÁRIO

1 INTRODUÇÃO

Cimentos à base de silicato tricálcico, também denominados de biocerâmicos, são o resultado da combinação entre silicatos de cálcio, apresentando propriedades biológicas adequadas, biocompatibilidade, bioatividade e ausência de citotoxicidade. Estes materiais promovem a formação de hidrato de silicato de cálcio e hidróxido de cálcio em contato com a água, proporcionando selamento em condições de umidade[1,2], o que possibilita ampla aplicação clínica.

Os cimentos reparadores são indicados para capeamento pulpar, pulpotomia, tratamento de dentes com ápice aberto e reparo de perfuração[2]. Estes são classificados de acordo com sua funcionalidade clínica apresentando variadas composições.

O NeoPutty (NuSmile, Houston, TX, EUA) é um novo cimento reparador pronto para uso composto por um pó inorgânico extremamente fino de silicato tricálcico e silicato dicálcico em meio orgânico, que segundo o fabricante foi projetado para tomar presa *in vivo* na presença de umidade. Suas indicações incluem capeamento pulpar direto e indireto, pulpotomia e apicigênese, além de reparo de perfurações, reabsorção, retrobturação e apicificação. O Neoputty exibe maior biocompatibilidade do que o EndoSequence BC RRM em células fibroblásticas e células-tronco pulpares[1]. No entanto, estudos *in vivo* não foram relatados até o momento. Quando comparado ao NeoMTA Plus e MTA HP, o MTA exibiu liberação de íons de cálcio significativamente maior em relação ao NeoPutty e NeoMTA Plus. Em células de polpa dentária humana, o NeoPutty mostrou citocompatibilidade[2]. Até o momento, as evidências científicas sobre as propriedades biológicas do NeoPutty permanecem limitadas.

O Bio-C Repair (Angelus, Londrina, PR, Brasil) é um material de reparo biocerâmico pronto para uso. Um estudo *in vitro* comparou a citocompatibilidade de Bio-C Repair, Biodentine e ProRoot MTA e revelou um alto índice de viabilidade de células de polpa dentária humana (hDPCS) expostas a esses cimentos. Além disso, nenhuma alteração do citoesqueleto foi observada em hDPCS, que estavam aderidas aos cimentos de reparo[3]. Ao ser avaliado em subcutâneo de ratos o material apresentou biocompatibilidade e sugeriu um potencial bioativo[4].

Outro cimento reparador, o MTA Repair (Angelus, Londrina, PR, Brasil), foi lançado na forma de um material biocerâmico com alta plasticidade visando manter as propriedades biológicas do MTA, melhorando suas propriedades químicas e físicas através da adição de um plastificante orgânico à água destilada. Acerca do MTA Repair, estudos indicam que o plastificante inserido na formulação líquida favoreceu a redução do tempo de presa e proporcionou um aumento do pH, sendo então considerado como parâmetro para outros materiais reparadores, apresentando ainda biocompatibilidade[4-6].

Visando melhorias nas propriedades dos cimentos reparadores, a adição do óleo essencial de tomilho (TEO), um líquido oleoso aromático complexo utilizado para prevenir e tratar doenças humanas devido às suas propriedades anticâncer, antioxidantes, anti-inflamatórias e antimicrobianas[7] pode resultar no aumento da atividade antibacteriana essencial para o sucesso clínico. O óleo essencial de tomilho, ou *Thyme Essential Oil* (TEO), pode resultar no aumento da atividade antibacteriana. O TEO apresenta atividade antimicrobiana e propriedades antifúngicas, antiinflamatórias e antibacterianas[8]. TEO inibe efetivamente microrganismos resistentes como *C. albicans*[9]. TEO demonstra ação antibacteriana e antibiofilme em cremes dentais contra bactérias associadas a doenças bucais, aumentando a eficiência dos dentifrícios contendo clorexidina[7-9].

Os cimentos obturadores devem permitir o selamento do sistema de canais radiculares de forma biocompatível e idealmente favorecer o processo de reparação[10,11].

O NeoSealer Flo (NuSmile, Houston, TX, EUA) é um novo material biocerâmico de preenchimento radicular pronto para uso composto de silicato dicálcico e tricálcico com aluminato de cálcio, aluminato tricálcico e tantalita. Segundo o fabricante, este selante apresenta capacidade de formação de hidroxiapatita, biocompatibilidade, estabilidade dimensional e ação antimicrobiana. Além disso, atendeu aos padrões químicos e físicos exigidos e liberou íons biologicamente relevantes, como cálcio e fosfato[6]. Porém, até o momento, não existem pesquisas *in vivo* sobre o NeoSealer Flo quanto à biocompatibilidade e bioatividade.

O BioRoot ™ RCS (Septodont, Saint-Maur-des-Fossés, França) é um cimento obturador que apresenta base mineral em forma de pó/líquido. A composição do pó consiste principalmente em silicato tricálcico, óxido de zircônio e povidona. A parte

líquida é uma solução aquosa de cloreto de cálcio com policarboxilato, altos valores de de Ca^{2+} e OH^{-} em soluções de PBS e maior resistência de união[13]. Colombo et al.[12] descrevem que BioRoot RCS apresenta uma atividade antibacteriana discreta, demonstrando a necessidade de melhorias em sua composição e de estudo in vivo que avaliem suas propriedades biológicas.

A cetrimida é um surfactante catiônico, que tem demonstrado eficácia contra bactérias gram-positivas e gram-negativas. É pouco irritante e reduz a tensão superficial dos líquidos, favorecendo sua entrada em locais de difícil acesso, como os túbulos dentinários. Estudos demonstram que a cetrimida apresenta a capacidade de erradicação de microrganismos após um minuto de exposição[13,14]. Estas características justificam sua associação ao cimento obturador, sendo necessário estudos *in vivo*.

O cimento obturador Bio-C Sealer (Angelus, Brasil) é um cimento endodôntco biocerâmico pronto para uso com pH alcalino, baixa alteração volumétrica demonstra biocompatibilidade e potencial bioativo[10].

A biocompatibilidade de materiais refere-se à capacidade de um material interagir de forma segura com sistemas biológicos, como células, tecidos e organismos vivos, sem causar danos ou respostas adversas. A avaliação da biocompatibilidade e potencial bioativos dos materiais endodônticos é essencial, devido ao íntimo contato destes com os tecidos periapicais e pode ser realizada através do estudo em tecido subcutâneo de ratos. Um material é considerado biocompatível quando sua resposta inflamatória apresenta redução com o decorrer do tempo[15-17]. A biocompatibilidade de um cimento endodôntico depende diretamente de seus componentes, de seu tempo de presa e de sua solubilidade[18]. Por sua vez, um material bioativo é aquele que tem a capacidade de interagir de forma benéfica com sistemas biológicos, como células e tecidos vivos, promovendo respostas específicas que favorecem a regeneração ou reparo tecidual.

O estudo em tecido conjuntivo subcutâneo de ratos é uma metodologia controlada recomendada pela Fédération Dentaire International e International Standard-ISO como indicativo para comparar o grau de irritabilidade dos materiais odontológicos, apresentando a capacidade de avaliar de forma precisa a reação causada pelo material e proporcionando a descrição do tipo, extensão de lesão e a duração. Ainda, estudos utilizando tecido subcutâneo de ratos demonstram

resultados importantes sobre os efeitos de diferentes materiais endodônticos sobre marcadores de inflamação e biomineralização.

A avaliação de formação de estruturas contendo cálcio é obtida por meio de técnicas histoquímica como o método de von Kossa, baseado na detecção de cálcio em cortes de material incluído em parafina, que pode ser associada a detecção imuno-histoquímica de proteínas não colágenas encontradas nos tecidos mineralizados, dentre elas a osteocalcina, osteopontina, osteonectina[4,10,11]. A osteocalcina é um peptídeo secretado pelos osteoblastos e odontoblastos durante a formação da matriz óssea e da matriz de dentina, respectivamente.

A avaliação da reação tecidual e do potencial bioativo dos cimentos endodônticos biocerâmicos é fundamental para compreender os mecanismos envolvidos na reparação e regeneração dos tecidos periapicais, bem como para aprimorar o desempenho clínico desses materiais. Diante do exposto, tornam-se relevantes os estudos que avaliem as propriedades biológicas dos novos materiais endodônticos.

2 PROPOSIÇÃO

Avaliar *in vivo* o comportamento biológico e o potencial bioativo dos materiais biocerâmicos reparadores e obturadores associados ou não a antimicrobianos.

2.1 Objetivos Específicos

Avaliar a reação inflamatória e potencial bioativo dos cimentos endodônticos biocerâmicos: NeoSealer Flo e Bio-C Sealer em comparação ao AH Plus.

Avaliar a reação inflamatória e potencial bioativo dos materiais reparadores: Neoputty em comparação ao Bio-C Repair e MTA Repair.

Verificar *in vivo* a reação inflamatória e potencial bioativo dos materiais biocerâmicos NeoSealer e BioRoot ™ RCS com adição de Cetramida.

Analisar *in vivo* a reação tecidual e potencial bioativo dos materiais MTA Repair e Bio-C Repair com adição do *Thime Essential Oil* (TEO).

3 PUBLICAÇÕES

Nessa sessão é realizada à apresentação dos artigos elaborados durante a realização da tese de doutorado. Durante esta sessão, são demonstrados os resultados, metodologias utilizadas e conclusões alcançadas ao longo do estudo.

3.1 Artigo 1*

Biocompatibility and bioactive potential of bioceramic endodontic sealer: Neosealer Flo

ABSTRACT

Introduction: NeoSealer Flo (NeoFlo, NuSmile, Houston) is a new ready-to-use bioceramic sealer. The aim of this study was to evaluate the biocompatibility and bioactive potential of the NeoFlo in comparison to Bio-C Sealer (Angelus, Londrina) and AH Plus (Dentsply DeTrey GmbH). **Methods:** The tissue reaction provoked by materials in the rat subcutaneous tissues was evaluated after 7, 15, 30 and 60 days of implantation. The number of inflammatory cells (IC), fibroblasts and the cells immunolabelled for osteocalcin (OCN) was obtained. von Kossa method and polarized light were used to identify amorphous calcite. Data were evaluated by two-way ANOVA followed by Tukey's test, with a significance level of 5%. OCN data were submitted Kruskal-Wallis test and the Dunn and Friedman and Nemenyi post hoc test for analysis over time. **Results:** Although NeoFlo showed higher values of IC than BC and AHP ($P < 0.05$), the capsules of NeoFlo presented a moderate inflammatory reaction, similarly to the AHP at 15, 30 and 60 days. Moreover, significant reduction in the number of IC and an increase in the fibroblasts and in the amount of birefringent collagen was observed in the capsules around over time. Immunoexpression of OCN was only observed in the capsules of NeoFlo and BC specimens, but the capsules of BC showed the highest values in all periods ($P <0.05$). **Conclusion:** In the present study, NeoFlo showed lower biocompatibility than Bio-C Sealer cement and similar inflammation intensity to AH Plus and presents bioactive potential in connective tissues.

* Artigo segue as normas de formatação do periódico *Journal of Endodontics* no qual foi submetido.

INTRODUCTION

Hydration of calcium silicate materials promotes calcium silicate hydrate and calcium hydroxide responsible for biological properties. These products, also named bioceramics, have wide clinical application and can be used as ready-to-use materials that setting with moisture in dentin and adjacent tissues[1,2,3]. Resulting in the continuous development of new endodontic sealers based on calcium silicate based on its excellent biological properties[4].

NeoSealer Flo (NeoFlo, NuSmile, Houston, TX, USA) is a ready-to-use bioceramic root filling material composed of dicalcium and tricalcium silicate with calcium aluminate, tricalcium aluminate and tantalite[1]. According to the manufacturer, this sealer presents hydroxyapatite formation capacity, biocompatibility, dimensional stability, and antimicrobial action. Furthermore, it has been proposed that NeoFlo complies with chemical and physical standards and can release biologically effective ions such as calcium and phosphate[1]. However, there is still no *in vivo* study on NeoFlo regarding biocompatibility and bioactivity.

Biocompatibility is the ability of a material to promote a biological response that point to an evident reduction in the inflammatory reaction culminating with the structural and functional tissue repair. In turn, a bioactive material can interact with living tissues, resulting in the formation of an apatite layer at the material-tissue interface[2]. The evaluation of the biocompatibility and bioactivity properties is required for endodontic sealers, due to the contact of these materials with the periapical tissues and the influence on the repair process[1,5,6,7].

Thus, the aim of this study was to evaluate the biocompatibility and bioactive potential of the NeoFlo bioceramic sealer in comparison to Bio-C Sealer and AH Plus. The null hypothesis was that the difference among the composition of the materials would not interfere with the tissue reaction induced by the different sealers.

MATERIALS AND METHODS

The research protocol was approved by the Ethical Committee for Animal (Protocol # 19/2021). Twenty-four male *Holtzman* rats (*Rattus norvegicus albinus*) were distributed into 4 groups (n = 6/group) The materials evaluated in this study, their manufacturers, compositions, and proportions are shown in Table 1. Polyethylene tubes (Embramed Ltda., São Paulo, Brazil) were filled with one sealer or left empty (control group). The animals were anaesthetized with ketamine

hydrochloride (80 mg/kg, Virbac do Brasil Indústria e Comércio Ltda., São Paulo, SP, Brazil) and xylazine chloride (8 mg/kg, União Química Farmacêutica Nacional S/A, São Paulo, SP, Brazil). Subsequently, 4 tubes were implanted in the connective tissue of dorsal subcutaneous. After 7, 15, 30 and 60 days, the animals were euthanized with anesthetic overdose and the implants with adjacent tissues were removed.

Table 1: The Endodontic Sealers Used.

Sealers	Composition	Manufacturers	Proportion
NeoSealer Flo (NeoFlo)	Dicalcium and tricalcium silicate with calcium aluminate, tricalcium aluminate and tantalite and thickening agent	NuSmile, Houston, TX	Ready to use
Bio C- Sealer (BC)	Tricalcium silicate, dicalcium silicate, tricalcium aluminate, calcium oxide, zirconia oxide, silicon oxide, polyethylene glycol, and iron oxide	Angelus, Londrina, PR, Brazil	Ready to use
AH Plus (AHP)	Paste A: epoxy bisphenol-A resin and epoxy bisphenol-F, calcium tungstate (CaWO4), zirconium oxide (ZrO2), silica, and iron oxide Paste B: dibenzyl-diamine, aminoadamantane, $CaWO_4$, ZrO_2, silica, and silicone	Dentsply DeTrey GmbH, Konstanz, Germany	1 g:1 g (paste/paste)

Histologic Procedures

After 7, 15, 30 and 60 days, the implants and adjacent tissues were removed and immersed for 72 hours in a 4% formaldehyde buffered with 0.1M sodium phosphate at pH 7.2. After fixation, the specimens were then dehydrated, cleared, embedded in paraffin, and longitudinal sections (6 μm thick) were obtained. Non-

serial sections were stained with hematoxylin-eosin (H&E) to estimate the capsule thickness, and the number of inflammatory cells and the fibroblasts in the capsules.

Thickness of capsules

In each implant, the thickness of the capsules (TC) was estimated in three H&E-stained non-serial sections of each specimen. Capsule thickness was estimated in the middle portion from its surface adjacent to the material to its boundary with adjacent tissues[2,7,8,9].

Numerical density of inflammatory cells and fibroblasts

The number of inflammatory cells (IC) and fibroblasts (Fb) was evaluated using the Image-Pro Express 6.0 Olympus program. In each section, a standard area of 0.09 mm^2 of the capsule adjacent to the opening of the implanted tubes was captured. In each implant, the number of IC (neutrophils, lymphocytes, plasma cells and macrophages) and Fb was obtained from 3 sections, totalling an area of 0.27 mm^2 per implant. At the end, the mean value per group and period was obtained.

After obtaining of IC number, the inflammation reaction intensity was classified according to the following parameter[7,9]: mild inflammatory reaction (capsule containing until 25 IC/field), moderate inflammatory reaction (capsule containing from 26 until 125 IC/field), and severe/intense inflammatory reaction (capsule containing over 125 IC/field).

Content of collagen in the capsules

To evaluate the amount of birefringent collagen, three non-serial sections per specimen were stained with picrosirius red solution and analyzed under polarized light (BX51, Olympus)[5-8]. The amount of birefringent collagen was computed using an image analysis software (ImageJ; National Institutes of Health; Bethesda, USA). The birefringent collagen was estimated considering the standardized hue definitions: red/orange (2-23 and 230-256), yellow (39-51) and green (52-128). The amount of birefringent collagen was calculated and expressed as the percentage of the number of pixels occupied by collagen.

Immunohistochemical detection of OCN

Sections were incubated with rabbit anti-OCN antibody (1:150, code SAB1306277; Sigma-Aldrich, St Louis, MO). After a period of 16 hours in a humidified chamber, the sections were then incubated in streptavidin-biotin kit (Universal Dako LSAB, K0675). After buffer washes, peroxidase activity was revealed by 3,3'-diaminobenzidine chromogen (ImmPACTTM DAB) and sections were counterstained with Carazzi's hematoxylin. Using an image analysis system (Image Pro-Express 6.0), the OCN-immunostained cells were counted in a standardized area (0.09 mm^2) at ×695.

von Kossa reaction and analysis under polarized light

The sections were immersed in a 5% silver nitrate solution and subsequently incubated in a 5% sodium hyposulfite solution. After washing, the sections were stained with picrosirius red and mounted in resin medium.

Unstained sections were analyzed under a light microscope (Olympus, BX51) equipped with polarization filters to investigate the presence of birefringent structures in the capsules[2,3].

Statistical analysis

With the aid of the Sigma Stat 2.0 program (Jandel Scientific, Sausalito, CA, USA) the data were evaluated by two-way ANOVA followed by the Tukey test, with a significance level of $p \leq 0.05$. Osteocalcin data were submitted to the Kruskal-Wallis non-parametric test and Dunn's post hoc multiple comparison test for comparison between groups, and Friedman's test and Nemenyi's post hoc test for analysis over time.

RESULTS

At 7 days, the capsules around all specimens showed several IC and few collagen fibres (Figs. 1A-1D). However, an intense inflammatory reaction was observed in the NeoFlo specimens while in BC and AHP specimens the capsules exhibited a moderate inflammatory reaction (Table 2). After 15 days, a moderate inflammatory reaction was present in the capsules adjacent to the materials (Figs. 1E-1G; Table 2). At 30 and 60 days, the capsules of NeoFlo (Figs. 1I and 1M) and AHP (Figs. 1K and 1O) materials exhibited moderate inflammatory reaction (Table 2)

while in the BC few IC were present (Figs. 1J and 1N), characterizing a mild inflammatory reaction (Table 2). In all periods, a mild inflammatory reaction was seen in the capsules of CG specimens (Figs. 1D, 1H, 1L, 1P and Table 2).

Thickness of the capsules

As shown in Table 2, significant difference in the TC was not observed between NeoFlo and AHP showed while BC presented highest value at 7 days. After 15, 30 and 60 days, no difference was seen between NeoFlo and BC specimens. At 60 days, the AHP specimens showed greater TC than in NeoFlo, BC and CG specimens. Moreover, no significant difference was detected among NeoFlo, BC and CG at 60 days ($P > 0.05$). Significant reduction in the TC was seen in all specimens over time. However, at 60 days the mean TC values were still greater than 150 µm in the NeoFlo and AHP specimens.

Numerical density of ICs and Fb

The quantitative analyses (Table 2) revealed that the greatest values of IC were seen in the NeoFlo specimens in all time points. No significant difference in the number of IC was detected between BC and AHP specimens at 7 days, but the number of IC was significantly reduced in the BC specimens in comparison with AHP at 15, 30 and 60 days. In all periods, no significant difference was observed in the number of Fb among NeoFlo, BC and AHP specimens, except at 15 days. In this period, the number of Fb was significantly greater in the AHP than in NeoFlo and BC specimens, but no significant difference was seen between AHP and CG specimens. In all groups, a significant reduction in the number of IC and a significant increase in the number of Fb was observed over time.

Content of collagen in the capsules

At 7 days, the capsules contained few birefringent materials, which showed a significant increase over time (Table 2). In all periods, the capsules around AHP presented the lowest values. Although the NeoFlo had lower birefringent collagen than in capsules of BC at 7 days, no significant difference ($P > 0.05$) was observed between two groups at 15, 30 and 60 days (Table 2).

Figure 1 – HE-stained sections

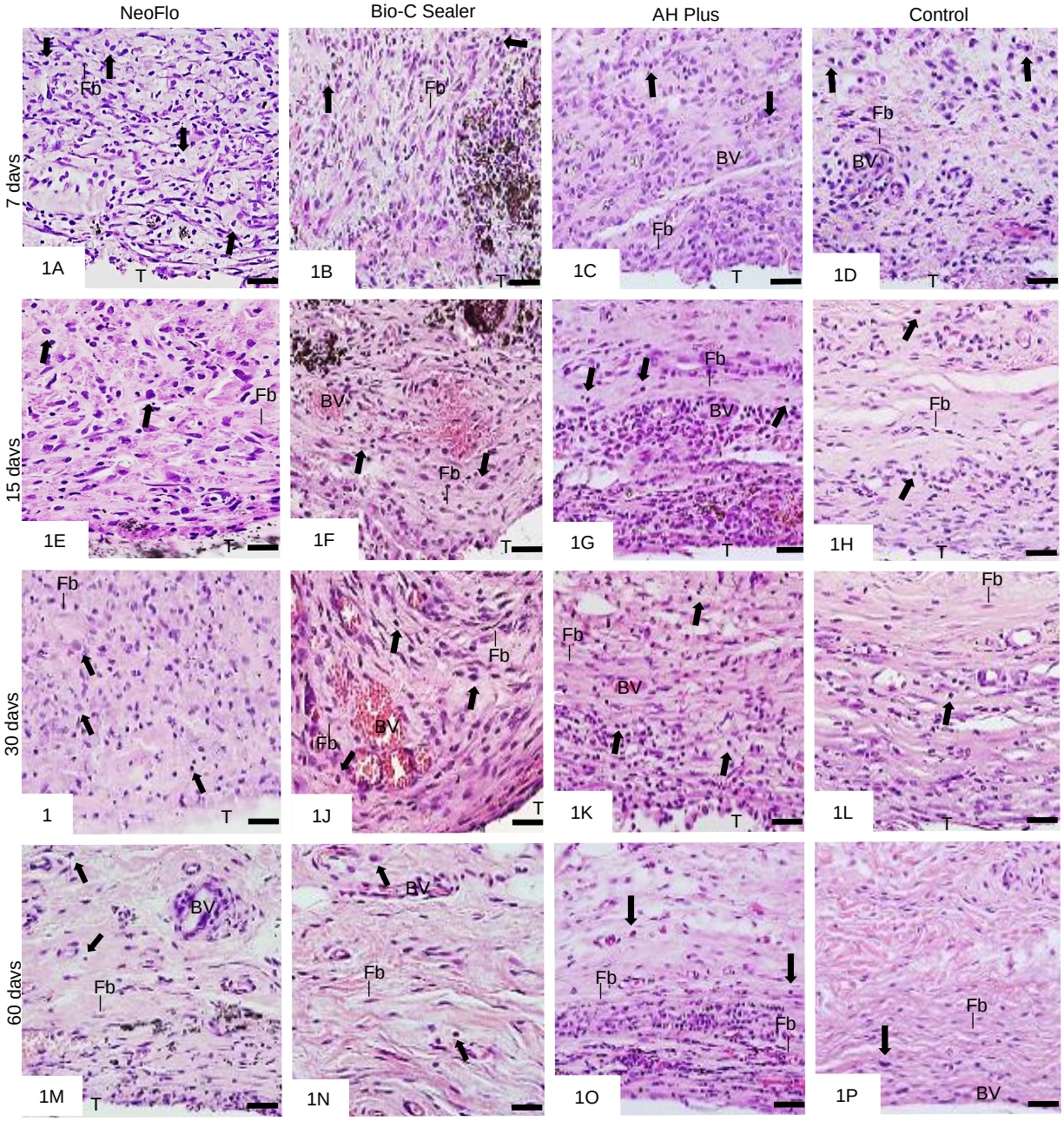

Figure 1: Photomicrographs of sections showing portions of capsules adjacent to the implanted tubes (T) after 7 (A-D), 15 (E-H), 30 (I-L) and 60 days (M-P). Arrows, inflammatory cells; Fb, fibroblasts; CF, collagen fibers; BV, blood vessels. Bars = 18 µm.

Immunohistochemical detection of OCN

OCN-immunolabelled cells were only observed in the capsules around NeoFlo and BC specimens (Figs. 2A-2P). According to Table 2, the number of OCN-immunolabelled cells was significantly greater in the BC specimens than in NeoFlo in

all periods (P<0.05). From 7 to 60 days, a significant increase in the immunoexpression was observed in the capsules around NeoFlo and BC specimens.

Table 2 – Thickness of the capsules (TC), number of inflammatory cells (IC), number of fibroblasts (Fb), number of OCN-immunolabelled cells, content of collagen (CF) and intensity of inflammatory reaction in the capsules around the NeoSealer Flo (NeoFlo), Bio-C Sealer (BC), AH Plus (AHP) and Control group (CG) at 7, 15, 30 e 60 days of implantation.

Periods		NeoFlo	BC	AHP	CG
7 days	**TC (µm)**	360 ± 46$^{a;1}$	485 ± 26$^{b;1}$	349 ± 65$^{a;1}$	149 ± 86$^{c;1}$
	IC/mm^2	1570 ± 24$^{a;1}$	720 ± 46$^{b;1}$	797 ± 73$^{b;1}$	251 ± 35$^{c;1}$
	Fb/mm^2	104±21 $^{a;1}$	128 ± 21 $^{a;1}$	104 ± 12 $^{a;1}$	168 ± 10 $^{a;1}$
	CF (%)	13.4±5 $^{a;1}$	21.8 ± 3 $^{b;1}$	3.4 ± 2 $^{c;1}$	16.4 ± 2 $^{a;1}$
	OCN/mm^2	11.11(11.11) $^{a;1}$	33.33(33.34) $^{b;1}$	0.00 (0.0) $^{c;1}$	0.00 (0.0) $^{c;1}$
	Inflammatory reaction	intense	moderate	moderate	mild
15 days	**TC (µm)**	363 ± 42$^{a;1}$	386 ± 31$^{a;1}$	242 ± 20$^{b;2}$	189 ± 11$^{c;1}$
	IC/mm^2	1252 ± 22$^{a;1}$	579 ± 27$^{b;2}$	636 ± 94$^{c;2}$	231 ± 15$^{d;1}$
	Fb/mm^2	151±21$^{a;1}$	158 ± 16 $^{a;1}$	202 ± 21 $^{b;2}$	236 ± 21 $^{b;2}$
	CF (%)	20.6±3 $^{a;2}$	22.8 ± 2 $^{a;1}$	11.5 ± 4 $^{b;2}$	28.9 ± 3 $^{a;2}$
	OCN/mm^2	22.22 (22.22) $^{a;2}$	33.33(33.34) $^{b;1}$	0.00 (0.0) $^{c;1}$	0.00 (0.0) $^{c;1}$
	Inflammatory reaction	moderate	moderate	moderate	mild
30 days	**TC (µm)**	281 ± 47$^{a;2}$	216 ± 11$^{a;2}$	229 ± 24$^{a;2}$	107 ± 04^{b,1}
	IC/mm^2	933 ± 67$^{a;2}$	262 ± 27$^{c;3}$	453 ± 39$^{b;3}$	176 ± 25^{c,2}
	Fb/mm^2	231±09 $^{a;2}$	221 ± 9 $^{a;2}$	203 ± 10 $^{a;2}$	310 ± 23 $^{b;3}$
	CF (%)	25.8±1 $^{a;3}$	28.2 ± 1 $^{a;2}$	20.9 ± 3 $^{a;3}$	26.8±2 $^{a;2}$
	OCN/mm^2	22.22 (22.22) $^{a;2}$	44.44 (33.34) $^{b;2}$	0.00 (0.0) $^{c;1}$	0.00 (0.0) $^{c;1}$
	Inflammatory reaction	moderate	mild	moderate	mild
60 days	**TC (µm)**	190 ± 49$^{a;3}$	146 ± 6$^{a;3}$	240 ± 43$^{b;2}$	104 ± 20^{a,1}
	IC/mm^2	486 ± 40$^{a;3}$	189 ± 7$^{b;4}$	352 ± 90$^{c;4}$	68 ± 11^{d,3}
	Fb/mm^2	360±23 $^{a;3}$	329 ± 27 $^{a;3}$	308 ± 12 $^{a;3}$	391 ± 23 $^{b;3}$
	CF (%)	29.9±2 $^{a;3}$	27.8 ± 1 $^{a;2}$	23.8 ± 1 $^{b;3}$	29.4 ± 1 $^{a;2}$
	OCN/mm^2	33.33(22.22) $^{a;3}$	55.56 (33.34) $^{b;3}$	0.00 (0.0) $^{c;1}$	0.00 (0.0) $^{c;1}$
	Inflammatory reaction	moderate	mild	moderate	mild

The comparison between groups in the same period is indicated by superscript letters in the lines; same letters = no significant difference.
The comparison between periods in the same group is indicated by superscript numbers in the columns; same numbers = no significant difference. Tukey test (p ≤ 0.05).

OCN: Values expressed as median and interquartile range. Analysis between groups in each period: Kruskal-Wallis followed by the Dunn test; analysis of each group over time: Friedman followed by the Nemenyi test ($p < 0.05$).

Figure 2 – Immunohistochemistry for osteocalcin detection

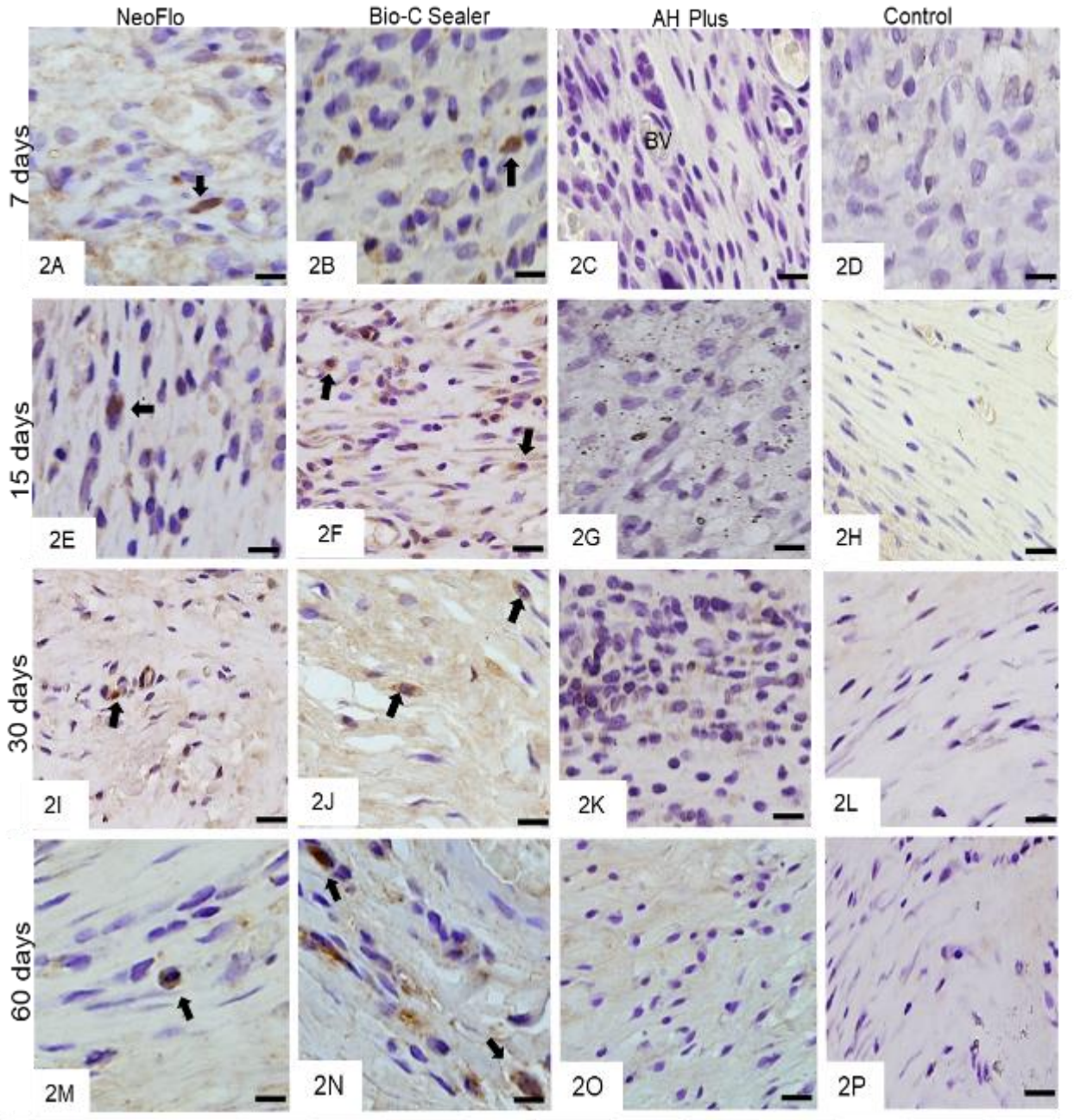

Figure 2: Photomicrographs of sections showing portions of capsules adjacent to the implanted tubes after 7 (2A-2D), 15 (2E-2H), 30 (2I-2L) and 60 days (2M-2P). The sections were subjected to the immunohistochemistry for OCN detection and counterstained with hematoxylin. OCN-immunolabelled cells (arrows) are seen in the capsules of NeoFlo and BC sealers. Bars = 18 µm.

von Kossa Reaction and Analysis under Polarized Light

The capsules around NeoFlo, BC and AHP specimens presented von Kossa-positive structures in all periods (Figs. 3A-3F). In all periods, birefringent structures

were observed in the capsules around NeoFlo and BC specimens (Figs. 3G, 3H, 3J and 3K); in the AHP specimens, birefringent structures were only seen in the innermost surface of the capsules (Figs. 3I and 3L). von Kossa-positive or birefringent structures were not observed in the CG specimens (data no shown).

Figure 3 – von Kossa and birefringent structures in unstained sections

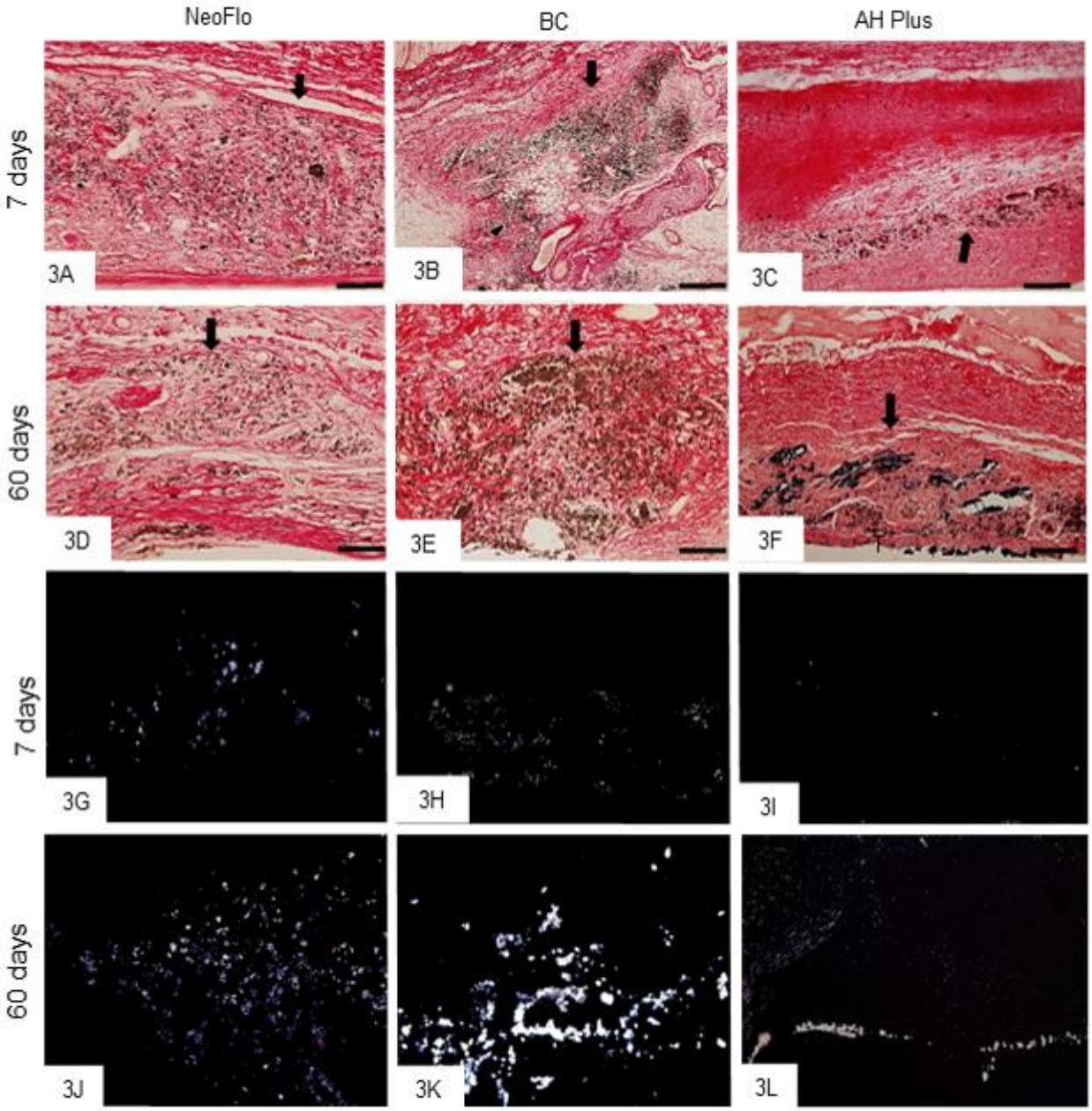

Figure 3: Photomicrographs of sections showing portions of capsules adjacent to the opening of the implanted tubes subjected to the von Kossa reaction (3A-3F) after 7 and 60 days. Capsules of NeoFlo (3A, 3D), BC (3B, 3E) and AHP (3C, 3F) exhibit von Kossa-positive structures (black/brown color). **Figs. 3G-3L:** unstained sections analyzed under polarized light. Birefringent structures are seen in the capsules. Bars = 36 µm.

DISCUSSION

The tissue reaction and bioactive potential of NeoFlo were compared to BC and AHP sealers after implantation in the subcutaneous connective tissue of rats. NeoFlo sealer induced greater recruitment of inflammatory cells than BC and AHP, leading to the maintenance of a moderate inflammatory reaction that lasted up to 60 days of subcutaneous implantation. On the other hand, NeoFlo was able to stimulate OCN immunoexpression and induce phosphate/calcium deposition, suggesting that this sealer has bioactive potential. Therefore, the null hypothesis was rejected due to differences in tissue reactions between sealers.

Although NeoFlo and BC have tricalcium and dicalcium silicate as their main component, their composition differs in other components. The BC material has calcium oxide, iron oxide, silicon dioxide and, as a radiopacifier, zirconium oxide. NeoFlo, on the contrary, presents calcium sulfate, grossite and tantalite, in addition to a thickening agent whose composition is not described by the manufacturer. Thus, it is possible that chemical composition of thickening agent may be related to different tissue reactions and the fact that at 7 days NeoFlo presented an intense inflammatory reaction, unlike BC and AHP, which promoted a moderate inflammatory process. This biological response may be also explained, at least in part, to the high solubility of NeoFlo.[1]

While a gradual reduction in the number of ICs around NeoFlo samples was observed over time, the capsules showed a mild inflammatory reaction within 60 days. In contrast, after 60 days, the capsules around the BC sealer showed a mild inflammatory reaction. The initial inflammatory reaction of BC is due to its high pH, which stimulates the recruitment of ICs and the production of cytokines.[2] The capsules of the CG specimens, on the other hand, showed a mild inflammatory process that may be related to the surgical procedure.[2]

Okamu et al.[10] also observed that the Bio-C Sealer demonstrates excellent healing of the periapical tissues. López-García et al.[11] demonstrated better cytocompatibility in terms of cell viability, migration, cell morphology, cell adhesion and mineralization ability for Bio-C Sealer in comparison to AH Plus.

AH Plus is an endodontic sealer based on epoxy resin, considered the gold standard for its physical properties and high bond strength to dentin. Tolosa-Monfà et al.[12] evaluated the effects of sealer on fibroblasts and concluded that it had severe cytotoxicity, the inflammatory potential found is justified by its composition. However,

Alves-Silva et al.[2] demonstrated that in subcutaneous tissues of rats at 60 days, the sealer is biocompatible, but does not have bioactive potential.

Endodontic sealers, including NeoFlo, can release irritating substances, especially during setting, promoting an inflammatory response in the connective tissue. Thus, the long setting time of NeoFlo (around 1344 minutes)[1] compared to Bio-C (around 220 minutes)[13] may also be responsible, at least in part, for the difference in the inflammatory reaction intensity induced by these sealers.

In all groups, significant reduction in the number of ICs was observed concomitantly with the gradual increase in the number of fibroblasts and in the content of birefringent collagen in the capsules around the NeoFlo, BC and AHP sealers. These findings support the concept that these endodontic sealers allow the connective tissue repair [9].

However, in NeoFlo and AHP capsules the rearrangement may take longer than in BC sealer capsules, as these capsules contained a moderate inflammatory infiltrate at 60 days. Furthermore, capsules adjacent to NeoFlo and AHP specimens were thick, while around BC thin capsules were observed at 60 days. The cytotoxicity of AH Plus has been mainly associated with the release of its amine and epoxy resin components.[14]

The chemical composition of endodontic materials plays an important role in biocompatibility, which explains the results found in the present study. The chemical reactions and properties of materials are directly related to their formula. Variation in the composition of calcium silicate-based materials can lead to differences in their clinical behavior.

Liu et al.[15] developed a sealer based on tricalcium aluminate and demonstrated that it showed biocompatibility and bioactive potential in fibroblastic cells. Calcium aluminate is mainly formed by three different phases, one of which is grossite.

NeoMTA Plus contains tantalum oxide in its composition as a radiopacifier and exhibited biocompatibility and bioactive potential when evaluated in the subcutaneous tissue of rats.[16] Tantalum oxide and tantalite are based on the same component, tantalum, however tantalite has a higher amount of tantalum which can cause different tissue reactions.

Neoputty is a repairing sealer that has the same composition as NeoSelaer Flo. Lozzáno-Guillén et al.[17] described that this material caused a decrease in cell

viability in higher dilutions. Periodontal ligament cells when cultured with NeoMTA 2 presented reduced cell viability. Although Ca^{2+} is an essential regulator of several intracellular processes, excessive intracellular Ca^{2+} accumulation and high alkalinity may be related to mitochondrial dysfunction and consequently reduced cell viability[18].

Endodontic sealers based on calcium silicate have been shown to be involved in osteoblastic differentiation.[19] OCN is a small glycoprotein, preferentially expressed by osteoblasts, mainly in the late stages of their differentiation, and consequently its presence can be considered as an indicator of the ability to form mineralized tissue [2,8,19,20,21]. OCN binds strongly to calcium and therefore this no collagenous protein seems to be involved in the regulation of matrix mineralization.

Here, OCN-immunolabelled cells were only observed in the capsules of NeoFlo and BC sealers, where BC presented the highest values at 60 days. BC sealer can contribute to the mineralization process of periapical tissues, as they demonstrate bioactive potential.[2]

In addition to the OCN immunoexpression, the capsules around these sealers also exhibited von Kossa-positive structures, indicating the salt deposits (calcium and/or phosphate)[22]. In the AHP specimens, birefringent structures were observed only on the innermost surface of the capsules, in agreement with other studies that demonstrated lower release of calcium ions for AH Plus than that promoted by bioceramic sealers[2,15,16]. Our results obtained from von Kossa combined with birefringent structures suggest a bioactive potential of NeoFlo like the BC sealer. The reaction process of calcium ions and carbon dioxide leads to the formation of calcite amorphous, birefringent structure that is considered as a parameter suggestive of the bioactive potential of an endodontic material[22,23, 24].

Biocompatibility and bioactive potential are necessary properties for endodontic materials, since these materials can have direct contact with periapical tissues and, consequently, interfere with the repair of periapical tissues, a process that aims at the success of endodontic treatment[2,22,25,26,27]. Our findings confirm that NeoSealer Flo presented inferior biocompatibility when compared to Bio-C Sealer.

CONCLUSION

In the present study, NeoFlo showed lower biocompatibility than Bio-C Sealer sealer and greater recruitment of inflammatory cells when compared to AH Plus. Furthermore, NeoFlo as well as BC was able to stimulate the immunoexpression of

OCN in the capsules as well as allowing the deposition of amorphous calcite suggesting a bioactive potential.

REFERENCES

1. Zamparini F, Prati C, Taddei P, Spinelli A, Di Foggia M, Gandolfi MG. Chemical-Physical Properties and Bioactivity of New Premixed Calcium Silicate-Bioceramic Root Canal Sealers. International Journal of Molecular Sciences 2022; 23(22): 13914.

2. Alves-Silva EC, Tanomaru-Filho M, da Silva GF, Delfino MM, Cerri PS, Guerreiro-Tanomaru JM. Biocompatibility and Bioactive Potential of New Calcium Silicate–based Endodontic Sealers: Bio-C Sealer and Sealer Plus BC. Journal of Endodontics 2020; 46: 1470-1477.

3. Camilleri J. Classification of hydraulic cements used in dentistry. Frontiers in dental medicine 2020; 1: 9.

4. Benetti F, Gomes-Filho JE, de Azevedo-Queiroz IO, Carminatti M, Conti LC, dos Reis-Prado AH, Cintra LTA. Biological assessment of a new ready-to-use hydraulic sealer. Restorative dentistry & endodontics 2021; 46(2).

5. Koutroulis A, Kuehne SA, Cooper PR, Camilleri J. The role of calcium ion release on biocompatibility and antimicrobial properties of hydraulic cements. Sci Rep 2019; 9:1–10.

6. Jung S et al. Evaluation of the biocompatibility of root canal sealers on human periodontal ligament cells ex vivo. Odontology 2019; 107: 54-63

7. Delfino MM, Jampani JLDA, Lopes CS, Guerreiro-Tanomaru JM, Tanomaru-Filho M, Sasso-Cerri E, Cerri PS. The participation of fibroblast growth factor-1 and interleukin-10 in connective tissue repair following subcutaneous implantation of bioceramic materials in rats. International Endodontic Journal 2022; 00:1-17.

8. de Pizzol Júnior JP, Sasso-Cerri E, Cerri PS. Matrix metalloproteinase-1 and acid phosphatase in the degradation of the lamina propria of eruptive pathway of rat molars. Cells 2018; *7*(11): 206.

9. Queiroz MB, Inada RN, Jampani JLDA, Guerreiro-Tanomaru JM, Sasso-Cerri E, Tanomaru-Filho M, Cerri P S. Biocompatibility, and bioactive potential of an experimental tricalcium silicate-based cement in comparison with Bio-C repair and MTA Repair HP materials. International Endodontic Journal 2023; 56:259-277.

10. Okamura T, Chen L, Tsumano N, Ikeda C, Komasa S, Tominaga K, Hashimoto Y. Biocompatibility of a high-plasticity, calcium silicate-based, ready-to-use material. Materials 2020; *13*(21): 4770.

11. López-García S, Pecci-Lloret MR, Guerrero-Gironés J, Pecci-Lloret MP, Lozano A, Llena C, Forner L. Comparative cytocompatibility and mineralization potential of Bio-C Sealer and TotalFill BC Sealer. Materials 2019; *12*(19): 3087.

12. Tolosa-Monfà A, Veroni A, Blasi-Cabús J, Ballester-Palacios ML, Berástegui-Jimeno E. Cytotoxicity comparison of Bio C Sealer against multiple root canal sealers. Journal of Clinical and Experimental Dentistry 2023; 15(2): e110.

13. Zordan-Bronzel CL, Torres FFE, Tanomaru-Filho M, Chávez-Andrade GM, Bosso-Martelo R, Guerreiro-Tanomaru JM. Evaluation of physicochemical properties of a new calcium silicate–based sealer, Bio-C Sealer. Journal of endodontics 2019; 45(10): 1248-1252.

14. Giacomino CM, Wealleans JA, Kuhn N, Diogenes A. Comparative biocompatibility and osteogenic potential of two bioceramic sealers. Journal of endodontics 2019; 45(1): 51-56.

15. Liu WN, Chang J, Zhu YQ, Zhang M. Effect of tricalcium aluminate on the properties of tricalcium silicate–tricalcium aluminate mixtures: setting time, mechanical strength and biocompatibility. International endodontic journal 2011; 44(1): 41-50.

16. Hoshino RA, Delfino MM, da Silva GF, Guerreiro-Tanomaru JM, Tanomaru-Filho M, Sasso-Cerri E, Cerri PS. Biocompatibility and bioactive potential of the NeoMTA Plus endodontic bioceramic-based sealer. Restorative dentistry & endodontics 2021; 46(1).

17. Lozano-Guillén A, López-García S, Rodríguez-Lozano FJ, Sanz JL, Lozano A, Llena C, Forner L. Comparative cytocompatibility of the new calcium silicate-based cement NeoPutty versus NeoMTA Plus and MTA on human dental pulp cells: an in vitro study. Clinical Oral Investigations 2022; 26(12): 1-10.

18. Rodríguez-Lozano FJ, Lozano A, López-García S, García-Bernal D, Sanz JL, Guerrero-Gironés J, Melo, M. Biomineralization potential and biological properties of a new tantalum oxide. Clinical Oral Investigations 2022; 26(2): 1427-1441.

19. Viana Viola N, Guerreiro-Tanomaru J, Ferreira da Silva G, Sasso-Cerri E, Tanomaru-Filho M, Cerri PS. Biocompatibility of an experimental MTA sealer implanted in the rat subcutaneous: quantitative and immunohistochemical evaluation.

Journal of Biomedical Materials Research Part B: Applied Biomaterials 2012; 100(7): 1773-1781.

20. Almeida LHS, Moraes RR, Morgental RD, Pappen FG. Are premixed calcium silicate–based endodontic sealers comparable to conventional materials? A systematic review of in vitro studies. Journal of endodontics 2017; 43(4): 527-535.

21. Silva ECA, Tanomaru-Filho M, Silva GF, Lopes CS, Cerri PS, Guerreiro Tanomaru, J. M. Evaluation of the biological properties of two experimental calcium silicate sealers: An in vivo study in rats. International Endodontic Journal 2020; 54(1): 100-111.

22. Silva GF, Tanomaru-Filho M, Bernardi MI, Guerreiro-Tanomaru JM, Cerri, PS. Niobium pentoxide as radiopacifying agent of calcium silicate-based material: evaluation of physicochemical and biological properties. Clinical oral investigations 2015; *19*: 2015-2025.

23. Bueno CRE, Valentim D, Marques VAS, Gomes-Filho JE, Cintra LTA, Jacinto R., Dezan-Junior E. (2016). Biocompatibility and biomineralization assessment of bioceramic-, epoxy-, and calcium hydroxide-based sealers. Brazilian oral research, 2016; 30 (1): e81.

24. Carvallo L, Henríquez B, Paredes R, Olate J, Onate S, Van Wijnen AJ, Montecino, M. 1α, 25-dihydroxy vitamin D3-enhanced expression of the osteocalcin gene involves increased promoter occupancy of basal transcription regulators and gradual recruitment of the 1α, 25-dihydroxy vitamin D3 receptor-SRC-1 coactivator complex. Journal of cellular physiology, 2008; 214(3): 740-749.

25. Kapralos V, Böcker J, Vach K, Altenburger M, Proksch S, Karygianni, L. On the biocompatibility of endodontic sealers. Swiss Dental Journal 2022; *132*(9): 586-597.

26. Donnermeyer D, Bürklein S, Dammaschke T, Schäfer E. Endodontic sealers based on calcium silicates: a systematic review. Odontology 2019; 107(4): 421-436.

27. Silva GF, Guerreiro-Tanomaru JM, Da Fonseca TS, Bernardi MIB, Sasso-Cerri E, Tanomaru-Filho M, Cerri PS. Zirconium oxide and niobium oxide used as radiopacifiers in a calcium silicate-based material stimulate fibroblast proliferation and collagen formation. International endodontic journal, 2017; 50: e95-e108.

3.2 Artigo 2*

Inflammatory reaction and bioactive potential of NeoPUTTY Calcium Silicate-based sealer: An in vivo study in rats

Aim: To evaluate the inflammatory reaction and the ability to induce the biological activity of a new repair material, NeoPUTTY (NPutty; NuSmile, USA), in comparison with Bio-C Repair (BC; Angelus, Brazil) and MTA Repair HP (MTA HP; Angelus, Brazil).

Methodology: Polyethylene tubes were filled with materials or left empty (control group, CG) and implanted subcutaneously in rats for 7, 15, 30, and 60 days (n = 6/group). Capsule thickness, number of inflammatory cells (ICs), fibroblasts, collagen content, von Kossa technique, and unstained sections under polarized light were evaluated in conjunction with immunohistochemistry for osteocalcin (OCN). Data were subjected to two-way ANOVA followed by Tukey's test ($P \leq 0.05$), except for OCN. Data were submitted to two-way ANOVA followed by Tukey's test ($P \leq 0.05$), except for OCN. OCN data were submitted to Kruskal-Wallis and Dunn and Friedman post hoc tests followed by the Nemenyi test at a significance level of 5%.

Results: At 7, 15, and 30 days, thick capsules containing numerous ICs were seen around the materials. At 60 days, a moderate inflammatory reaction was observed for NPutty, BC while MTA HP presented thin capsules with moderate inflammatory cells. In all periods, NPutty specimens contained the highest values of ICs ($P < 0.05$). From 7 to 60 days, the number of ICs reduced significantly while an increase in the number of fibroblasts and birefringent collagen content was observed. At 7 and 15 days, no significant difference in the immunoexpression of OCN ($P > 0.05$). At 30 and 60 days NPutty showed the lowest values of OCN ($P < 0.05$). At 60 days, similar immunoexpression was observed for BC and MTA HP ($P > 0.05$). In all time intervals, capsules around NPutty, BC, and MTA HP showed von Kossa-positive and birefringent structures.

Conclusions: Despite the greater inflammatory reaction promoted by NeoPutty compared to BC and MTA HP, the reduction in the thickness of capsules, the

* Artigo formatado segundo as normas do periódico *International Endodontic Journal* no qual foi submetido e aceito.

increase in the number of fibroblasts, and the reduction in the number of ICs indicate that this bioceramic material is biocompatible Furthermore, our findings suggest that NeoPutty presents the ability to promote biological interaction with tissue.

INTRODUCTION

Calcium silicate-based materials are commonly used to promote pulp regeneration and hard tissue repair, such as pulp capping, pulpotomy, apexification, perforation repair, and retrograde filling. Chemical composition and physical properties of endodontic materials can interfere with the cellular response promoting tissue repair (Silva *et al.* 2017, da Fonseca *et al*. 2019; Delfino *et al.* 2021, Queiroz *et al.* 2023). Bioceramic materials induce the formation of a bioactive layer at the material/tissue interface, thus stimulating biomineralization. It has been demonstrated that calcium silicate-based materials promote an increased deposition of hydroxyapatite over time, which is associated with a regenerative/reparative response (Silva et al., 2020; Alves-Silva *et al.* 2020, Queiroz *et al.* 2023).

NeoPUTTY (NPutty; NuSmile, Houston, TX, USA) is a new ready-to-use repair cement composed of fine inorganic powder of tricalcium silicate (<25) and dicalcium silicate (<10) in an organic medium, designed to set in the presence of moisture. NPutty indications include direct and indirect pulp capping, cavity lining, and base, pulpotomy, and apicogênese, as well as perforation repair, retrofilling, and apexification. NPutty exhibits greater citocompatibility than EndoSequence BC RRM putty on fibroblastic cells and pulpal stem cells (Sun *et al.* 2021). NPutty in a study using cultured human dental pulp cells (hDPCs) showed cell viability like NeoMTA Plus and MTA-Angelus (Lozano-Guillén *et al*. 2022). However, NPutty presented a lower release of calcium ions than NeoMTA Plus and MTA-Angelus (Lozano-Guillén *et al.* 2022). Alqahtani *et al.* (2023) demonstrated that NeoPUTTY® showed comparable success to mineral trioxide aggregate in primary molar pulpotomies over 12 months. However, the tissue reaction of the material has not yet been evaluated in the subcutaneous tissue of rats.

MTA Repair HP (MTA HP; Angelus, Londrina, PR, Brazil), a calcium silicate-based material, presents setting time, solubility, and radiopacity according to the ISO 6876/2012 standard (Queiroz *et al*. 2022). MTA HP is a bioceramic material with an organic plasticizer added to distilled water to improve plasticity (ElReash *et al.* 2019, Ferreira *et al*. 2019). Histological studies have shown that MTA HP implanted in the

subcutaneous tissue is biocompatible and has bioactive potential (Delfino *et al.* 2021, Queiroz *et al*. 2023, Inada *et al.* 2023).

Bio-C Repair (BC, Angelus, Londrina, PR, Brazil) is a ready-to-use repair bioceramic cement composed of calcium silicates, tricalcium silicate, in addition to dicalcium silicate, calcium aluminate, calcium oxide, zirconium oxide, iron oxide, silicon dioxide and dispersing agent (Queiroz *et al.* 2023, Inada *et al.* 2023). Despite moderate cytotoxicity due to reduced cell viability (Klein-Junior *et al.* 2021), BC is biocompatible, and this material shows bioactivity in subcutaneous connective tissue (Queiroz *et al.* 2023, Inada *et al.* 2023).

Studies using implantation of dental materials into subcutaneous tissues in rats is a methodology recommended by the Fédération Dentaire International and International Organization for Standardization (Silva *et al.* 2021). This methodology is useful for comparing the degree of injury caused by dental materials (Anderson *et al.* 2008, Silva *et al.* 2017, Fonseca *et al.* 2019, Delfino *et al.* 2020).

The present study aimed to evaluate the inflammatory reaction and the bioactive potential of the new NPutty repair in comparison to BC and MTA HP materials. The null hypothesis was that tissue response induced by the NPutty bioceramic material would not be different from BC and MTA HP materials when implanted in the subcutaneous connective tissue of rats.

MATERIALS AND METHODS

Experimental procedure

The manuscript of this animal study has been written according to Preferred Reporting Items for Animal Studies in Endodontology (PRIASE) 2021 guidelines (Nagendrababu *et al*. 2021). The PRIASE 2021 flowchart is represented in Figure 1.

This study was approved by the Animal Research Ethics Committee (Protocol Nº. 19/2021) in compliance with national legislation 11.794/08 on the use of animals. Twenty-four male Holtzman rats (*Rattus norvegicus albinus*) weighing ± 250-300 g were distributed into 4 groups (n = 6/group) filled with the respective sealers (Table 1) and control group (GC; empty polyethylene tubes). The sample size was estimated according to previous study (Silva *et al.* 2020) to detect a 50% difference among the experimental groups, considering a variability of 20%, test power of 90%, and an alpha error of 0.05 to recognize a significant difference. Thus, 5 rats per group was required at each period. Considering the possibility of animal loss, one animal was

added to each group. The animals were distributed randomly using a rotation system according to the periods: 7, 15, 30, 60 (Figure 1).

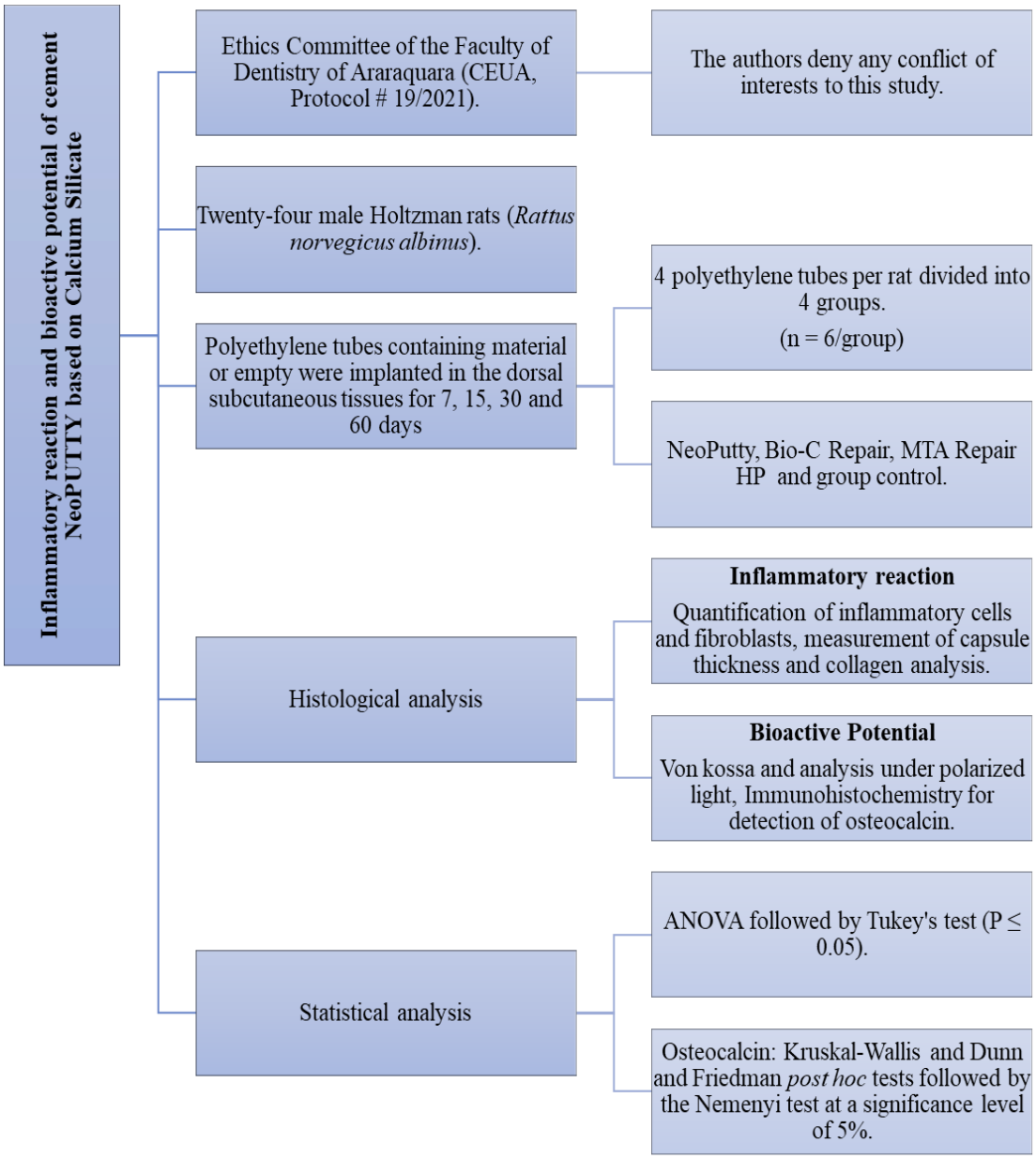

Figure 1 - Flowchart showing experimental design and analyses used to assess biocompatibility and bioactive potential.

The animals were housed in polyethylene cages (40 x 30 x 15 cm) with white pine shavings and maintained in the room under a light-dark 12:12 cycle at controlled temperature (23 ± 2º C) and humidity (55 ± 10%), with food (Guabi rat chow, Paulínia, SP, Brazil) and water provided *ad libitum*.

The materials (Table 1) were inserted into polyethylene tubes (10.0 mm in length and 1.6 mm in diameter) and subsequently implanted in the subcutaneous dorsum of the animals. Four tubes were inserted per animal, one from each group, in a quadrant rotation (ISO-10993-6, 2007). MTA Repair HP was mixed according to the manufacturer's instructions and inserted into the tubes while the ready-to-use sealants were inserted directly, totaling 0.04 g of sealant per tube. Then, these were carefully shaken to avoid failures and the ends were cleaned with gauze to remove excess. When necessary, more material was introduced.

The animals were anesthetized with ketamine hydrochloride (80 mg/kg of body weight; Virbac do Brasil Indústria e Comércio Ltda., São Paulo, SP, Brazil) and xylazine hydrochloride (8 mg/kg of body weight; União Química Farmacêutica Nacional S/A, São Paulo, SP, Brazil) by intraperitoneal route using insulin syringe. The dorsal skin was shaved and disinfected with 5% iodine solution, and an incision (measuring about 2 cm) was made in the cranio-caudal plane. After divulsion, the polyethylene tubes were placed in the dorsal subcutaneous pocket and, immediately, the skin was sutured with simple stitches using 4-0 silk thread (Ethicon Inc., São José dos Campos, São Paulo, Brazil).

After 7, 15, 30, and 60 days, the animals were euthanized with anesthetic overdose, and the portions of skin containing the implants were removed and processed for light microscopy (Figure 1).

Table 1: The Endodontic Sealers Used

Sealers	**Composition**	**Manufacturers**	**Proportion**
NeoPutty	Dicalcium and tricalcium silicate, tantalite, grossite, tricalcium aluminate, calcium sulfate in an organic medium.	NuSmile, Houston, TX	Ready to use
Bio-C Repair	Calcium Silicates, Calcium Aluminate, calcium oxide, zirconium oxide, iron oxide, silicon dioxide and dispersing agent.	Angelus, Londrina, PR, Brazil	Ready to use
MTA Repair HP	Powder: Tricalcium silicate; Dicalcium silicate; Tricalcium	Angelus, Londrina, PR,	1g powder: 300 µL liquid

	aluminate; Calcium oxide; Calcium Tungstate. Liquid: Water and plasticizer.	Brazil

Histological procedures

The implanted polyethylene tubes surrounded by tissues of the subcutaneous were removed and immediately immersed in a 4% formaldehyde solution (freshly prepared from paraformaldehyde) buffered with 0.1 mol/L sodium phosphate at pH 7.2 at room temperature. After 48 h, the samples were dehydrated, treated with xylene, and immersed in liquid paraffin at 60°C for 4 h. The samples were embedded in paraffin to obtain longitudinal sections (6 µm thick), which were obtained using a rotary microtome (Leica, model RM2125 RST) and disposable stainless-steel knives (Leica, model 818). Non-serial sections were stained with hematoxylin and eosin (HE) for morphological and morphometrical analyses (number of inflammatory cells and fibroblasts in the capsules, and the capsule thickness). Other sections were also subjected to the picrosirius-red, von Kossa method, and osteocalcin immunohistochemistry reactions.

Thickness of capsules

The thickness (in µm) of the capsules adjacent to the implanted tubes was measured in three non-serial HE-stained sections of each specimen. Using a camera (DP-71, Olympus - Japan) coupled to a light microscope (Olympus, BX-51, Japan), the images of capsules were obtained at x55 magnification. Capsule thickness was estimated in the middle portion from its surface adjacent to the material to its boundary with adjacent tissues using an image analysis program (Olympus Image-Pro Express 6.0 program, Olympus, Tokyo, Japan). After obtaining the values, the average value was calculated from the measurements obtained in the three sections of each specimen. This measure was obtained in all specimens (n = 6 per group) and in all time points (Delfino *et al.* 2021, Silva *et al.* 2020, Queiroz *et al.* 2023). Capsules exhibiting a thickness greater than 150 µm are classified as thick while capsules with measurements below 150 µm are classified as thin (Yaltirik *et al.* 2004, Delfino *et al.* 2021, Queiroz *et al.* 2023).

Numerical density of inflammatory cells and fibroblasts

Quantitative analysis of inflammatory cells and fibroblasts was performed in the capsules of all implants. In each specimen, the analysis was performed in three non-serial HE-stained sections at x545 magnification. The number of inflammatory cells and fibroblasts was computed using the Olympus Image-Pro Express 6.0 program in a standard field of 0.09 mm^2 of the capsule adjacent to the opening of the implanted tubes. The inflammatory cells (neutrophils, lymphocytes, plasma cells, and macrophages) and fibroblasts were recognized according to morphological characteristics. Inflammatory cells were identified as rounded or ovoid cells containing kidney-shaped nuclei (macrophages), dense nuclei (lymphocytes), nucleus eccentrically located (plasma cells), or multilobulated nuclei (neutrophils) whereas fusiform cells with elliptical nucleus were identified as fibroblasts. In each specimen, the number of inflammatory cells and fibroblasts was computed in a total field of 0.27 mm^2 (Silva *et al.* 2021, Queiroz *et al*. 2023).

Intensity of inflammatory reaction

After obtaining the number of inflammatory cells in the standardized field (x40 objective lens), the intensity of the inflammatory reaction was classified according to the following parameters: mild (capsule containing up to 25 inflammatory cells/field), moderate (capsule containing from 26 to 125 inflammatory cells/field) and severe/intense (capsule containing more than 125 inflammatory cells/field) inflammatory reaction (Yaltirik *et al.* 2004, Delfino *et al.* 2021).

Content of collagen in the capsules

The collagen in the capsule was evaluated in sections stained in 0.1% Sirius-red dissolved in picric acid-saturated solution and analyzed under a light microscope with polarisation filters (Silva *et al*. 2017, Delfino *et al.* 2023, Queiroz *et al.* 2023). In each specimen, three non-serial sections were captured at x695 magnification with rigorously standardized parameters (light intensity, diaphragm opening, condenser position, and exposure time). Afterward, the content of birefringent collagen in the capsules was estimated using image analysis software (ImageJ; National Institutes of Health). The definition of hue considered in birefringence was the following: red/orange, 2–38 and 230–256; yellow, 39-51; and green, 52–128 (de Pizzol-Júnior *et al.* 2018, Queiroz *et al.* 2023). Thus, the amount of collagen was represented by

the percentage of birefringent areas of the total area and calculated using an image analysis program.

Osteocalcin detection

For osteocalcin detection, rabbit anti-mouse osteocalcin antibody (Sigma-Aldrich Co., Saint Louis, Missouri, USA; code SAB1306277) diluted at 1:150 was used. After dewaxing and hydration, the slides were immersed in 0.001 M sodium citrate buffer at pH 6.0 and subjected to microwave treatment at 96-98□C. After cooling, the slides were washed in 0.01 M PBS buffer (pH 7.2) and then immersed in a 5% aqueous solution of hydrogen peroxide. The sections were again washed and incubated with 2% bovine serum albumin (Sigma-Aldrich Co., Saint Louis, Missouri, USA). Then, the sections were incubated overnight in a humidified chamber at 4ºC with an anti-osteocalcin rabbit antibody. After washing in 0.01 M PBS buffer, the sections were incubated for 1 hour in the Labeled StreptAvidin-Biotin kit (Universal Dako LSAB, Dako Inc., Carpinteria, CA, USA; K0675) at room temperature. After washing, the peroxidase activity was revealed by 3,3'-diaminobenzidine chromogen (ImmPACTTM DAB Vector, Burlingame, CA, USA), and the sections were counterstained with Carazzi's hematoxylin. As a negative control, sections were incubated with non-immune serum instead of primary antibody.

The number of immunopositive cells (brown-yellow color) was computed in a standardized field (0.09 mm^2) using an image analysis program (Image-Pro Express 6.0, Olympus, Tokyo, Japan). The number of osteocalcin-immunolabelled cells was performed in all specimens (6 specimens per group at each time point). Thus, the number of immunopositive cells/mm^2 of the capsule was estimated for each specimen.

von Kossa reaction and analysis under polarised light

Three non-serial sections were submitted to the von Kossa reaction for the detection of calcium/phosphate deposits in the capsules. After hydration, the sections were immersed in a cold 5% silver nitrate solution for 1 hour under an incandescent lamp (100 W). The slides were quickly washed in distilled water and then immersed in a 5% sodium hyposulfite solution for 5 min. After washing in distilled water, the sections were stained with picrosirius-red.

Considering that calcite deposits present birefringence (Holland *et al.* 1999, Benetti *et al*. 2019, Delfino *et al.* 2020, Queiroz *et al.* 2023), unstained sections were deparaffinized, mounted in resin medium, and analyzed under polarised illumination (BX-51, Olympus).

Statistical analysis

Statistical analysis was performed using the GraphPad Prism 9.02 software (GraphPad software). The data showed a standard normal variate Quantile-Quantile plot (Q–Q plot). Differences amongst the groups in each period and the differences of each group over time were evaluated by two-way ANOVA analysis followed by the Tukey post-test (GraphPad Prism 5.0 software) at significance level of $P \leq .05$. All data were presented as mean and standard deviation. OCN data were subjected to the non-parametric Kruskal-Wallis test and Dunn's post hoc multiple comparisons test to compare between groups at each time point, while Friedman's test and Nemenyi's post hoc test were used in the analysis throughout. of time.

RESULTS

Morphological findings, capsule thickness, number of inflammatory cells and fibroblasts, and birefringent collagen content

HE-stained sections revealed that capsules around the implanted materials contained inflammatory cells, mainly lymphocytes and macrophages, blood vessels, fibroblasts, and collagen fibres. Although the incidence of inflammatory cells and collagen fibres varied according to material and time point, a predominance of inflammatory cells in comparison with fibroblasts was seen in the capsules of all materials at 7 and 15 days (Figs. 2a-2h). At 30 and 60 days, an evident reduction in the inflammatory cells was observed in capsules around the implants (Figs. 2i-2p). At 60 days, the capsules around BC and MTA HP specimens (Figs. 2n and 2o) contained marked content of collagen bundles and fibroblasts similarly to the CG specimens (Fig. 2p). In contrast, evident presence of inflammatory cells was still observed in the capsules of NPutty specimens (Fig. 2m).

At 7 days, inflammatory reaction induced by materials culminated with thick capsules measuring about 300 µm around repair materials (Table 2). According to Table 2, no significant difference was observed in the capsule thickness among NPutty, BC and MTA HP at 7 days. However, the capsules around NPutty were

significantly thicker than in BC and MTA HP at 15, 30 and 60 days. In these periods, significant differences were not observed between BC and MTA HP in the capsule thickness. In all time points, the capsules of CG specimens were thinner than those around the materials. From 7 to 60 days, significant reduction in the thickness of capsules was seen in all groups. However, the capsules around NPutty specimens measured around 198 µm while in the BC and MTA HP the capsules measured about 146 µm and 132 µm, respectively.

The quantitative analysis (Table 2) revealed that, in all periods, the capsules around NPutty specimens contained a greater number of inflammatory cells than in other groups ($P < 0.0001$). At 7 and 15 days, the number of inflammatory cells was significantly greater in the BC than in MTA HP specimens ($P < 0.0001$) whereas, at 30 and 60 days, significant differences between these groups were not seen. A significant reduction in the number of inflammatory cells was observed in all groups over time. Regarding fibroblasts (Table 2), capsules around NPutty exhibited the lowest values of fibroblasts in comparison with BC and MTA HP in all time points, except at 15 days. In this period, significant difference in the number of fibroblasts was not seen between NPutty and BC ($P > 0.05$). A gradual and significant increase in the number of fibroblasts was found in the capsules of all the groups over time. In all periods, the number of fibroblasts was significantly greater in the CG specimens than in capsules around bioceramic materials.

In all time points, picrosirius red-stained sections analysed under polarised illumination revealed birefringent collagen fibres in the capsules of all groups (Figs. 3a-3p). In all periods, significant differences were not found in the content of birefringent collagen among NPutty, BC and MTA HP. The highest percentage of birefringent collagen was observed in the capsules around CG specimens, in all time points (Table 2).

Immunohistochemical detection of osteocalcin (OCN)

The sections subjected to the immunohistochemistry for OCN detection revealed cytoplasmic immunolabelling (in brown yellow colour) in some cells of capsules around NPutty, Bio-Repair and MTA HP materials (Figs. 4a-c, 4e-g, 4i-4k, 4m-4o). In contrast, immunolabelling was not seen in the capsules of CG specimens (Figs. 4d, 4h, 4i, 4p). None immunolabelled cell was found in the sections used as negative control (data not shown).

Quantitative analysis (Table 2) revealed that no significant difference in the number of OCN-immunolabelled cells was observed among NPutty, BC and MTA HP specimens. Although at 30 days significant difference in the immunoexpression of OCN in the capsules of NPutty and BC was not observed, after 60 days of implantation, the number of immunolabelled cells was significantly greater in the BC and MTA HP than in NPutty specimens ($P < 0.0001$). Moreover, no significant difference between BC and MTA HP was detected at 60 days. The capsules around all materials showed gradual increase in the number of OCN-immunolabelled cells over time.

Figure 2 – HE-stained sections

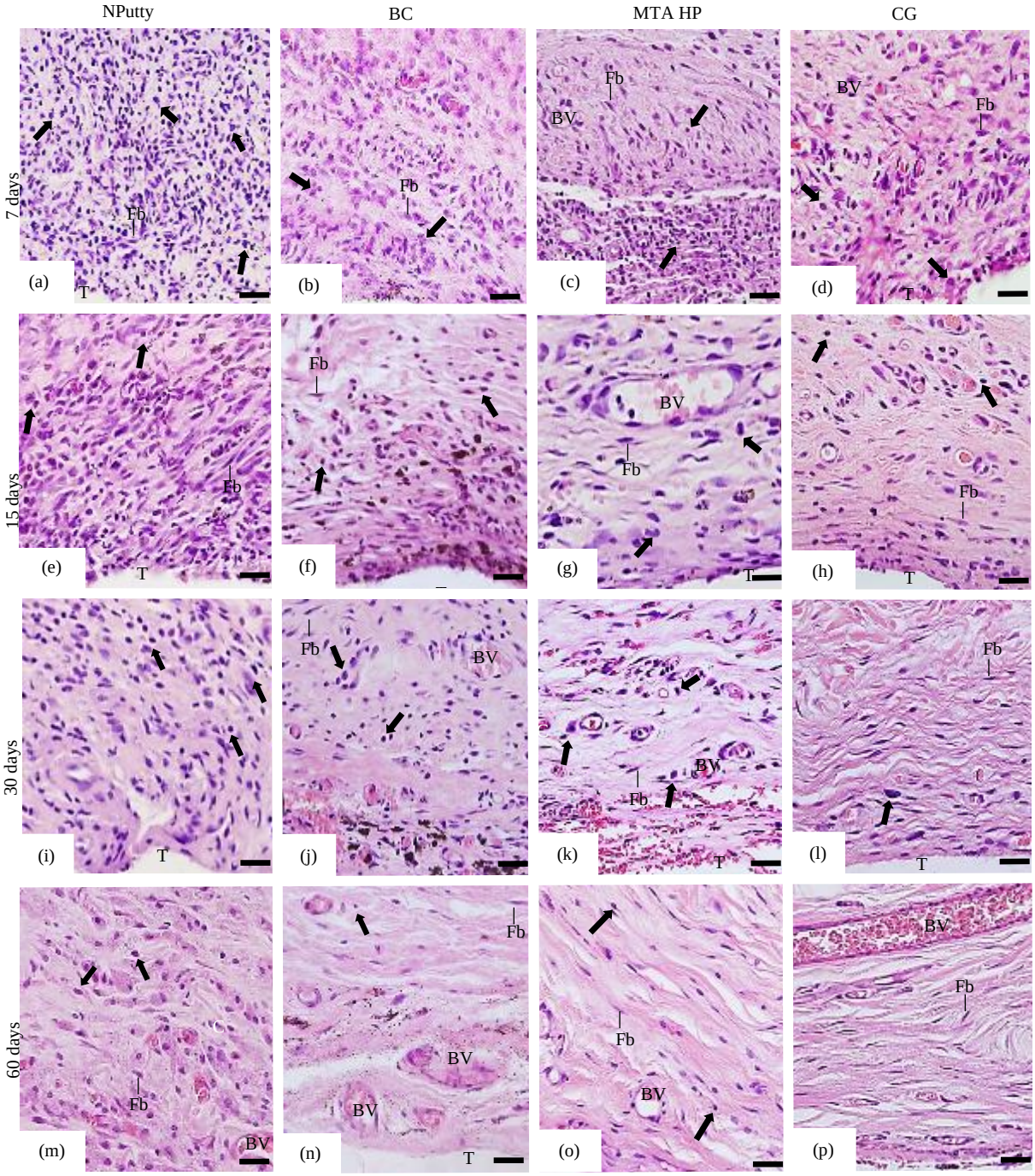

Figure 2: Light micrographs showing portions of sections of capsules adjacent to the implanted tubes (T) after 7 (a-d), 15 (e-h), 30 (i-l), and 60 days (m-p). Arrows, inflammatory cells; Fb, fibroblasts; CF, collagen fibers; BV, blood vessels. NPutty (NuSmile, USA), BC (Angelus, Brazil) and MTA HP (Angelus, Brazil). GC (group control). Bars: 18 µm.

Figure 3: Sections stained with picrosirius Red.

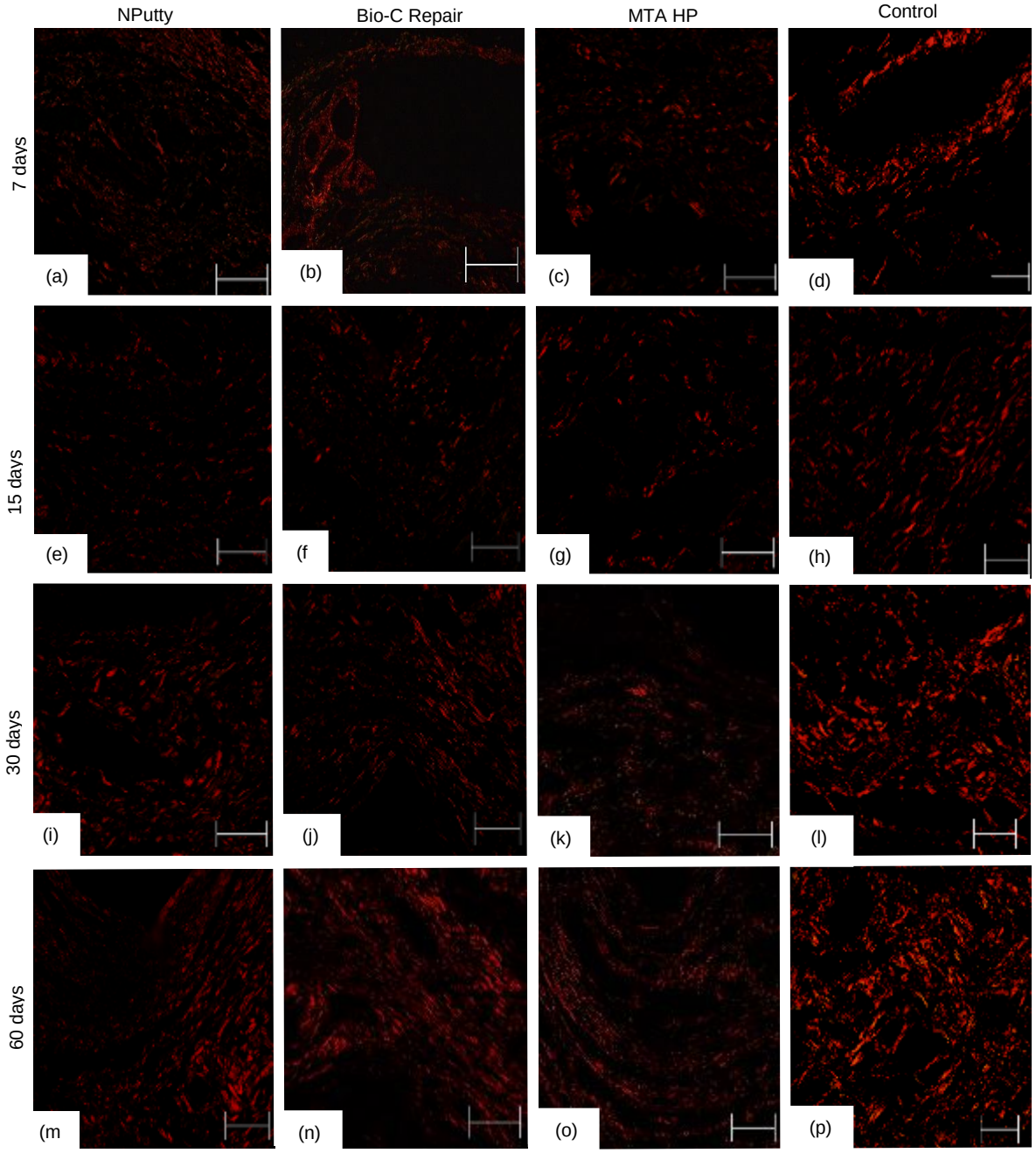

Figure 3 - Light micrographs showing portions of sections of capsules adjacent to the implanted tubes after 7 (a-d), 15 (e-h), 30 (i-l), and 60 (m-p) days of implantation. Sections were stained with picrosirius-red and photographed under polarised light. Birefringent collagen fibers are mainly seen in red color. NPutty (NuSmile, USA), BC (Angelus, Brazil) and MTA HP (Angelus, Brazil). GC (group control). Bars: 20 µm.

Table 2 - Capsule thickness (CT, µm), number of inflammatory cells (IC) and fibroblasts per mm^2 and number of osteocalcin-immunolabelled cells per mm^2 (OCN/ mm^2), percentage of collagen (CF) and inflammatory reaction intensity (IR) in the capsules around the NPutty, BC, MTA HP and Control Group (GC) after 7, 15, 30 and 60 days. Mean (standard deviation).

Periods		NPutty	BC	MTA HP	CG
7 days	CT (µm)	331 ± 12$^{a; A}$	312 ± 26$^{a; A}$	307 ± 22$^{a; A}$	149 ± 86$^{b; A}$
	IC/mm^2	1389 ± 24$^{a; A}$	972 ± 13$^{b; A}$	689 ± 30$^{c; A}$	251 ± 35$^{d; A}$
	Fb/mm^2	91±14$^{a; A}$	128 ± 11$^{b;}$ A	104 ± 12 $^{b; A}$	168 ± 10$^{c; A}$
	CF (%)	19±11$^{a; A}$	21.8 ± 3$^{a; A}$	22 ± 4$^{a; A}$	25.9 ± 3$^{b; A}$
	OCN/mm^2	12.12(12.12) $^{a; A}$	11.11(11.11) $^{a; A}$	11.11(11.11) $^{a; A}$	0.00(0.0) $^{b; A}$
	IR	intense	intense	moderate	mild
15 days	CT (µm)	311 ± 22$^{a; A}$	282 ± 11$^{b; B}$	241 ± 20$^{b; B}$	189 ± 11$^{c; A}$
	IC/mm^2	1153 ± 14$^{a; B}$	862 ± 30$^{b; A}$	590 ± 22$^{c; B}$	231 ± 15$^{d; A}$
	Fb/mm^2	106 ± 6 $^{a; B}$	178 ± 16 $^{a; A}$	203 ± 2 $^{b; B}$	236 ± 21 $^{b; B}$
	CF (%)	20 ±8$^{a; A}$	22 ± 2$^{a; A}$	23 ± 4$^{a; A}$	31 ± 5 $^{b; B}$
	OCN/mm^2	19.19(19.19) $^{a; A}$	11.11(11.11) $^{b; A}$	22.22(22.22) $^{a; A}$	0.00 (0.0) $^{c; A}$
	IR	intense	moderate	moderate	mild
30 days	CT (µm)	301 ± 17$^{a; A}$	206 ± 11$^{b; B}$	209 ± 24$^{b; B}$	107 ± 04$^{c, A}$
	IC/mm^2	933 ± 22$^{a; C}$	372 ± 37$^{b; B}$	309 ± 12$^{b; C}$	176 ± 25$^{c, B}$
	Fb/mm^2	233±09 $^{a; C}$	302 ± 9 $^{b; B}$	304 ± 10 $^{b; C}$	381 ± 23 $^{c; C}$
	CF (%)	23 ±6$^{a; A}$	23 ± 1 $^{a; A}$	25 ± 3 $^{a; A}$	31.9 ± 3 $^{b; B}$
	OCN/mm^2	19.19(19.19) $^{a; A}$	22.22(22.22) $^{a; A}$	44.44 (33.34) $^{b; B}$	0.00 (0.0) $^{c; A}$
	IR	intense	moderate	moderate	mild
60 days	CT (µm)	198 ± 11$^{a; B}$	146 ± 6$^{b; C}$	132 ± 22$^{b; C}$	104 ± 20$^{c, A}$
	IC/mm^2	590 ± 23$^{a; C}$	246 ± 42$^{b; C}$	198 ± 27$^{c; D}$	68 ± 11$^{d, C}$
	Fb/mm^2	318±23 $^{a; D}$	429 ± 27 $^{b; C}$	488 ± 12 $^{b; D}$	583 ± 23 $^{c; D}$
	CF (%)	27 ±5$^{a; B}$	28 ± 1 $^{a; A}$	29.8 ± 1 $^{a; B}$	33.4 ± 1 $^{b; A}$
	OCN/mm^2	22.22(22.22) $^{a; B}$	44.44(22.22) $^{b; B}$	55.56 (33.34) $^{b; B}$	0.00 (0.0) $^{c; A}$
	IR	moderate	mild	mild	mild

Mean (standard deviation).
The comparison between groups in the same period is indicated by superscript letters in the lines, same letters = no statistically significant difference.
The comparison between periods in the same group is indicated by superscript numbers in the columns; same numbers = no statistically significant difference. Tukey test ($p \leq 0.05$).
OCN: Values expressed as median and interquartile range. Analysis between groups in each period: Kruskal-Wallis followed by the Dunn test; analysis of each group over time: Friedman followed by the Nemenyi test ($p < 0.05$)

Figure 4 – Immunohistochemistry for osteocalcin detection.

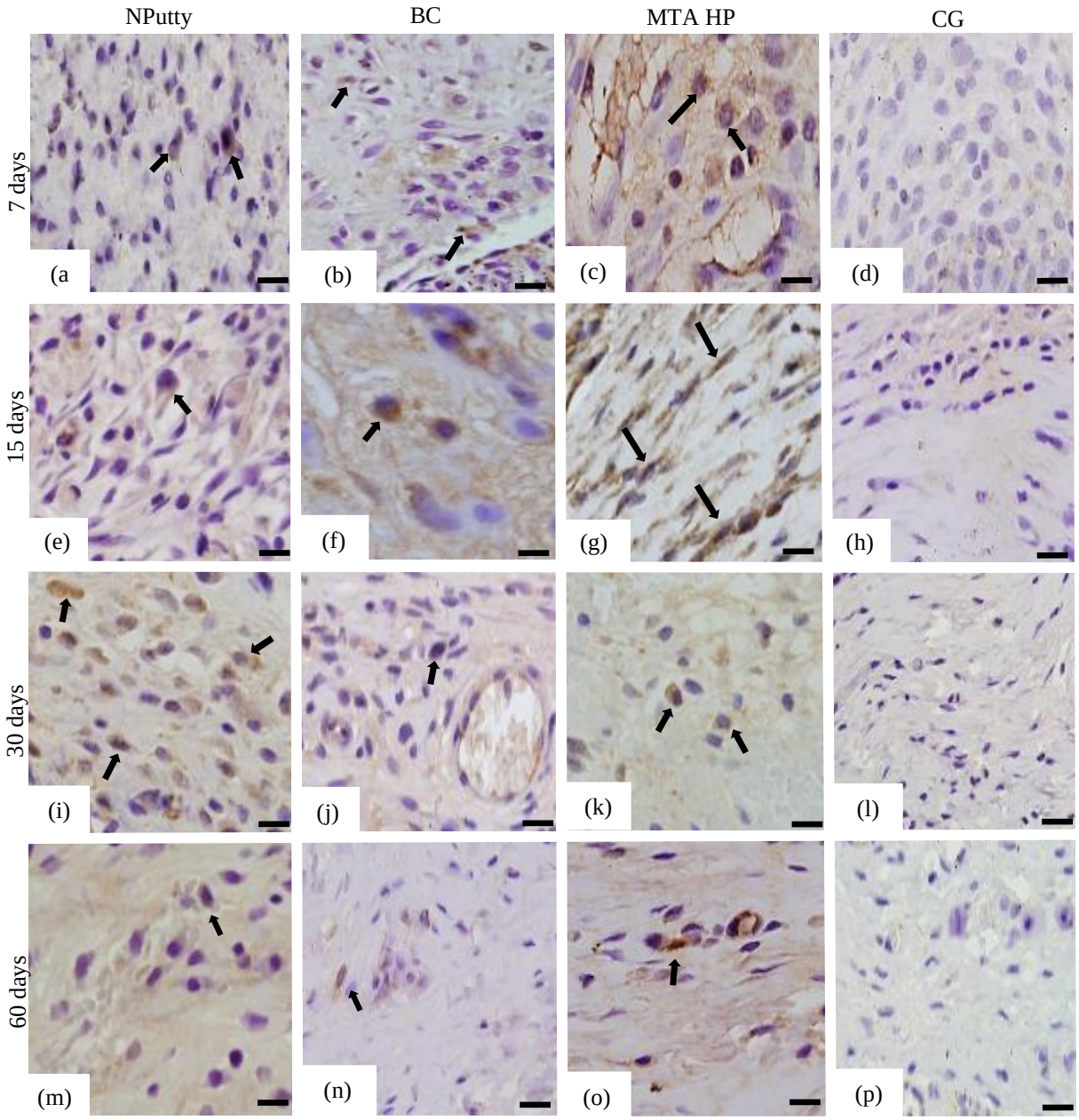

Figure 4 - Light micrographs showing portions of capsules adjacent to the implanted tubes after 7 (a-d), 15 (e-h), 30 (i-l), and 60 days (m-p). Sections were submitted to immunohistochemistry for OCN detection and counterstained with hematoxylin. OCN-immunolabelled cells (arrows) are seen in the capsules of NPutty, BC, and MTA HP. NPutty (NuSmile, USA), BC (Angelus, Brazil) and MTA HP (Angelus, Brazil). GC (group control). Bars: 18 µm.

von Kossa reaction and analysis under polarised light

von Kossa-positive structures (black/brown colour) were present in the capsules around NPutty, BC and MTA HP materials (Figs. 5a-5c; 5i-5k). Furthermore, unstained sections analyzed under polarised light revealed birefringent structures in regions compatible with the results obtained with von Kossa (Figs. 5d-5f; 5m-5o). von Kossa-positive structures and birefringent deposits were not found in the CG capsules (data not shown).

Figure 5: von Kossa and birefringent structures in unstained sections.

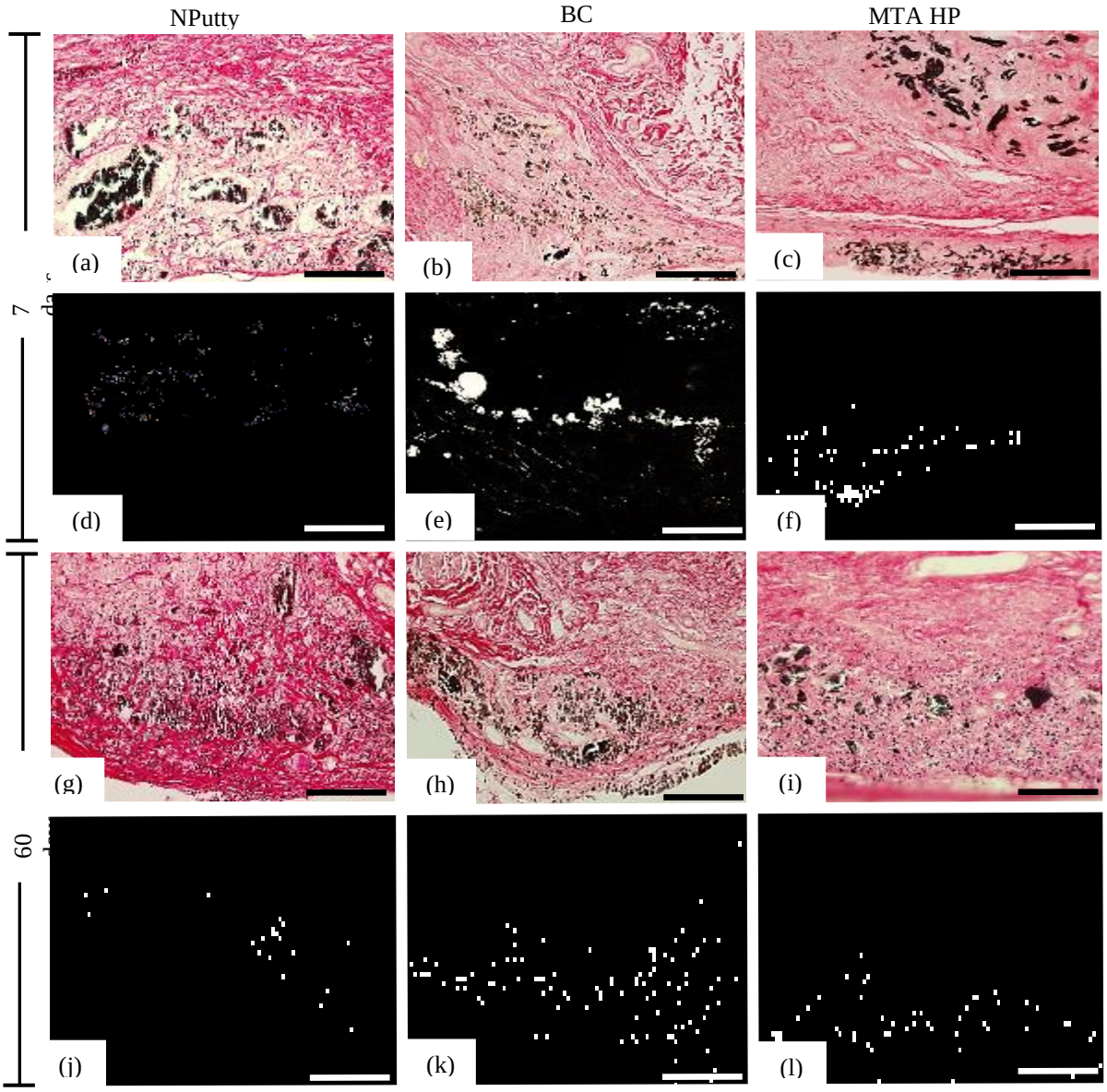

Figure 5 - Photomicrographs of sections showing portions of capsules subjected to the von Kossa reaction after 7 (a-c) and 60 days (g-i). von Kossa-positive structures (black-brown color) are observed in the capsules of NPutty, BC, and MTA HP specimens. NPutty (NuSmile, USA), BC (Angelus, Brazil)

and MTA HP (Angelus, Brazil). GC (group control). Unstained sections analyzed under polarized light demonstrate birefringent structures in the capsules after 7 (d-f) and 60 (i-l) days. Bars: 36 µm.

DISCUSSION

In the present study, histological analyses were used to assess the initial inflammatory response the regression of this process, and the bioactive potential promoted by repair materials for up to 60 days. The null hypothesis was rejected because NPutty repair material presented the highest inflammatory potential compared to BC and MTA HP materials in the connective tissue of rats subcutaneously.

Calcium silicate-based materials implanted in the subcutaneous connective tissue initially stimulate the recruitment of inflammatory cells next to the materials (Silva *et al.* 2015, Delfino *et al.* 2021, Silva *et al.* 2021, Queiroz *et al*. 2023). The degree of inflammatory reaction induced is associated with the chemical composition and physical properties of materials. NPutty induced recruitment of several inflammatory cells than BC and MTA HP in all time points. The recruitment of inflammatory cells is usually associated with alkaline pH provided by bioceramic materials in contact with tissue fluids and, the release of calcium and other substances, as dispersing agents. Saber *et al.* (2023) demonstrated that the pH of Neoputty decreases over time (pH between 8 and 9) and is lower than that of Biodentine. The pH of MTA HP is around 9.3 (Queiroz e*t al*. 2021) while BC showed 7.0 (Oliveira *et al.* 2021). Therefore, our findings suggest that other substances could be responsible for different patterns in the recruitment of inflammatory cells by NPutty in comparison with BC and MTA HP.

The inflammatory reaction caused by NPutty until on 30th may be related to some substance present in the “organic medium”. Although the components of “organic medium” were not reported by the manufacturer, often the plasticizer agents contain calcium chloride and methylparaben. It has been suggested that methylparaben, one of the substances in the liquid of BC (Lima *et al.* 2020) might be responsible for the initial damage caused by this repair material in comparison with MTA HP (Queiroz *et al*. 2023). Although organic substances improve the plasticity of the repair materials (Silva *et al.* 2016, Guimarães *et al*. 2018, Tomás-Catalá *et al.* 2018, Benetti *et al*. 2019, ElReash *et al.* 2019, Ferreira *et al.* 2019), these substances may be initially irritant to cells and tissues. Moreover, the plasticizers may also interfere with the

setting time of the materials increasing the period of releasing substances in the microenvironment culminating in prolonged injury to the tissues and, consequently, delaying the tissue repair. This hypothesis is supported by the highest values of inflammatory cells and the lowest number of fibroblasts observed in the capsules around NPutty specimens at 60 days.

NPutty induced an intense inflammatory reaction and promoted the formation of thicker capsules than BC and MTA HP after 60 days of implantation. Moreover, the greater number of inflammatory cells was accompanied by a lower number of fibroblasts in the capsules around NPutty, supporting the hypothesis that NPutty repair material caused a delay in the reestablishment of structural integrity of connective tissue. In human dental pulp cells (hDPCs), NeoPUTTY demonstrated lower cell viability than MTA Angelus and the control group, suggesting low cytocompatibility (Lozano-Guillén *et al.* 2022).

Despite the delay in the rearrangement of connective tissue around the NPutty, the reduction in the number of inflammatory cells and thickness of capsules concomitantly to the increase in the number of fibroblasts are suggestive parameters of regression in the connective tissue damage over time (Delfino *et al.* 2021, Queiroz *et al.* 2023). In fact, from 30 to 60 days a significant reduction in the number of inflammatory cells in the capsules around NPutty specimens culminated in the characterization of a moderate inflammatory reaction.

NPutty has tantalum oxide (Ta_2O_5) as a radiopacifying agent. It is known that radiopacifying agents may interfere with the chemical and physical properties of dental materials (Silva *et al*. 2015, Lozano-Guillén *et al.* 2022). However, NeoMTA Plus, a calcium silicate-based material that contains tantalum oxide as a radio pacifier, presented biocompatibility and bioactive potential (Hoshino *et al*. 2021).

Tricalcium silicate-based materials are used for regeneration and repair procedures in endodontics due to their bioactivity. The bioactivity is related to the hydration reaction of tricalcium and dicalcium silicates, promoting the formation of calcium silicate hydrate and calcium hydroxide (Silva *et al.* 2020, Camilleri, 2020, Queiroz *et al*. 2023). Calcium hydroxide dissociates into Ca^{+2} and OH^- promoting an alkalinization of the microenvironment (Niu *et al.* 2014). Furthermore, calcium supersaturation in the extracellular fluid can result in calcium precipitation stimulating apatite nucleation (Bonewald *et al.* 2003, Ding *et al.* 2009). In phosphate-containing solutions, bioceramic materials promote the formation of amorphous calcium

phosphate (ACP). ACP has biological importance as it represents the main precursor phase of calcium phosphate that precedes the biological formation of apatite in osteogenesis (Niu *et al.* 2014).

The calcium phosphate precipitation is under the control of several mediators such as alkaline phosphatase (ALP), bone sialoprotein, osteopontin, and OCN. ALP is an enzyme highly expressed during the differentiation of matrix-producing cells from mineralized tissues (Zordan-Bronzel *et al.* 2019, Delfino *et al.* 2021, da Silva Sasso *et al*. 2021, Zordan-Bronzel *et al.* 2021) and participates in the phosphate (Pi) production from pyrophosphate (Bellows *et al.* 1991, Register *et al.* 1986, Daltoé *et al*. 2016). ALP-immunolabelled cells in close juxtaposition to von Kossa-positive structures were observed in the capsules around Bio-C Pulpo, MTA AH, and MTA-Angelus suggesting the bioactive potential of these bioceramic materials (Delfino *et al*. 2021).

Another protein synthetized by cells of mineralized tissues is OCN which constitutes one of the main non-collagenous components of the bone matrix (Nefussi *et al.* 1997, Sodek & Mckee, 2000). Since osteocalcin interacts with calcium from hydroxyapatite, it has been suggested that this protein has an essential role in the alignment of apatite crystals with the collagen fibrils (Manolagas, 2020) controlling therefore the growth of hydroxyapatite (Moreira *et al.* 2013). In the present study, OCN-immunolabelled cells were observed in the capsules of bioceramic materials suggesting a bioactive potential of the materials evaluated. However, a varied pattern in the immunoexpression of osteocalcin was seen among the bioceramic materials, particularly, in the NPutty in comparison with BC and MTA HP specimens at 60 days. In this period, immunoexpression of OCN was reduced in the capsules of NPutty suggesting that delay in the regression of inflammatory reaction and the repair of connective tissue may interfere with the bioactivity of bioceramic materials. Moreover, it is possible that the new bioceramic material – NeoPUTTY – releases slower calcium ions and, consequently, exerts a subtle inducing role in connective tissue cells compared to other bioceramic materials. In addition to immunoexpression of OCN, von Kossa structures were also seen in the capsules around bioceramic materials, including the NPutty, suggesting the presence of calcium/phosphate deposits in these capsules (Viola *et al*. 2012, Silva *et al*. 2015, Hoshino *et* al. 2021, Delfino *et al*. 2021, Queiroz *et al*. 2023).

Calcium silicate-based materials release calcium ions during setting reactions (Niu *et al.* 2014, Silva *et al*. 2015, Bosso-Martelo *et al.* 2016; Camilleri, 2020). A bioactive material promotes an environment compatible with osteogenesis and tissues through the development of an interface between living and non-living materials (Niu *et al.* 2014).

Therefore, von Kossa-positive structures were observed in the capsules around the bioceramic materials implanted in the subcutaneous connective tissue. However, the presence of birefringent deposits detected by polarised illumination from unstained sections strongly suggest the formation of amorphous calcite (calcium carbonate), which originates from reaction of calcium released by bioceramic materials with carbonate dioxide of tissue fluids (Holland *et al.* 1999, Camilleri *et al.* 2014, Cintra *et al.* 2017, Bueno *et al*. 2019, Delfino *et al.* 2021; Queiroz *et al*. 2023).

The von Kossa histochemical method promotes a reaction with phosphate in calcium deposits, which may be associated with cations other than calcium. However, significant amounts of calcium ions are released by calcium silicate-based materials. Calcium ions released into the microenvironment may be responsible, at least in part, for the bioactive behavior of these materials (Queiroz *et al*. 2023). Therefore, the immunoexpression of OCN, von Kossa-positive structures, and the presence of amorphous calcite are suggestive that bioceramic NPutty material presents bioactive potential. Additional studies of the biological properties of Neoputty are needed, in addition to clinical studies.

CONCLUSION

The findings taken together indicate that NeoPutty is biocompatible, although the irritant potential this bioceramic material in the connective tissue is higher than the Bio C Repair and MTA HP. Moreover, the immunoexpression of osteocalcin by connective tissue cells as well as von Kossa-positive structures and birefringent deposits are suggestive parameters that NeoPutty exhibits bioactive potential.

CONFLICT OF INTEREST

The authors have stated explicitly that there are no conflicts of interest in connection with this article.

REFERENCES

Alves- Silva ECA, Tanomaru-Filho M, da Silva GF, Delfino MM, Cerri PS, Guerreiro-Tanomaru JM. (2020) Biocompatibility and bioactive potential of new calcium silicate–based endodontic sealers: Bio-C Sealer and Sealer Plus BC. *Journal of Endodontics* **46**, 1470-1477.

Alqahtani AS, Alsuhaibani NN, Sulimany AM, Bawazir OA (2023). NeoPUTTY® versus NeoMTA 2® as a pulpotomy medicament for primary molars: a randomized clinical trial. *Pediatr Dent.* **15**;45(3):240-244.

Anderson JM, Rodriguez A, Chang DT. (2008) Foreign body reaction to biomaterials. *Seminars in Immunology* **20,** 86-100.

Benetti F, Queiroz ÍOA, Cosme-Silva L, Conti LC, de Oliveira SHP, Cintra LTA. (2019) Cytotoxicity, the biocompatibility of a new ready-for-use bioceramic repair material. *Brazilian Dental Journal* **30**, 325–332.

Bellows CG, Aubin JE, Heersche JNM. (1991) Initiation and progression of mineralization of bone nodules formed in vitro: the role of alkaline phosphatase and organic phosphate. *Bone and Mineral **14***, 27-40.

Bonewald LF, Harris SE, Rosser J, Dallas MR, Dallas SL, Camacho NP. et al. (2003) von Kossa staining alone is not sufficient to confirm that mineralization in vitro represents bone formation. *Calcified Tissue International* **72**, 537–547.

Bosso-Martelo R, Guerreiro-Tanomaru JM, Viapiana R, Berbert FL, Duarte MA, Tanomaru-Filho M. (2016) Physicochemical properties of calcium silicate cements associated with microparticulate and nanoparticulate radiopacifiers. *Clinical Oral Investigations* **20,** 83–90.

Bueno, C. R. E., Vasques, A. M. V., Cury, M. T. S., Sivieri-Araújo, G., Jacinto, R. C., Gomes-Filho, J. E., ... & Dezan-Júnior, E. (2019). Biocompatibility and biomineralization assessment of mineral trioxide aggregate flow. *Clinical Oral Investigations* **23**, 169-177.

Camilleri J. (2020) Classification of hydraulic cement used in dentistry. *Frontiers in Dental Medicine* **1**, 9. Available from: https://doi.org/10.3389/fdmed.2020.00009

Camilleri J, Grech L, Galea K, Keir D, Fenech M, Formosa L, *et al*. (2014) Porosity and root dentine to material interface assessment of calcium silicate-based root-end filling materials. *Clinical Oral Investigations* **18,** 1437–1446.

Cintra LTA, Benetti F, de Azevedo Queiroz ÍO, Ferreira LL, Massunari L, Bueno CRE, Gomes-Filho JE. (2017) Evaluation of the cytotoxicity and biocompatibility of new resin epoxy–based endodontic sealer containing calcium hydroxide. *Journal of Endodontics* **43**, 2088-2092.

da Fonseca TS, da Silva GF, Tanomaru-Filho M, Sasso-Cerri E, Guerreiro-Tanomaru JM, Cerri PS. (2016) In vivo evaluation of the inflammatory response and IL-6 immunoexpression promoted by Biodentine and MTA Angelus. *International Endodontic Journal* **49**, 145–153.

da Fonseca TS, Silva GF, Guerreiro-Tanomaru JM, Delfino MM, Sasso-Cerri E, Tanomaru-Filho M, Cerri PS. (2019) Biodentine and MTA modulate immunoinflammatory response favoring bone formation in sealing of furcation perforations in rat molars. *Clinical Oral Investigations* **23**, 1237-1252.

Daltoé MO, Paula-Silva FWG, Faccioli LH, Gatón-Hernández PM, De Rossi A, Silva LAB. (2016). Expression of mineralization markers during pulp response to Biodentine and Mineral Trioxide Aggregate. *Journal of Endodontics* **42,** 596-603.

da Silva Sasso, G. R., Florencio-Silva, R., Sasso-Cerri, E., Gil, C. D., de Jesus Simões, M., & Cerri, P. S. (2021). Spatio-temporal immunolocalization of VEGF-A, Runx2, and osterix during the early steps of intramembranous ossification of the alveolar process in rat embryos. *Developmental Biology* **478**, 133-143.

Delfino MM, Guerreiro-Tanomaru JM, Tanomaru-Filho M, Sasso-Cerri E, Cerri PS. (2020) Immunoinflammatory response and bioactive potential of GuttaFlow bioseal and MTA Fillapex in the rat subcutaneous tissue. *Scientific Reports* **10,** 7173.

Delfino MM, de Abreu Jampani JL, Lopes CS, Guerreiro-Tanomaru JM, Tanomaru-Filho M, Sasso-Cerri E, *et al.* (2021) Comparison of Bio-C Pulpo and MTA repair HP with White MTA: effect on liver parameters and evaluation of biocompatibility and bioactivity in rats. *International Endodontic Journal* **54,** 1597–1513.

Delfino, M. M., Jampani, J. L. D. A., Lopes, C. S., Guerreiro-Tanomaru, J. M., Tanomaru-Filho, M., Sasso-Cerri, E., & Cerri, P. S. (2023). Participation of fibroblast growth factor-1 and interleukin-10 in connective tissue repair following subcutaneous implantation of bioceramic materials in rats. *International Endodontic Journal* **56**(3), 385-401.

de Pizzol Júnior, J. P., Sasso-Cerri, E., & Cerri, P. S. (2018). Matrix metalloproteinase-1 and acid phosphatase in the degradation of the lamina propria of eruptive pathway of rat molars. *Cells* **7**(11), 206.

Ding SJ, Shie MY, Wang CY. (2009) Novel fast-setting Calcium silicate bone cement with high bioactivity and enhanced osteogenesis in vitro. *Journal of Materials Chemistry* 1**9**, 1183–1190.

ElReash AA, Hamama H, Abdo W, Wu Q, El-Din AZ, Xiaoli X. (2019) Biocompatibility of new bioactive resin composite versus calcium silicate cement: an animal study. *BMC Oral Health* **19,** 194.

Ferreira C, Sassone LM, Gonçalves AS, de Carvalho JJ, Tomás-Catalá CJ, García-Bernal D, *et al.* (2019) Physicochemical, cytotoxicity and in vivo biocompatibility of a high-plasticity calcium-silicate based material. *Scientific Reports* **9,** 3933.

Guimarães BM, Prati C, Duarte M, Bramante CM, Gandolfi MG. (2018) Physicochemical properties of calcium silicate-based formulations MTA Repair HP and MTA Vitalcem. *Journal of Applied Oral Science* **26**, e2017115.

Holland R, de Souza V, Nery MJ, Otoboni Filho JA, Bernabé PFE, Dezan Jr, E. (1999). Reaction of dogs' teeth to root canal filling with mineral trioxide aggregate or a glass ionomer sealer. *Journal of Endodontics* **25,** 728-730.

Hoshino, R. A., Delfino, M. M., da Silva, G. F., Guerreiro-Tanomaru, J. M., Tanomaru-Filho, M., Sasso-Cerri, E., & Cerri, P. S. (2021). Biocompatibility and bioactive potential of the NeoMTA Plus endodontic bioceramic-based sealer. *Restorative Dentistry & Endodontics* **46(**1).

Inada RNH, Queiroz MB, Lopes CS, Silva ECA, Torres FFE, da Silva GF *et al.* (2023) Biocompatibility, bioactive potential, porosity, and interface analysis calcium silicate repair cement in a dentin tube model. *Clinical Oral Investigations*, 1-15.

ISO10993-6. International Organization for Standardization: Biological evaluation of medical devices, 2016.

Klein-Junior CA, Zimmer R, Dobler T, Oliveira V, Marinowic DR, Özkömür A, Reston EG. (2021) Cytotoxicity assessment of Bio-C Repair ion^{+}: A new calcium silicate-based cement. *Journal of Dental Research, Dental Clinics, Dental Prospects* **15,** 152.

Lima SPR, Santos GLD, Ferelle A, Ramos SP, Pessan JP, Dezan-Garbelini CC. (2020) Clinical and radiographic evaluation of a new stain-free tricalcium silicate cement in pulpotomies. *Brazilian Oral Research* **34,** e102.

Lozano-Guillén A, López-García S, Rodríguez-Lozano FJ, Sanz JL, Lozano A, Llena C, Forner L. (2022) Comparative cytocompatibility of the new calcium silicate-based cement NeoPutty versus NeoMTA Plus and MTA on human dental pulp cells: an in vitro study. *Clinical Oral Investigations* **26,** 7219-7228.

Manolagas SC. (2020) Osteocalcin promotes bone mineralization but is not a hormone. *PLoS Genetics* **16,** e1008714.

Moreira P, Genari SC, Goissis G, Galembeck F, An YH, Santos Jr,AR. (2013) Bovine osteoblasts cultured on polyanionic collagen scaffolds: an ultrastructural and immunocytochemical study. *Journal of Biomedical Materials Research Part B: Applied Biomaterials* **101**, 18-27.

Nagendrababu V, Kishen A, Murray PE, Nekoofar MH, de Figueiredo JAP, Priya E, Dummer PMH. (2021) PRIASE 2021 guidelines for reporting animal studies in Endodontology: a consensus-based development. *International Endodontic Journal* **54**, 848-857.

Nefussi JR, Brami G, Modrowski D, Obcuf M, Forest N. (1997) Sequential expression of bone matrix proteins during rat calvaria osteoblast differentiation and bone nodule formation in vitro. *Journal of Histochemistry & Cytochemistry* **45,** 493-503.

Niu LN, Jiao K, Zhang W, Camilleri J, Bergeron BE, Feng HL, Tay FR. (2014) A review of the bioactivity of hydraulic calcium silicate cements. *Journal of Dentistry* **42**, 517-533.

Oliveira LV, de Souza GL, da Silva GR, Magalhães TE, Freitas GA, Turrioni AP. et al. (2021) Biological parameters, discolouration and radiopacity of calcium silicate-based materials in a simulated model of partial pulpotomy. *International Endodontic Journal* **54**, 2133–2144.

Queiroz MB, Torres FFE, Rodrigues EM, Viola KS, Bosso-Martelo R, Chavez-Andrade GM, Tanomaru-Filho M. (2021) Physicochemical, biological, and antibacterial evaluation of tricalcium silicate-based reparative cements with different radiopacifiers. *Dental Materials* **37**, 311-320.

Queiroz MB, Inada RN, Jampani JLDA, Guerreiro-Tanomaru JM, Sasso-Cerri E, Tanomaru-Filho M, Cerri PS. (2023) Biocompatibility and bioactive potential of an experimental tricalcium silicate-based cement in comparison with Bio-C repair and MTA Repair HP materials. *International Endodontic Journal* **56**, 259-277.

Queiroz, M. B., Inada, R. N. H., Lopes, C. S., Guerreiro-Tanomaru, J. M., Sasso-Cerri, E., Tanomaru-Filho, M., & Cerri, P. S. (2022). Bioactive potential of Bio-C Pulpo is evidenced by presence of birefringent calcite and osteocalcin immunoexpression in the rat subcutaneous tissue. *Journal of Biomedical Materials Research Part B: Applied Biomaterials* **110**(10), 2369-2380.

Register TC, McLean FM, Low MG, Wuthier RE. (1986) Roles of alkaline phosphatase and labile internal mineral in matrix vesicle-mediated calcification. Effect of selective release of membrane-bound alkaline phosphatase and treatment with isosmotic pH 6 buffer. *Journal of Biological Chemistry*, **261** 9354-9360.

Saber SM, Gomaa SM, Elashiry MM, El-Banna A, Schäfer E. (2023). Comparative biological properties of resin-free and resin-based calcium silicate-based endodontic repair materials on human periodontal ligament stem cells. *Clinical Oral Investigations*, 1-12.

Silva ECA, Tanomaru-Filho M, Silva GF, Lopes CS, Cerri PS, Guerreiro-Tanomaru, JM. (2021) Evaluation of the biological properties of two experimental calcium silicate sealers: an in vivo study in rats. *International Endodontic Journal* **54,** 100–111.

Silva GF, Guerreiro-Tanomaru JM, da Fonseca TS, Bernardi MIB, Sasso-Cerri E, Tanomaru-Filho M, *et al.* (2017) Zirconium oxide and niobium oxide used as radio pacifiers in a calcium silicate-based material stimulate fibroblast proliferation and collagen formation. *International Endodontic Journal* **50,** e95–e108.

Silva GF, Tanomaru-Filho M, Bernardi MIB, Guerreiro-Tanomaru JM, Cerri PS. (2015) Niobium pentoxide as a radiopacifying agent of calcium silicated-based material: evaluation of physicochemical and biological properties. *Clinical Oral Investigations* **19**, 2015–2025.

Silva EJNL, Carvalho NK, Senna PM, De-Deus G, Zuolo ML, Zaia AA. (2016) Push-out bond strength of MTA HP, a new high-plasticity calcium silicate-based cement. *Brazilian Oral Research* **30**, e84.

Sodek J, Mckee MD. (2000) Molecular and cellular biology of alveolar bone. *Periodontology 2000* **24**, 99-126.

Sun Q, Meng M, Steed JN, Sidow SJ, Bergeron BE, Niu LN, Tay FR. (2021) Manoeuvrability and biocompatibility of endodontic tricalcium silicate-based putties. *Journal of Dentistry* **104**, 103530.

Tomás-Catalá CJ, Collado-González M, García-Bernal D, Oñate-Sánchez RE, Forner L, Llena C, *et al.* (2018) Biocompatibility of new pulp-capping materials NeoMTA Plus, MTA Repair HP, and Biodentine on human dental pulp stem cells. *Journal of Endodontics* **44**, 126–132.

Viola NV, Guerreiro-Tanomaru JM, da Silva GF, Sasso-Cerri E, Tanomaru-Filho M, Cerri PS. (2012) Biocompatibility of experimental MTA sealer implanted in the rat

subcutaneous: quantitative and immunohistochemical evaluation. *Journal Biomedical Materials Research Part B, Applied Biomaterials* **100**, 1773–1781.

Yaltirik M, Ozbas H, Bilgic B, Issever H. (2004) Reactions of connective tissue to mineral trioxide aggregate and amalgam. *Journal of Endodontics* **30**, 95–99.

Zamparini F, Prati C, Taddei P, Spinelli A, Di Foggia M Gandolfi MG. (2022). Chemical-Physical Properties and Bioactivity of New Premixed Calcium Silicate-Bioceramic Root Canal Sealers. *International Journal of Molecular Sciences* **23,** 13914.

Zordan-Bronzel, C. L., Torres, F. F. E., Tanomaru-Filho, M., Chávez-Andrade, G. M., Bosso-Martelo, R., & Guerreiro-Tanomaru, J. M. (2019). Evaluation of physicochemical properties of a new calcium silicate–based sealer, Bio-C Sealer. *Journal of Endodontics* **45**(10), 1248-1252.

Zordan-Bronzel, C. L., Tanomaru-Filho, M., Torres, F. F. E., Chávez-Andrade, G. M., Rodrigues, E. M., & Guerreiro-Tanomaru, J. M. (2021). Physicochemical properties, cytocompatibility and antibiofilm activity of a new calcium silicate sealer. *Brazilian Dental Journal* **32**, 8-18.

3.3 Artigo 3*

Biocompatibility and bioactive potential of bioceramic sealers associated with Cetramide

ABSTRACT

NeoSealer Flo (NeoFlo - NuSmile, Houston) is a new ready-to-use endodontic bioceramic sealer. Cetrimide (CTR) has an antimicrobial effect and can be added to endodontic sealers to increase antimicrobial activity. The study evaluated biocompatibility and bioactive potential of BioRoot ™ RCS (BROOT - Septodont, France) and NeoFlo and their associations with 1% CTR. The tissue reaction was evaluated after implantation of tubes with the materials into subcutaneous connective tissue for 7, 15, 30 and 60 days. Number of inflammatory cells (ICs), fibroblasts, osteocalcin (OC)-immunostained cells were evaluated. von Kossa reaction was performed. Data were evaluated by two-way ANOVA followed by Tukey's test, with a significance level of 5%. The OCN data were submitted to the Kruskal-Wallis test and the Dunn and Friedman and Nemenyi post hoc test for analysis over time. CIs was significantly higher for NeoFlo CTR than for NeoFlo at 7 and 60 days ($p < 0.05$). There was a reduction in the thickness of the capsules and the number of ICs from 7 to 60 days and a significant increase in the number of fibroblasts and birefringent collagen for all specimens. NeoFlo showed immunoexpression of OCN in all periods, while NeoFlo CTR, BROOT and BROOT CTR only at 60 days. Von Kossa structures were observed in the capsules around all materials at all periods. Addition of cetrimide promoted a greater inflammatory reaction, but the reduction of inflammatory cells and rearrangement of connective tissue suggests biocompatibility. Amorphous calcite deposits and OCN immunoexpression suggest bioactive potential.

Keywords: Biocompatible materials, Root canal filling materials, rats, osteocalcin.

* Artigo formato segundo as normas do periódico *Brazilian Oral Research* para o qual foi submetido.

Introduction

Controlling endodontic infection in the root canal system is essential for the success of endodontic treatment. Although mechanical instrumentation of root canals considerably reduces endodontic microbiota, microbial elimination cannot be achieved[1-4].

The antimicrobial activity is desirable for repair cements and root canal filling materials and may collaborate for the disinfection of contaminated dentine[2,3]. Thus, the incorporation of antimicrobial agents into endodontic materials can improve their effect against remaining microorganisms. Cetrimide (CTR) is a cationic surfactant, which has demonstrated efficacy against gram-positive and gram-negative bacteria[2,3]. CTR added to a tricalcium silicate-based cement improved the antibiofilm activity of the cement without compromising its physicochemical properties such as setting time, pH, and solubility[3]. However, in vivo studies are needed to evaluate whether CTR impairs the tissue response when added to the endodontic sealers.

Endodontic sealers should ideally be biocompatible and have bioactive potential to stimulate periapical repair[4,5]. BioRoot™ RCS (BROOT; Septodont, Saint-Maur-des-Fossés, France) is a calcium silicate-based bioceramic sealer in powder/liquid composition. The biocompatibility of BioRoot RCS has been reported in several in vitro studies, where the effects on cells depend on the dilution of their extracts and time of exposition[4,5]. Chlorhexidine improved the antibacterial activity of bioceramic sealers such as BioRoot, but decreased cell viability, in addition to affecting their physicochemical properties [6]. Therefore, the association of bioceramic sealers with antimicrobial agents aiming for better antimicrobial activity is beneficial, as if does not alter physicochemical and biological properties.

NeoSealer Flo (NeoFlo, NuSmile, Houston, TX, USA) is a new ready-to-use bioceramic root sealer composed of dicalcium and tricalcium silicate. This bioceramic sealant met the standards required by ISO (9917-1) demonstrating adequate radiopacity, setting time, film thickness and a pH of 8 up to 28 days, in addition to exhibiting the formation of a thin layer of phosphate phase calcium[7].

This study aimed to evaluate the biocompatibility and bioactive potential of BioRoot™ RCS and NeoSealer Flo and and their associations with the antimicrobial cetrimide (CTR). The null hypothesis is that the addition of cetrimide will not interfere with the tissue reaction and bioactive potential of the sealers.

Methodology

Ethical approval (Protocol #19/2021) was obtained for a study involving 30 Rats (*Rattus norvegicus albinus*), divided into Sealers (Table 1) and a Control Group (CG). The animals were kept in plastic cages with controlled temperature, humidity and light cycles and access to food and water ad libitum. The ARRIVE (Animal Research: Reporting of In Vivo Experiments) guidelines were followed by the authors.

The animals were anesthetized with ketamine chloride (80 mg/kg, Virbac do Brasil Indústria e Comércio Ltda., Brazil) and xylazine chloride (8 mg/kg, National Pharmaceutical Chemical Union, Brazil) administered by intraperitoneal. After 7, 15, 30, and 60 days the animals were sacrificed with anesthetic overdose implants with adjacent tissues were removed and the samples were fixed with 4% buffered formaldehyde at pH 7.2. After 48 h, the samples were dehydrated, treated with xylene, immersed in liquid paraffin, and embedded in paraffin to obtain longitudinal sections of the implants surrounded by capsules. Serial sections were obtained for hematoxylin & eosin (HE), picrosirius-red, von Kossa reaction staining, and immunohistochemistry for the detection of osteocalcin (OCN).

Thickness of capsules around implants

In each specimen, the thickness of capsules was estimated from three HE-stained non-serial sections. The thickness of the capsules was measured in the middle portion from its innermost surface adjacent to the material until its limit with adjacent tissues[8,9]. According to thickness, the capsules were characterized as thin when measured below 150 µm and thick those exhibiting values above 150 µm[8].

Numerical density of inflammatory cells and fibroblasts

The number of inflammatory cells (IC) and fibroblasts (Fb) was computed using the Image-Pro Express 6.0 Olympus software. The quantitative analysis was performed in the capsules of all implants. In each section a standard field of the capsule adjacent to the opening of the implanted tubes (measuring 0.09 mm^2) was captured at x40. The number of IC and Fb was obtained from 3 sections/implant in each time point, as previously described[8,9].

The intensity of inflammatory reaction was estimated according to number of IC per field[9,10], the inflammatory reaction was classified as mild (containing until 25

IC/field), moderate (containing from 26 to 125 IC /field) and severe/intense (containing more than 125 IC /field).

Table 1: The Endodontic Sealers Used.

Sealers and Manufacturers	Proportion	Composition
NeoSealer Flo (NeoFlo)/ NuSmile, Houston (USA)	Ready to use	Dicalcium and tricalcium silicate with calcium aluminate, tricalcium aluminate, and tantalite and thickening agent.
+ CTR 1% (cetrimide, # (Sigma-Aldrich, USA)	990 mg of sealer NeoSealer and 10 mg CTR	
BioRoot RCS/ Septodont (Saint-Maur-des-Fossé, France).	1 portion of dust and 5 drops of liquid according to the manufacturer, with measurement on a scale	Powder: Knitting silicate, zirconium oxide, and povidone. Liquid: dihydrate calcium chloride, sand, purified water
+ CTR 1% (cetrimide, # (Sigma-Aldrich, USA)	990 mg of already manipulated sealer BioRoot and 10 mg CTR	

Content of collagen in the capsules

In each specimen, the amount of birefringent collagen was analyzed from three non-serial sections stained with 0.1% picrosirius-red solution. Using a polarized light microscope, a field of the capsule was captured (at ×40 objective lens) with rigorously standardized parameters (light intensity, diaphragm aperture, condenser position and exposure time). The birefringent collagen was computed using an image analysis software (ImageJ; National Health Institutes; Bethesda, USA)[11,12].

Immunohistochemical detection of OCN

The deparaffinized sections were immersed in sodium citrate and heated at 98º C in a microwave oven for 30 min. After washings, the sections were immersed in 5% aqueous hydrogen peroxide solution, and they were incubated with 2% bovine serum albumin (Sigma-Aldrich, USA). The sections were incubated in a humidified chamber at 4º C with rabbit anti-OCN primary antibody diluted 1:150 (Sigma-Aldrich, USA. Code # Sab1306277). The sections were washed and incubated for 1 hour in the Labelled StreptAvidin-Biotin Kit (Universal Dako LSAB, Dako Inc.). After washings, the peroxidase activity was revealed by 3.3'-diaminobenzidine chromogen (Dako Inc.; code: K3468) and counterstained with Carazzi's hematoxylin.

The number of immunolabelled cells/mm^2 of capsule was obtained with help of an image analysis software (Image-Pro Express 6.0, Olympus, Japan). In each specimen, a standardized field (at x40 objective lens) was captured using a digital camara (DP-71, Olympus) attached to a light microscope (Olympus, Japan). The number of immunolabelled cell (in brown/yellow colour) was computed by a blinded examiner in each image previously captured. Thus, the number of OCN-immunolabelled cells/mm^2 was estimated.

von Kossa reaction and analysis under polarized light

Dewaxed sections were immersed in the 5% silver nitrate solution for 1 hour under incandescent light. After washings, the slides were immersed for 5 min. in 5% sodium hyposulfite solution. Afterwards, the sections were stained with 0.1% picrosirius-red solution and mounted.

Sections near the those subjected to von Kossa reaction were dewaxed, dehydrated, and mounted; these unstained sections were analyzed under a light microscope equipped with polarization filters (Olympus, BX51).

Statistical analysis

The data were evaluated by two -way ANOVA followed by the Tukey test, with a level of significance of $P \leq 0.05$. Osteocalcin data were subjected to the non-parametric Kruskal-Wallis test and Dunn's Multipson Post Hoc test for groups comparison and Friedman's test and Nemenyi's post hoc test for analysis over time.

Results

Morphological findings, capsule thickness and numerical density of IC and Fb

At 7 and 15 days, thick capsules containing numerous IC were seen around the implanted materials (Figs. 1A-1D and 1F-1I). After 30 days of implantation (Figs. 1K-1O), thick capsules with dense IC population were still observed juxtaposed to the NeoFlo CTR material (Fig. 1L). At 60 days, the capsules around all specimens were characterized by well-defined layer of connective tissue (Figs. 1P-1T). The measuring of capsules (Table 2) revealed that, at 7 days, all materials were surrounded by thick capsules, but the highest values were observed in the NeoFlo CTR and BROOT CTR. At 7 and 15 days, the thickness of the capsules around the NeoFlo was significantly lower than in other materials. At 30 days, no significant difference among NeoFlo, BROOT and BROOT CTR. At 60 days, no significant difference was observed between the materials.

At high magnification revealed massive presence of macrophages and lymphocytes (Figs. 2A-2D). These capsules exhibited an intense inflammatory reaction, except in the BROOT specimens that presented a moderate inflammatory reaction (Table 2). At 15 days, an intense inflammatory reaction was found in the capsules of NeoFlo and NeoFlo CTR specimens (Figs. 2F and 2G) while, BROOT and BROOT CTR specimens exhibited moderate reaction (Figs. 2H-2I and Table 2). At 30 (Figs. 2K-2N) and 60 (Figs. 2P-2S), although the IC were more sparsely distributed in comparison with the periods of 7 (Figs. 2A-2D) and 15 (Figs. 2F-2I) days, the capsules around all materials still showed a moderate inflammatory reaction (Table 2).

Regarding to numerical density (Table 2), the number of IC was significantly greater in NeoFlo CTR than in NeoFlo at 7, 30 and 60 days ($p < 0.05$) while, at 15 days, the number of IC was significantly lower in the NeoFlo CTR specimens. In all time points, a greater number of IC was found in the capsules around BROOT CTR than in BROOT specimens, The number of ICwas significantly lower in BROOT CTR than in NeoFlo specimens at 15, 30 and 60 days ($p < 0.05$). In all periods, capsules around BROOT material contained lower number of IC ($p < 0.05$) than in NeoFlo, NeoFlo CTR and BROOT CTR materials.

At 7 days, the number of Fb was greater in the capsules of NeoFlo and BROOT materials than in NeoFlo CTR and BROOT CTR ($p<0.0001$), respectively whereas no significant difference was seen between NeoFlo CTR and BROOT CTR

specimens. After 15 days of implantation, no significant difference was observed among NeoFlo, BROOT and BROOT CTR specimens. At 30 and 60 days, capsules around NeoFlo had greater number of Fb than other capsules adjacent to the materials.

Content of collagen in the capsules

As shown in the Table 2, few bundles of birefringent collagen were seen in the capsules of all specimens at 7 days (Figs. 3A-3E). However, in all specimens a significant increase in the amount of birefringent collagen was observed over time (Figs. 3A-3P; Table 2).

At 7 days, the content of collagen was lower significantly in the BROOT CTR than in BROOT ($p<0.0001$), NeoFlo CTR ($p<0.0001$). After 15 days, no significant difference was seen between CG with NeoFlo and with BROOT ($p > 0.05$) which showed the highest values of collagen. In contrast, the lowest values were found in the NeoFlo CTR and BROOT CTR specimens. At 30 days, the percentage of collagen was greater significantly in the NeoFlo, BROOT and CG specimens than in NeoFlow CTR and BROOT CTR specimens. At 60 days, significant differences were not observed between NeoFlo and NeoFlo CTR, NeoFlo and BROOT, and NeoFlo CTR and BROOT.

Immunohistochemical detection of OCN

The immunoexpression of OCN was observed in the capsules surrounding the NeoFlo samples in all periods (Figs. 4A-4F). Otherwise, OCN-immunolabelled cells in NeoFlo CTR, BROOT and BROOT CTR specimens were only observed at 60 days (Figs. 4F-4I). OCN-immunolabelled cells were not seen in the capsules around CG specimens (Figs. 4E-4J; Table 2). As shown in Table 2, at 60 days NeoFlo showed the highest values of OCN-immunolabelled cells, while no significant difference was observed between BROOT and BROOT CTR.

Figure 1 – HE-stained sections

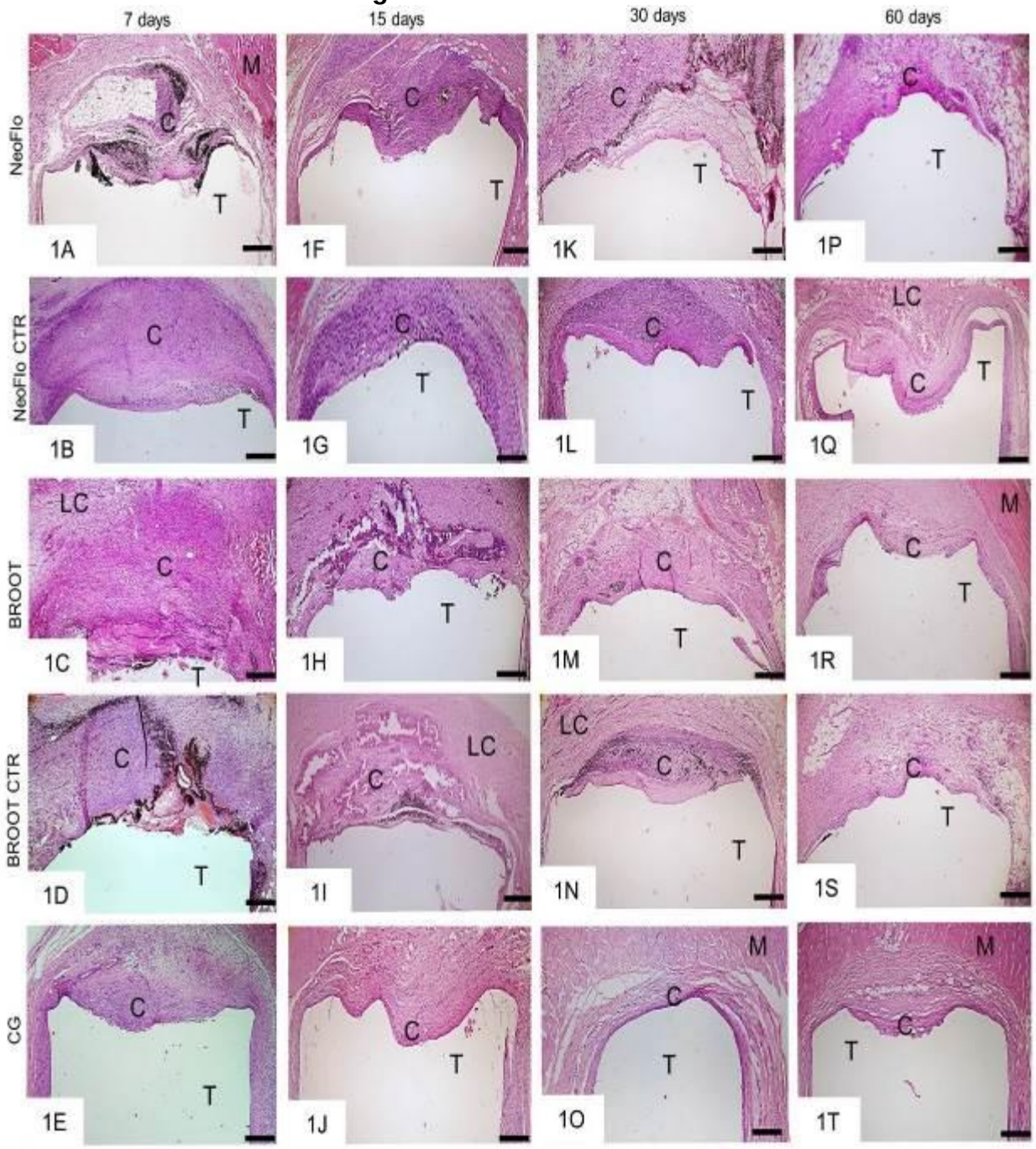

Figure 1: Photomicrographs show a general view of capsules (C) adjacent to the opening of the tubes implanted (T). M, muscle tissue; LC, loose connective tissue. Scale bars: 900 μm.

Figure 2– HE-stained sections

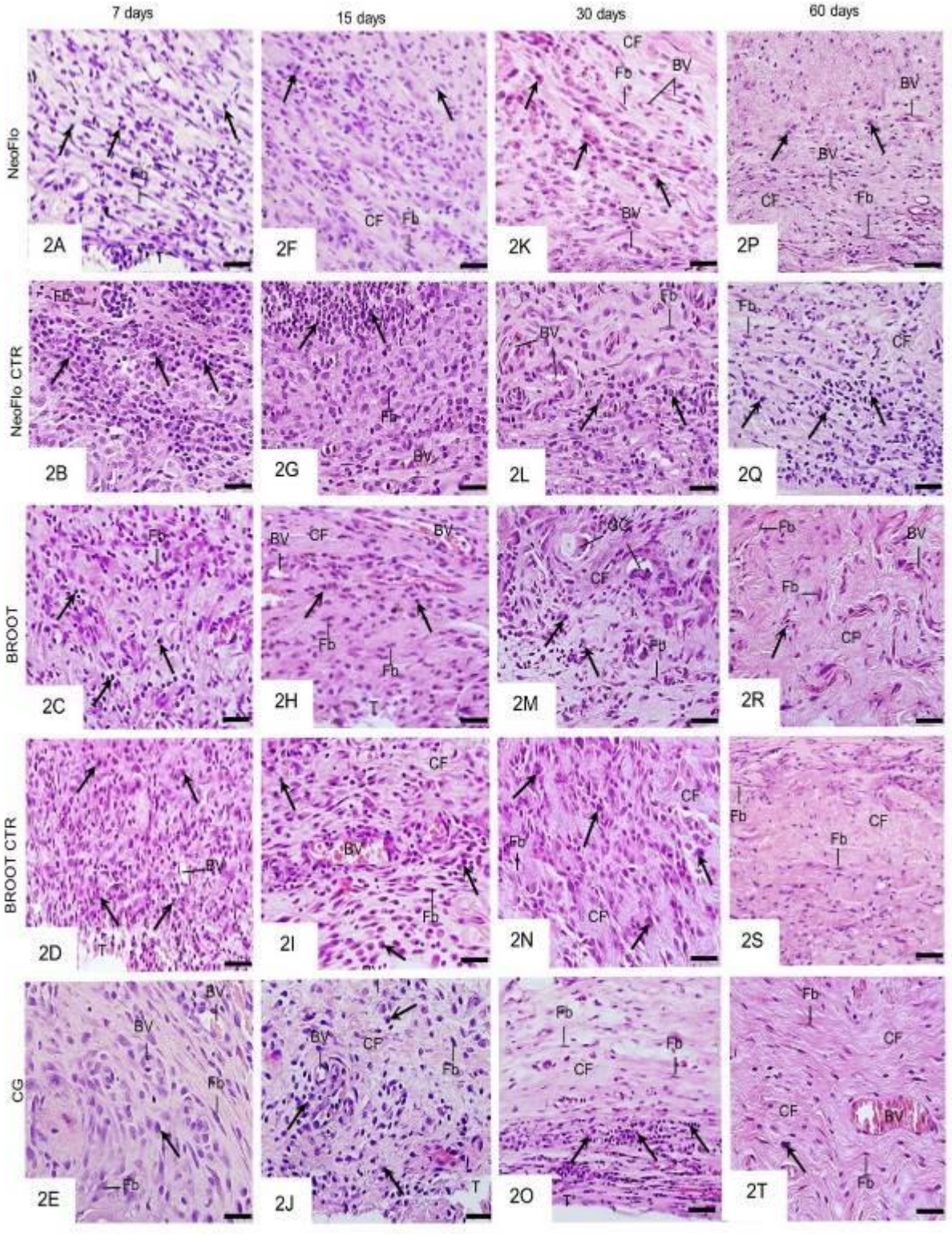

Figure 2: Photomicrographs of sections of portions of capsule adjacent to the implanted tubes (T) after 7 and 60 days. Arrows, inflammatory cells; Fb, fibroblasts; CF, collagen fibers; BV, blood vessels; GC, giant cell. Scale bars: 18 µm.

Figure 3: Sections stained with picrosirius Red

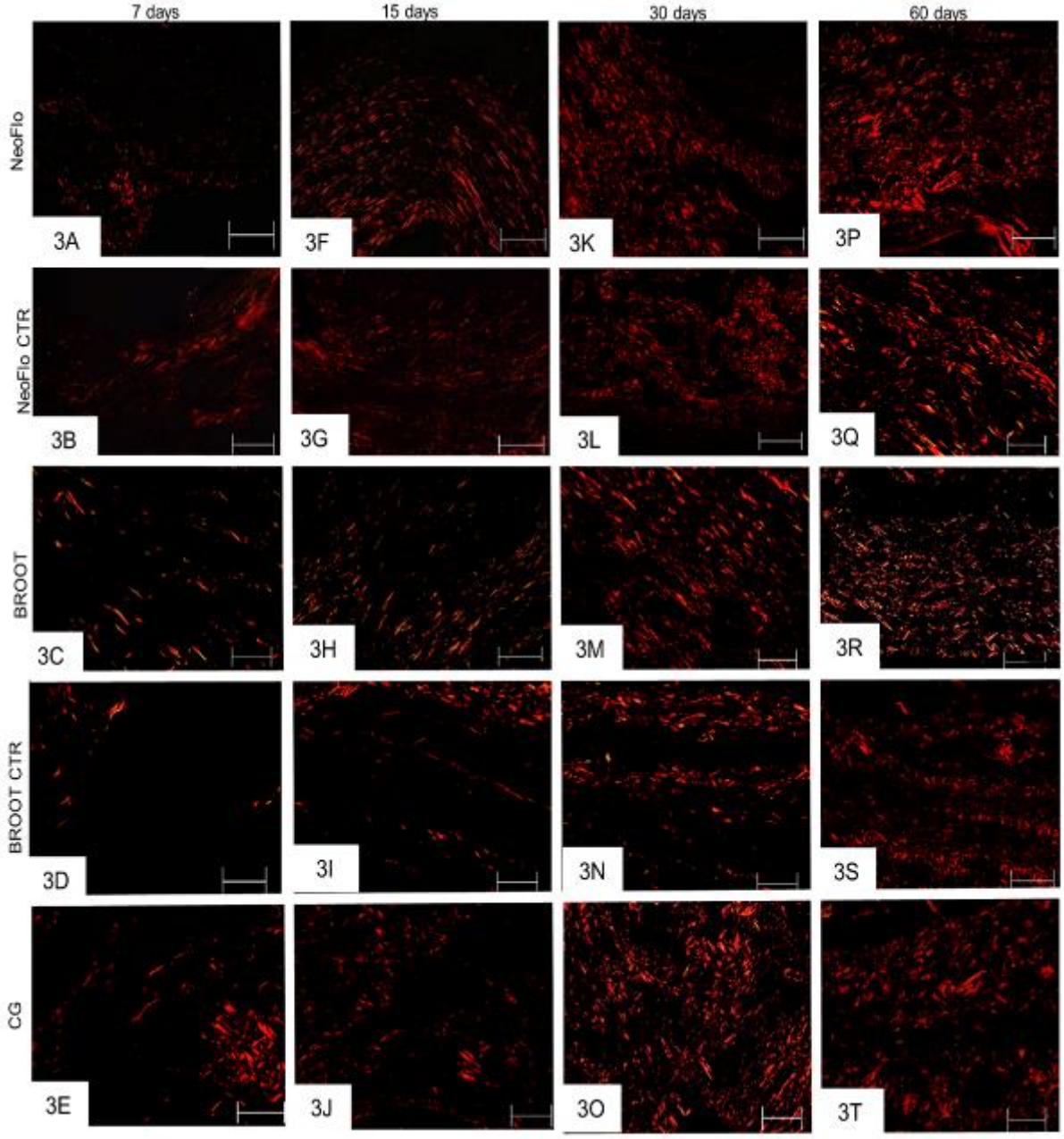

Figure 3: Photomicrographs of sections showing portions of capsule adjacent to the implanted tubes after 7 (3A-3E), 15 (3F-3J), 30 (3K-3O) and 60 (3P-3T) days of implantation. Sections were stained with picrosirius-red and analyzed under polarised light. Scale bars: 20 µm.

Figure 4: Immunohistochemistry for osteocalcin detection

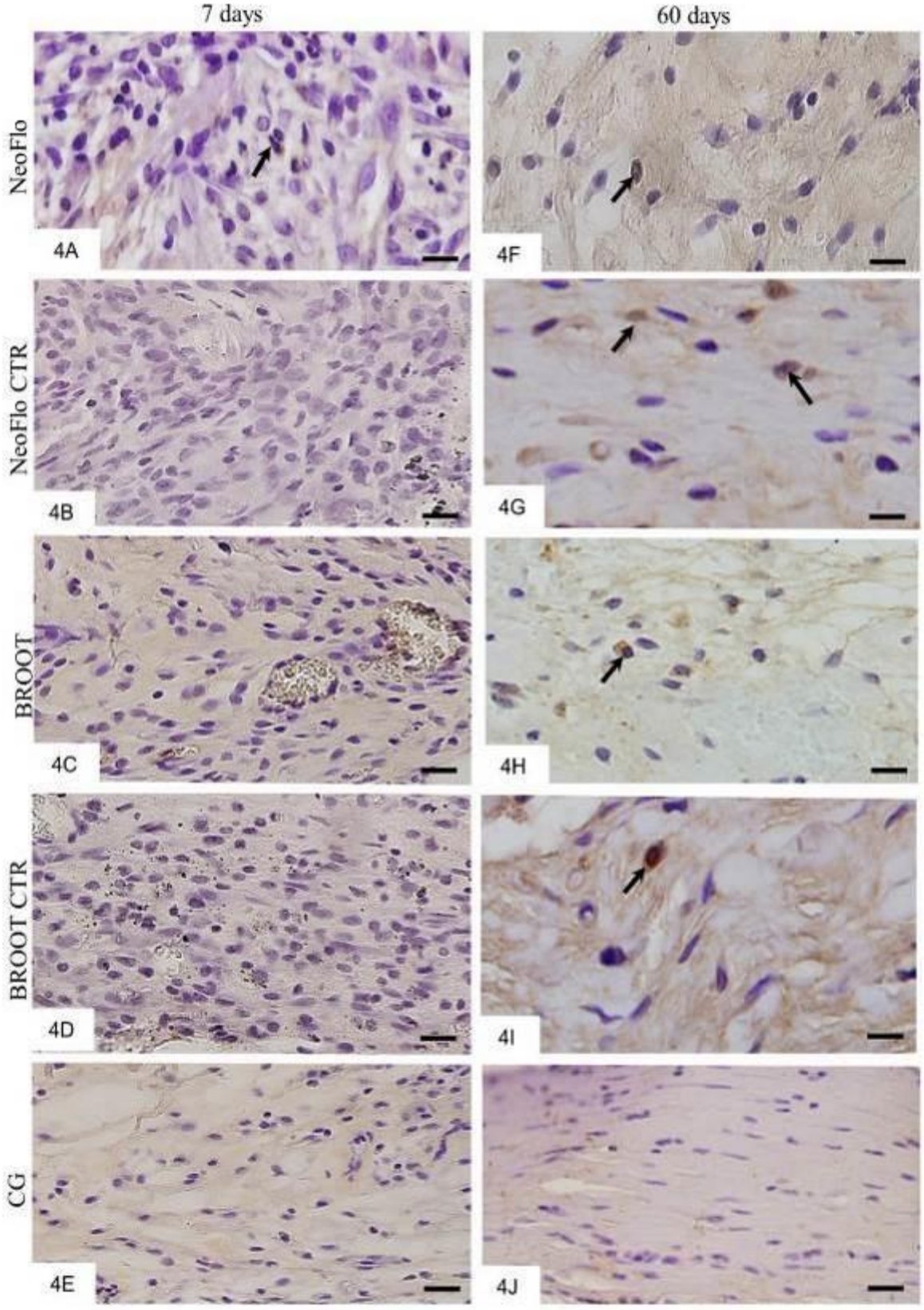

Figure 4: Photomicrographs showing portions of capsules adjacent to the implanted tubes after 7 (4A-4E) and 60 days (4F-4J). Scale bars: 18 µm.

Table 2 – Thickness of capsules (TC), number of inflammatory cells (ICs), number of fibroblasts (Fb), number of OCN-immunolabelled cells, content of collagen (CF) and inflammatory reaction intensity (IR) in the capsules around the NeoSealer Flo (NeoFlo), NeoSealer Flo + Cetrimide (NeoFlo CTR), BioRoot (BROOT), BioRoot + Cetrimide (BROOT CTR) and Control group (CG) at 7, 15, 30 e 60 days of implantation.

Periods	Analyses	NeoFlo	NeoFlo CTR	BROOT	BROOT CTR	CG
7 days	TC (µm)	366 ± 43$^{a;1}$	733 ± 24$^{b;1}$	489 ± 25$^{c;1}$	772 ± 25$^{b;1}$	168 ± 13$^{d;1}$
	ICs/mm^2	1569 ± 27$^{a;1}$	1650 ± 15$^{b;1}$	971 ± 19$^{c;1}$	1555 ± 22$^{a;1}$	249 ± 32$^{d;1}$
	Fb/mm^2	104±21$^{a;1}$	93 ± 16$^{b;1}$	129 ± 16$^{a;1}$	80 ± 9$^{b;1}$	168 ± 10$^{c;1}$
	CF (%)	13.1±4$^{a;1}$	9.7± 1$^{b;1}$	14.9 ± 2$^{c;1}$	5.9 ± 1$^{c;1}$	16.4 ± 2$^{a;1}$
	OCN/mm^2	11.11(11.11)$^{a;1}$	0.00(0.0)$^{b;1}$	0.00(0.0)$^{b;1}$	0.00(0.0)$^{b;1}$	0.00 (0.0)$^{b;1}$
	IR	intense	intense	intense	intense	mild
15 days	TC (µm)	323 ± 40$^{a;1}$	491 ± 26$^{b;2}$	439 ± 20$^{b;1}$	504± 18$^{c;2}$	181 ± 11$^{d;1}$
	ICs/mm^2	1429 ± 21$^{a;1}$	1324 ± 12$^{b;2}$	902 ± 10$^{c;1}$	1012 ± 26$^{d;2}$	233 ± 14$^{e;1}$
	Fb/mm^2	151±21$^{a;2}$	114 ± 12$^{b;2}$	141 ± 6$^{a;1}$	130 ± 9$^{a;2}$	236± 21$^{c;2}$
	CF (%)	20.6±3$^{a;2}$	16.9 ± 1$^{a;2}$	18.5 ± 2$^{b;2}$	14.8 ± 2$^{b;2}$	28.9 ± 3$^{a;2}$
	OCN/mm^2	22.22(22.22)$^{a;2}$	0.00(0.0)$^{b;1}$	0.00(0.0)$^{b;1}$	0.00(0.0)$^{b;1}$	0.00(0.0)$^{b;1}$
	IR	intense	intense	intense	intense	mild
30 days	TC (µm)	279 ± 41$^{a;2}$	304 ± 22$^{b;3}$	246 ± 24$^{a;2}$	276 ± 20$^{a;3}$	111 ± 03$^{c;1}$
	ICs/mm^2	990 ± 21$^{a;2}$	1103 ± 22$^{b;3}$	684 ± 22$^{c;2}$	804 ± 17$^{d;3}$	175 ± 26$^{e;2}$
	Fb/mm^2	231±09$^{a;3}$	190 ± 9$^{b;3}$	196 ± 10$^{b;2}$	180 ± 13$^{b;3}$	313 ± 14$^{c;3}$
	CF (%)	25.8±1$^{a;3}$	19.3 ± 1$^{a;3}$	20.9 ± 3$^{a;3}$	16.6 ± 1$^{b;2}$	26.8±2$^{a;2}$
	OCN/mm^2	22.22(22.22)$^{a;2}$	0.00(0.0)$^{b;1}$	0.00(0.0)$^{b;1}$	0.00(0.0)$^{b;1}$	0.00(0.0)$^{b;1}$
	IR	moderate	moderate	moderate	moderate	mild
60 days	TC (µm)	215 ± 45$^{a;2}$	237 ± 24$^{a;4}$	223 ± 23$^{a;2}$	247 ± 13$^{a;3}$	101 ± 10$^{b;1}$
	ICs/mm^2	503 ± 24$^{a;3}$	611 ± 15$^{b;4}$	297 ± 23$^{c;3}$	401 ± 15$^{d;4}$	67 ± 11$^{e;3}$
	Fb/mm^2	360±23$^{a;4}$	243 ± 10$^{b;4}$	268 ± 16$^{b;3}$	232 ± 6$^{b;4}$	341 ± 16$^{a;3}$
	CF (%)	29.9±2$^{a;3}$	26.8 ± 1$^{a;2}$	23.2 ± 1$^{b;3}$	20.1 ± 4$^{b;3}$	29.4 ± 1$^{a;2}$
	OCN/mm^2	33.33(22.22)$^{a;3}$	22.22(22.22)$^{b;2}$	11.11(11.1)$^{c;2}$	11.11(11.11)$^{c;2}$	0.00(0.0)$^{d;1}$
	IR	moderate	moderate	moderate	moderate	mild

The comparison between groups in the same period is indicated by superscript letters in the lines, same letters = no statistically significant difference.
The comparison between periods in the same group is indicated by superscript numbers in the columns; same numbers = no statistically significant difference. Tukey test ($p \leq 0.05$).
OCN: Values expressed as median and interquartile range. Analysis between groups in each period: Kruskal-Wallis followed by the Dunn test; analysis of each group over time: Friedman followed by the Nemenyi test ($p < 0.05$).

von Kossa reaction and analysis under polarized light

The capsules around all sealers exhibited von Kossa-positive structures in all time points (Figs. 5A-5H). Moreover, the analyses under polarized light of unstained sections revealed birefringent structures diffused by capsules adjacent to the materials (Fig 5I-5P). Either von Kossa-positive or birefringent structures were not seen in the CG specimens (data not shown).

Figure 5: von Kossa and birefringent structures in unstained sections

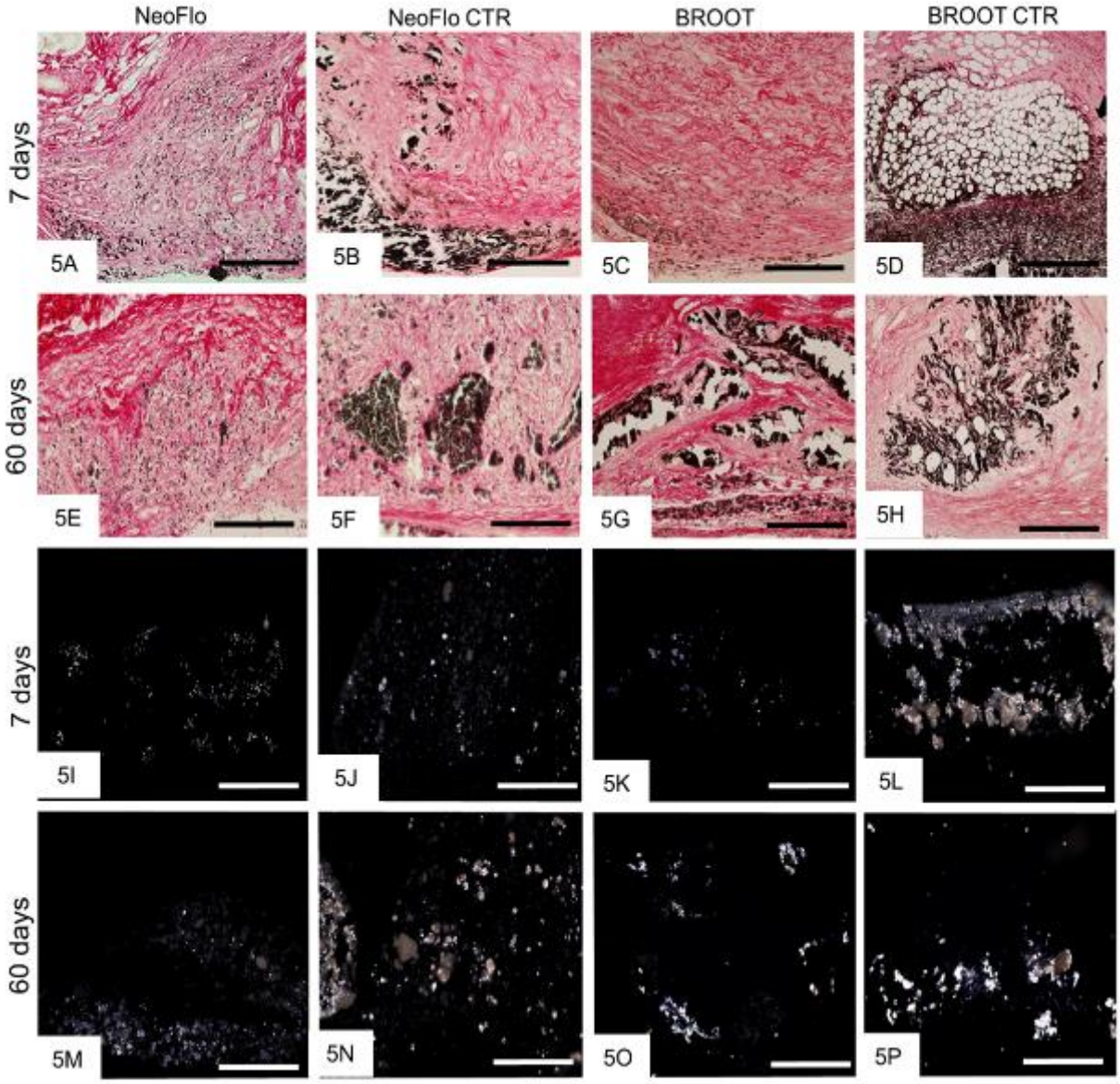

Figure 5: In 5A-5H - Photomicrographs of sections showing portions of capsule subjected to the von Kossa reaction at 7 (5A-5D) and 60 days (5E-5H). Figs. 5I-5P: Photomicrographs showing unstained sections analyzed under polarized light. Scale bars: 36 µm.

Discussion

The present study evaluated the biocompatibility and bioactive potential of BioRoot ™ RCS and NeoSealer Flo sealers with the addition of CTR. The addition of CTR to bioceramic sealers promoted greater recruitment of IC, which culminated with the maintenance of moderate inflammatory reaction until 60 days after subcutaneous implantation. Therefore, the null hypothesis was rejected because the addition of CTR interfered directly in tissue reaction.

The physical and antimicrobial properties of bioceramic sealers, along with the biological properties, are promising and can potentially improve the clinical success of treatment[14]. Thus, the addition of antimicrobials to endodontic sealers aims to improve their antibacterial activity and maintain the sterile nature of the root canal prepared. CTR is a cationic surfactant with excellent antibacterial activity[1,2,15] that has a strong ability to reduce bacterial adhesion[4], justifying the choice for its addition to the materials in the present study. Moreover, 1% or 0.5% CTR did not cause significant changes in the setting time, flow, solubility and radiopacity when added to the AH[15] Plus. However, no in vivo study evaluating tissue reaction of CTR added to the bioceramic sealers was found.

An important goal of endodontic therapy is the complete elimination of all microorganisms from the root canal system. Unfortunately, it appears to be impossible in certain clinical circumstances since root canal biofilm is the main reason for endodontic treatment failure[3-5]. However, the use of endodontic sealers with antibacterial properties can help reduce or eradicate bacteria. However, low antibacterial effectiveness of BROOT was demonstrated by agar diffusion and direct contact assays against *E. faecalis*[5]. Moreover, BROOT was not able to prevent the formation of different stages of biofilm[10]. Regarding NeoFlo there are still no studies that have evaluated its antimicrobial activity.

In the present study, the addition of 1% CTR to NeoFlo or BROOT caused greater damage to connective tissue than these pure sealers. The CTR addition to NeoFlo and BROOT recruited the greatest number of IC, culminating in the maintenance of the inflammatory reaction for a prolonged time. CTR added to V79 Chinese hamster cells caused high rate of cell death demonstrated by MTT, clonogenic and micronucleus assays[16]. It has been suggested that CTR promotes disruption of cell membrane lipids, resulting in cell lysis[16].

Our findings also revealed that, the capsules around all materials exhibited a moderate inflammatory reaction, indicating that endodontic sealers induced a prolonged injury to the structural arrangement of connective tissue of the subcutaneous. However, the significant reduction in the number of IC and in the capsule thickness observed over time, suggests that NeoFlo and BROOT sealers as well as the experimental sealers are biocompatible. On the other hand, the highest degree the tissue injury initially induced by sealers containing CTR leads us to raise the idea that perhaps the best sealer will depend on the degree of infection of the root canal. Thus, usage of bioceramic sealers associated with CTR would be indicated for teeth with infection in the canal system, justifying the addition of the antimicrobial agent despite its greater irritating potential than pure sealers.

Although CTR added to the BROOT sealer caused greater tissue injury than pure BROOT, it is important to emphasize that damage promoted by BROOT CTR decreased more quickly in comparison with NeoFlo. BioRoot RCS (BROOT; Septodont, Saint-Maur-des-Fossés, France) was developed as a calcium silicate-based root canal sealer. This bioceramic sealer is composed of a powder that contains tricalcium silicates, zirconium oxide and povidone, while the liquid contains polycarboxylate and calcium chloride. There is evidence that BROOT releases calcium, has alkalizing activity and induces the apatite formation[4]. Although NeoFlo presents calcium sulfate, grossite and tantalite, this difference in composition may explain the different pattern of tissue reaction between these two root sealers.

The higher values of IC culminating in intense inflammatory process in the initial period can be also explained by alkaline pH and high solubility presented by NeoFlo and BROOT sealers[4,7]. BROOT presents pH around 8.7 at 28 days, in turn AH Plus displays values close to 7, while BROOT's solubility at 7 days is 14.2%, compared to 0.8 for AH Plus[4].

Despite intense inflammatory reaction, the high values of Ca^{2+} and OH^{-1} release by these bioceramic sealers may provide a suitable microenvironment to induce the differentiation of mesenchymal cells into cells with the typical phenotype of producing-mineralized-tissue cells[22]. Here, the NeoFlo sealer induced the OCN immunoexpression by cells of subcutaneous connective tissue in all time points. OCN is a small glycoprotein, expressed by differentiating osteoblasts[17,18]. Studies have shown that calcium silicate-based endodontic materials induce the OCN immunoexpression suggesting that these materials may stimulate the differentiation

of mesenchymal cells into cells able to produce proteins of mineralized tissues[17,18]. Therefore, it is conceivable to suggest that CTR may initially inhibit the mesenchymal cell differentiation, since OCN-immunolabelled cells in NeoFlo CTR capsules were only seen at 60 days. The addition of 0.12% CHX gluconate, an antimicrobial agent, to the ProRoot ® MTA induced macrophages and fibroblasts apoptosis indicating that this antimicrobial agent may cause a delay in the tissue repair and, consequently, may possibly interfere with bioactive potential of the materials[23].

In contrast, von Kossa-positive structures were observed in the capsules around all sealers in all time points. Considering that von Kossa reaction is a histochemical method that detects calcium[20], these findings suggest that these sealers can promote the precipitation of calcium in the connective tissues. The formation of calcium carbonate either as calcite or aragonite was demonstrated on the surface of NeoFlo sealer after Hanks balanced salt solution immersion for 28 days and analyzed under micro-Raman spectroscopy[7]. Few von Kossa-positive areas were also demonstrated in the culture of BROOT-grown A4 cells, which were associated with calcium deposits probably derived from leakage and diffusion of repair material[24]. Therefore, our results indicated that pure sealers or associated with CTR allowed the deposition of calcite amorphous in the connective tissue.

The composition of endodontic sealers plays an important role in their biocompatibility and bioactive potential. Cetrimide directly influenced the inflammatory reaction of the materials, leading to greater recruitment of inflammatory cells. Despite tissue damage, all sealers evaluated induced a response in connective tissue suggestive of bioactive potential.

Conclusion

The addition of cetrimide to NeoSealer and BioRoot RCS bioceramic sealers induced greater recruitment of inflammatory cells. However, the reduction in the inflammatory reaction was accompanied by a gradual increase in the fibroblasts and collagen content over time, indicating therefore, that these sealers are biocompatible. Birefringent structures and OCN immunoexpression suggest bioactive potential of pure NeoFlow and BROOT as well as these sealers with addition of 1% cetrimide.

References

1- Zhang R, Chen M, Lu Y, Guo X, Qiao F, Wu L. Antibacterial and residual antimicrobial activities against *Enterococcus faecalis* biofilm: A comparison between EDTA, chlorhexidine, cetrimide, MTAD and QMix. Scientific Reports 2015; 5(1): 1-5. http://dx.doi.org/10.1038/srep12944

2- Ruiz-Linares M, Ferrer-Luque CM, Arias-Moliz T, de Castro P, Aguado B, Baca P. Antimicrobial activity of alexidine, chlorhexidine and cetrimide against *Streptococcus mutans* biofilm. Annals of Clinical Microbiology and Antimicrobials 2014 Aug; 13: 1-6. http://dx.doi.org/10.1186/s12941-014-0041-5

3- Rodrigues GB, Tanomaru-Filho M, Chavez-Andrade GM, Torres FFE, Guerreiro-Tanomaru JM. Physicochemical properties and antibiofilm activity of tricalcium silicate cement and its association with cetrimide. Odovtos-International Journal of Dental Sciences. 2022; 24(1): 113-121. http://dx.doi.org/10.15517/ijds.2021.47607

4- Siboni F, Taddei P, Zamparini F, Prati C, Gandolfi MG. Properties of BioRoot RCS, a tricalcium silicate endodontic sealer modified with povidone and polycarboxylate. International Endodontic Journal. 2017;2: e120-e136. https://doi.org/10.1111/iej.12856

5- Colombo M. Poggio C, Dagna A, Meravini MV, Riva P, Trovati F, Pietrocola G. Biological, and physico-chemical properties of new root canal sealers. Journal of Clinical and Experimental Dentistry. 2018; 10(2): e120. http://dx.doi.org/10.4317/jced.54548

6- Kapralos V, Sunde PT, Camilleri J, Morisbak E, Koutroulis A, Ørstavik D, Valen H. Effect of chlorhexidine digluconate on antimicrobial activity, cell viability and physicochemical properties of three endodontic sealers. Dental Materials. 2022; 38(6): 1044-1059. http://dx.doi.org/10.1016/j.dental.2022.04.013

7- Zamparini F, Prati C, Taddei P, Spinelli A, Di Foggia M, Gandolfi MG. Chemical-physical properties and bioactivity of new premixed calcium silicate-bioceramic root canal sealers. International Journal of Molecular Sciences. 2022; 23(22): 13914. https://doi.org/10.3390/ijms232213914

8- Delfino MM, de Abreu Jampani JL, Lopes CS, Guerreiro-Tanomaru JM, Tanomaru-Filho M, Sasso-Cerri E, Cerri PS. Comparison of Bio-C Pulpo and MTA Repair HP with White MTA: effect on liver parameters and evaluation of

biocompatibility and bioactivity in rats. International Endodontic Journal. 2021; 54(9): 1597-1613. https://doi.org/10.1111/iej.13567

9- Queiroz MB, Inada RN, Jampani JLDA, Guerreiro-Tanomaru JM, Sasso-Cerri E, Tanomaru-Filho M, Cerri P S. Biocompatibility, and bioactive potential of an experimental tricalcium silicate-based cement in comparison with Bio-C repair and MTA Repair HP materials. International Endodontic Journal. 2023; 00:1-19. http://dx.doi.org/ 10.1111/iej.13863.

10- Yaltirik M, Ozbas H, Bilgic B, Issever H. Reactions of connective tissue to mineral trioxide aggregate and amalgam. Journal of Endodontics. 2004; 30(2): 95-99. https://doi.org/10.1097/00004770-200402000-00008

11- Silva GF, Guerreiro-Tanomaru JM, Da Fonseca TS, Bernardi MIB., Sasso-Cerri E, Tanomaru-Filho M, Cerri PS. Zirconium oxide and niobium oxide used as radiopacifiers in a calcium silicate-based material stimulate fibroblast proliferation and collagen formation. International Endodontic Journal. 2017; 50: e95-e108. https://doi.org/10.1111/iej.12789

12- de Pizzol Júnior JP, Sasso-Cerri, E, Cerri, PS. Matrix metalloproteinase-1 and acid phosphatase in the degradation of the lâmina propria of eruptive pathway of rat molars. Cells. 2018; 7(11): 206. https://doi.org/10.3390/cells7110206

13- Camilleri J. Will bioceramics be the future root canal filling materials? Current Oral Health Reports. 2017; 4: 228-238. http://dx.doi.org/ 10.1007/s40496-017-0147-x

14- Arias-Moliz M, Ferrer-Luque CM, González-Rodríguez MP, Valderrama MJ, Baca P. Eradication of *Enterococcus faecalis* biofilms by cetrimide and chlorhexidine. Journal of Endodontics. 2010;36(1): 87-90. http://dx.doi.org/ 10.1016/j.joen.2009.10.013.

15- Ruiz-Linares M, Bailón-Sánchez ME, Baca P, Valderrama M, Ferrer-Luque CM. Physical properties of AH Plus with chlorhexidine and cetrimide. Journal of Endodontics. 2013; 39(12): 1611-1614. http://dx.doi.org/ 10.1016/j.joen.2013.08.002

16- Giardino L, Bidossi A, Del Fabbro M, Savadori P, Maddalone M, Ferrari L, Rao BS. Antimicrobial activity, toxicity and accumulated hard-tissue debris (AHTD) removal efficacy of several chelating agents. International Endodontic Journal. 2020; 53(8): 1093-1110. http://dx.doi.org/ 10.1111/iej.13314.

17- Alves-Silva EC, Tanomaru-Filho M, da Silva GF, Delfino MM, Cerri PS, Guerreiro-Tanomaru JM. Biocompatibility and bioactive potential of new calcium

silicate-based endodontic sealers: Bio-C Sealer and Sealer Plus BC. Journal of Endodontics. 2020; 46: 1470. http://dx.doi.org/ 1477. 10.1016/j.joen.2020.07.011

18- Silva ECA, Tanomaru-Filho M, Silva GF, Lopes CS, Cerri PS, Guerreiro-Tanomaru, J. M. Evaluation of the biological properties of two experimental calcium silicate sealers: An in vivo study in rats. International Endodontic Journal. 2021; 54(1): 100-111. http://dx.doi.org/ 10.1111/iej.13398.

19- Meloan SN, Puchtler H. Chemical mechanisms of staining methods: von Kossa's technique: what von Kossa really wrote and a modified reaction for selective demonstration of inorganic phosphates. Journal of Histotechnology. 1985; 8(1):11-13. https://doi.org/10.1179/his.1985.8.1.11

20- Loison-Robert LS, Tassin M, Bonte E, Berbar T, Isaac J, Berdal A, Fournier BP. In vitro effects of two silicate-based materials, Biodentine and BioRoot RCS, on dental pulp stem cells in models of reactionary and reparative dentinogenesis. PLoS One. 2018; 13(1): e0190014. http://dx.doi.org/10.1371/journal.pone.0190014.

21- Malheiros CF, Marques MM, Gavini G. In vitro evaluation of the cytotoxic effects of acid solutions used as canal irrigants. Journal of Endodontics. 2005; 31: 746–8. http://dx.doi.org/ 10.1097/01.don.0000157994.49432.67.

22- Bueno CRE, Valentim D, Marques VAS, Gomes-Filho JE, Cintra LTA, Jacinto R., Dezan-Junior E. Biocompatibility and biomineralization assessment of bioceramic-, epoxy-, and calcium hydroxide-based sealers. Brazilian Oral Research. 2016; 30 (1): e81. https://doi.org/10.1590/1807-3107BOR-2016.vol30.0081.

23- Hernandez EP, Botero TM, Mantellini MG, McDonald NJ, Nör JE. Effect of ProRoot® MTA mixed with chlorhexidine on apoptosis and cell cycle of fibroblasts and macrophages in vitro. International Endodontic Journal. 2005; 38(2): 137-143. https://doi.org/10.1111/j.1365-2591.2004.00922.x

24- Dimitrova-Nakov S, Uzunoglu E, Ardila-Osorio H, Baudry A, Richard G, Kellermann O, Goldberg M. In vitro bioactivity of Bioroot™ RCS, via A4 mouse pulpal stem cells. Dental Materials. 2015; 31(11): 1290-1297. http://dx.doi.org/10.1016/j.dental.2015.08.163.

3.4 Artigo 4*

Biocompatibility and bioactive potential of repair materials with the addition of Thyme Essential Oil in the subcutaneous tissues of rats

Aim: *Thyme Essential Oil* (TEO) has antibacterial effect, including resistant microorganisms and, therefore, its addition to the repair materials could improve the biological properties of bioceramic materials. This study evaluated the tissue reaction and bioactive potential of MTA Repair HP (MTA HP) and Bio-C Repair (BC) with the addition of TEO.

Methodology: Polyethylene tubes filled with one of the materials (BC; MTA HP; BC+TEO; MTA+TEO) or empty tubes (control group) were implanted into subcutaneous tissues for 7, 15, 30 and 60 days. After fixation, the implants surrounded by adjacent tissues were embedded in paraffin. Morphological and quantitative analyses were carried out in sections stained with haematoxylin and eosin. Collagen content was estimated in picrosirius red-stained sections. Bioactive potential was investigated using von Kossa method, analysis of unstained sections under polarized light, and immunohistochemistry for osteocalcin (OCN) detection. The data were subjected to ANOVA and Tukey tests, with a significance level of 5%. OCN data were submitted to Kruskal-Wallis and Dunn and Friedman post hoc tests followed by the Nemenyi test at a significance level of 5%.

Results: At 7 days, BC+TEO and MTA+TEO revealed lower inflammatory cells compared with BC ($p < 0.0001$), but no significant differences were observed amongst the materials after 30 and 60 days. At 15, 30 and 60 days, the BC+TEO and MTA+TEO materials showed greater amount of collagen fibers compared to BC and MTA HP. In all periods, the number of fibroblasts was greater in the capsules of BC+TEO and MTA+TEO than in BC and MTA HP specimens. von Kossa-positive and birefringent structures, suggestive of amorphous calcite, were seen in the material capsules at all time points, but OCN immunoexpression was only observed in the capsules around BC+TEO and MTA+TEO after 60 days. Moreover, the highest values were observed in MTA HP while the lowest values in BC+TEO specimens.

* Artigo formatado segundo as normas do periódico *International Endodontic Journal* para o qual pretende-se submeter.

Conclusions: The addition of TEO did not harm the biocompatibility of Bio-C Repair and MTA HP Repair. Furthermore, considering the immunostaining for OCN and presence of amorphous calcite in the capsules, it is conceivable to suggest that all materials may have bioactive potential.

*

INTRODUCTION

Repair materials should present adequate characteristics to be used in different clinical applications (Parirokh, Torabinejad, 2010). Antimicrobial action is important to collaborate with the disinfection of the contaminated and provide an increase in treatment success rates (Ruiz-Linares *et al.* 2014). It was already demonstrated that antibacterial properties of calcium silicate-based materials are enhanced by the addition of different substances or changing on their powder-to-liquid ratio (Parirokh, Torabinejad, 2010; Lima et al. 2021). However, these modifications might adversely affect other properties of the material, such as, biocompatibility (Parirokh, Torabinejad,2010).

Essential oils (EOs) are defined as volatile secondary metabolites of plants that give the plant a distinct smell, taste, or both, and are generally obtained because of hydrodistillation, steam distillation, dry distillation, or cold mechanical pressing of plants (Ruiz-Linares *et al.* 2014). Thyme and its volatile oil have long been used for the treatment of upper respiratory tract infections, symptoms of bronchitis, parasitic infections, pruritus associated with dermatitis, bruises, and sprains. It exerts antibacterial effect on Gram-positive and Gram-negative bacteria together with antifungal, anti-inflammatory properties. The main components of thyme EO are thymol (36-55%) and p-cymene (15-28%) (Zhang *et al.* 2015). Schött *et al.* (2017) described those essential oils of Thymus species presented antibacterial activity against S. mutans. Another study demonstrated that thyme oil can be used as an agent in the treatment of biofilm associated with *C. albicans* and *C. tropicalis* infections (Jafri, Ahmad, 2020). Thyme Essential Oil (TEO), can result in increased antibacterial activity, effectively inhibiting resistant microorganisms such as *C. albicans* (Zhang *et al.* 2015) and has demonstrated antibacterial and antibiofilm effect in toothpastes against bacteria associated with oral diseases (Ruiz-Linares *et al.* 2014).

Bio-C Repair (BC, Angelus, Londrina, PR, Brazil) is a ready-to-use bioceramic repair material. An in vitro study compared the cytocompatibility of Bio-C Repair, Biodentine and ProRoot MTA and revealed a high viability index of human dental pulp cells (hDPCS) exposed to these sealers. Furthermore, no cytoskeletal changes were observed in hDPCS, which were adhered to repair cements (Klein-Junior *et al.* 2021). When evaluated in the subcutaneous tissue of rats, the material showed biocompatibility and suggested a bioactive potential (Queiroz *et al*. 2023; Inada *et al.* 2023).

MTA Repair (MTA HP, Angelus, Londrina, PR, Brazil), has been introduced as a bioceramic material featuring elevated plasticity to preserve the biological characteristics of MTA. This improvement in chemical and physical attributes is achieved by incorporating an organic plasticizer into distilled water. Research suggests that the inclusion of the plasticizer in the liquid composition contributes to a reduction in the setting time and leads to an elevation in pH. This factor is regarded as a benchmark for other restorative materials, further confirming its biocompatibility in both vitro and in vivo studies (Lozano-Guillén *et al.* 2022; Queiroz *et al.* 2023).

The present study aimed to evaluate the inflammatory reaction and the bioactive potential of Bio-C Repair and MTA Repair bioceramic materials with addition of TEO. The null hypothesis is that the association of TEO would not play any role in the inflammatory reaction and in the bioactive potential of the Bio-C Repair and MTA Repair.

MATERIALS AND METHODS

Experimental procedure

This study was approved by the Animal Research Ethics Committee (CEUA, Protocol # 19/2021) in compliance with Brazilian national law on animal use. Thirty-two male Holtzman rats (*Rattus norvegicus albinus*) weighing ± 250-300 g were distributed into 5 groups (n = 6/group) filled with the respective sealers (Table 1) and control group (CG; empty polyethylene tubes)

The sample size was estimated using previous study (Silva *et al.* 2021) for the detection of a 50% difference between the experimental groups, considering a variability of 20% and test power of 90% and an alpha error of 0.05 to recognize a significant difference. Thus, a sample of 5 rats per group was required at each time point, considering the possibility of loss of animals, one animal was added to each

group. Thus, a sample of 5 rats per group was required at each time point, considering the possibility of loss of animals or samples during histological processing, one sample of each group was added to each time point. The study has been written according to Preferred Reporting Items for Animal studies in Endodontology (PRIASE) 2021 guidelines (Nagendrababu *et al*. 2021). The PRIASE 2021 flowchart is represented in Figure 1.

The materials (Table 1) were inserted into polyethylene tubes (10.0 mm in length and 1.6 mm in diameter) and subsequently implanted in the subcutaneous dorsum of the animals. Four tubes were inserted per animal, one from each group, in a quadrant rotation (ISO-10993-6, 2007). The animals were anesthetized with ketamine hydrochloride (80 mg/kg of body weight; Virbac do Brasil Indústria e Comércio Ltda., São Paulo, SP, Brazil) and xylazine hydrochloride (8 mg/kg of body weight; União Química Farmacêutica Nacional S/A, São Paulo, SP, Brazil) by intraperitoneal route using insulin syringe. The dorsal skin was shaved and disinfected with 5% iodine solution, and an incision (measuring about 2 cm) was made in the cranio-caudal plane. After divulsion, the polyethylene tubes were placed in the dorsal subcutaneous pocket and, immediately, the skin was sutured with simple stitches using 4-0 silk thread (Ethicon Inc., São José dos Campos, São Paulo, Brazil).

Table 1: The Endodontic Cements Used.

Cement and Manufacturers	Proportion	Composition
Bio-C Repair (BC; Angelus, Brazil)	Ready to use	Calcium silicates, calcium aluminate, calcium oxide, zirconium oxide, iron oxide, silicon dioxide and dispersing agent.
Bio-C Repair (BC; Angelus, Brazil) + TEO 1% Sigma-Aldrich) (BC+ TEO)	990 mg of BC sealer and 10 µl TEO	Calcium silicates, calcium aluminate, calcium oxide, zirconium oxide, iron oxide, silicon dioxide, dispersing agent and Thymol.

MTA Repair HP (MTA; Angelus, Brazil)	1g powder: 300 µL liquid	Powder: Tricalcium silicate; Dicalcium silicate; Tricalcium aluminate; Calcium oxide; Calcium Tungstate; Liquid: Water and plasticizer.
MTA HP (Angelus, Brazil) + TEO 1% (Sigma-Aldrich) (MTA+ TEO)	990 mg of sealer MTA and 10 µl TEO	Powder: Tricalcium silicate; Dicalcium silicate; Tricalcium aluminate; Calcium oxide; Calcium Tungstate; Liquid: Water and plasticizer.

After 7, 15, 30, and 60 days, the animals were euthanized with anesthetic overdose, and the portions of skin containing the implants were removed and processed for light microscopy.

The implanted polyethylene tubes surrounded by tissues of the subcutaneous were removed and immediately immersed in a 4% formaldehyde solution (freshly prepared from paraformaldehyde) buffered with 0.1 mol/L sodium phosphate at pH 7.2 at room temperature. After 48 h, the samples were dehydrated, treated with xylene, and immersed in liquid paraffin at 60°C for 4 h. The samples were embedded in paraffin to obtain longitudinal sections (6 µm thick), which were obtained using a rotary microtome (Leica, model RM2125 RST) and disposable stainless-steel knives (Leica, model 818). Non-serial sections were stained with hematoxylin and eosin (HE) and Masson's trichrome for morphological and morphometrical analyses. Other sections were also subjected to the picrosirius-red, von Kossa method, and osteocalcin immunohistochemistry reactions.

The analyses were performed using a light microscope (BX51, Olympus, Tokyo, Japan) and an image analysis software (Image Pro-Express 6.0, Olympus, Tokyo, Japan). The quantitative analyses were performed by one calibrated and blinded examiner and the measurements were repeated (in duplicate).

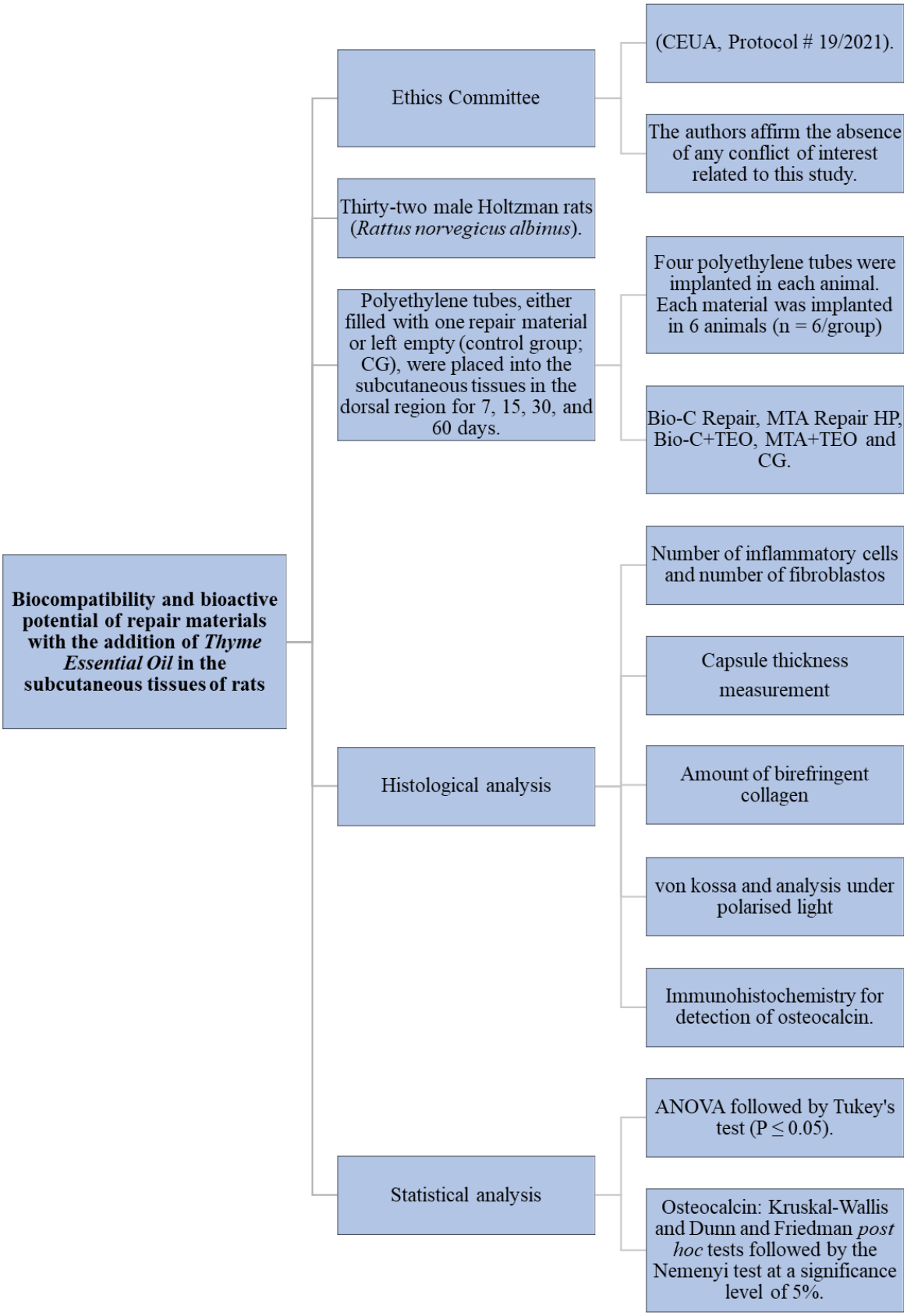

Figure 1: Diagram illustrating the experimental design and methodologies employed for evaluating both biocompatibility and bioactive potential.

Thickness of capsules

The thickness of capsules was estimated from three non-serial HE-stained sections per specimen. In each section, using a digital camera (DP-71, Olympus – Japan) attached to the Olympus microscope, one image of the capsule adjacent to the polyethylene tube opening was captured with an objective lens at x4 magnification. The thickness of the capsule was estimated from the inner portion of the capsule (adjacent to the tube opening) to its interface with adjacent tissues (muscle tissue, loose connective tissue) using image analysis software (Olympus), as previously described (Alves-Silva *et al.* 2020; Queiroz *et al.* 2023). The capsule thickness was estimated in all specimens (n=6 per group) and at various time points. Capsules were categorized as thick when measured over 150 µm and as thin when measured up to 150 µm (Yaltirik *et al.* 2004; Queiroz *et al.* 2023).

Numerical density of inflammatory cells

The number of inflammatory cells (IC) was computed using the Image-Pro Express 6.0 Olympus program. Images were captured using a digital camera attached to a light microscope with objective lens at x40. In each section, a standard area of 0.09 mm^2 of the capsule adjacent to the opening of the implanted tubes was captured. The number of IC was obtained from 3 sections of each implant, totaling an area of 0.27 mm^2 per implant. The number of IC (neutrophils, lymphocytes, plasma cells and macrophages) was computed considering the morphological characteristics. In each area, the number of IC was calculated, obtaining the number of IC and fibroblasts per mm^2 of each sample. At the end, the average value per group and period was obtained.

Numerical density of fibroblasts

In every sample, the count of fibroblasts (Fb) was evaluated within the capsules using Masson trichrome-stained sections. Three non-sequential sections were examined in each specimen. Within each section, a standardized area (0.09 mm^2) at the central region of the capsule, near the opening of the implanted tube, was captured at a magnification of ×695. The fibroblasts, characterized by their elongated/fusiform morphology, were quantified within the standardized field. Consequently, for each specimen, the fibroblast count per square millimeter of the

capsule was determined by dividing the total number of fibroblasts by the total capsule fields (0.27 mm^2).

Content of collagen in the capsules

The collagen content in the capsules was quantified in sections stained with 0.1% picrosirius-red solution and examined using a polarized light microscope (BX-51, Olympus). For each sample, three non-consecutive sections were utilized. Using a digital camera connected to the light microscope with polarized filters, a field of each capsule was captured with the objective lens at x40 magnification (final magnification: x695). To evaluate the content of birefringent collagen, the images were carefully obtained using rigorously standardized parameters such as light intensity, diaphragm opening, condenser position, and exposure time. The birefringent content in the capsules was assessed using image analysis software (ImageJ; National Institutes of Health). Birefringence was defined based on the following hue parameters: red/orange, 2–38 and 230–256; yellow, 39-51; and green (Delfino *et al.* 2021; Queiroz *et al.* 2023). Consequently, the collagen quantity was expressed as the percentage of birefringent area occupied in the total area.

Immunohistochemical detection of osteocalcin

For detection of osteocalcin, rabbit anti-mouse osteocalcin antibody (1:150; Sigma-Aldrich Co., Saint Louis, Missouri, USA; code SAB1306277) was used. After dewaxing and hydration, the slides were immersed in 0.001 M sodium citrate buffer at pH 6.0 and subjected to microwave treatment. After cooling, the slides were washed in 0.01 M PBS at pH 7.2 and then immersed in a 5% aqueous solution of hydrogen peroxide. The sections were washed and incubated with 2% bovine serum albumin (Sigma-Aldrich Co., Saint Louis, Missouri, USA). Then, the sections were incubated overnight in a humidified chamber at 4º C with anti-osteocalcin rabbit antibody. After washing in 0.01 M PBS buffer, the sections were incubated for 1 hour in the Labeled StreptAvidin-Biotin kit (Universal Dako LSAB, Dako Inc., Carpinteria, CA, USA; K0675) at room temperature. After washing, the peroxidase activity was revealed by 3,3'-diaminobenzidine chromogen (ImmPACTTM DAB Vector, Burlingame, CA, USA) and the sections were counterstained with Carazzi's haematoxylin. As negative control, sections were incubated with non-immune serum instead of anti-osteocalcin antibody. The number of immunopositive cells was

calculated using an image analysis software (Image-Pro Express 6.0, Olympus, Tokyo, Japan). Thus, the number of immunopositive cells/mm^2 of capsule was obtained for each implant.

von Kossa Reaction and analysis under polarised light

Sections of capsules were subjected to the von Kossa technique to identify calcium deposits. Following deparaffinization and hydration, the sections were immersed in a 5% silver nitrate solution for 1 hour under an incandescent lamp (100 Watts). Subsequently, the slides were rinsed in distilled water for 3 minutes and immersed in a 5% sodium hyposulfite solution for 5 minutes. The sections were then once again rinsed in distilled water for 5 minutes and subsequently stained with picrosirius-red and mounted in a resin medium.

Statistical analysis

Statistical analysis was conducted using GraphPad Prism 9.02 software (GraphPad Software). The data exhibited a Quantile-Quantile plot for the standard normal variate (Q–Q plot). Variations among the groups at each time point and the changes within each group over time were assessed through two-way ANOVA analysis, followed by the Tukey post-test (GraphPad Prism 5.0 software) with a significance level set at $p \leq .05$. All presented data were expressed as mean and standard deviation. Osteocalcin data underwent the non-parametric Kruskal-Wallis test, and Dunn's post hoc multiple comparisons test was employed to compare between groups at each time point. Friedman's test and Nemenyi's post hoc test were utilized for the analysis across different time points.

RESULTS

Morphological findings, capsule thickness, number of inflammatory cells and fibroblasts

The analysis of sections stained with Masson’s trichrome revealed well-defined capsules around the implanted tubes in all time points (Figs. 2a-2t). In all periods, the capsules of BC+TEO and MTA+TEO specimens were significantly thinner than those around the BIO-C and MTA HP. Moreover, no significant differences were observed in the thickness of capsules around the BIO-C and MTA HP specimens in all time

points. At 60 days, no significant difference was observed in capsules measurements among BC+TEO, MTA+TEO, and CG specimens (Table 2).

The analysis in higher magnification of HE-stained sections revealed that, at 7 and 15 days, the capsules surrounding all implanted materials presented a moderate inflammatory reaction with predominance of lymphocytes and macrophages intermingled with evident blood vessels, fibroblasts, and collagen fibers. At 7 and 15 days, there was a predominance of inflammatory cells over fibroblasts in the capsules of all tubes filled with materials (Figs. 3a-3d and 3f-3i). At 30 and 60 days, the capsules around the implanted materials exhibited an evident reduction in cell population and an increase in extracellular matrix components, particularly, in collagen fibers (Figs. 3k-3n and 3p-3s). After 60 days of implantation, the capsules invariably showed the predominance of fibroblasts and collagen fibers, besides blood vessel (Figs. 3p-3t).

As shown in Table 2, the number of IC was significantly greater in the capsules around the BIO-C than in BC+TEO and MTA+TEO specimens at 7 and 15 days ($p < 0.0001$). At 7 days, no significant difference in the number of IC was seen between BC+TEO and MTA+TEO specimens ($p = 0,1376$), but at 15 days the number of IC was significantly reduced in the BC+TEO capsules compared to the MTA+TEO specimens ($p = 0.0222$). In these periods, the capsules around the MTA HP exhibited lower number of IC than in MTA+TEO ($p = 0.0002$) specimens. At 30 and 60 days, significant differences in the number of IC were not observed amongst BC+TEO, BIO-C, MTA+TEO and MTA HP specimens. In all periods, the lowest values of number of IC were found in the CG capsules. A significant reduction in the number of IC accompanied by significant increase in the number of Fb was observed in the capsules of all groups over time. In all time points, the number of Fb was significantly greater ($p < 0.0001$) in the capsules around the BC+TEO and MTA+TEO than in BIO-C and MTA HP specimens, respectively, as shown in Table 2. In all periods, significant differences in the number of Fb were not seen between BIO-C and MTA HP specimens. The capsules of CG specimens exhibited the highest values of Fb, in all periods.

Figure 2: General view of capsules

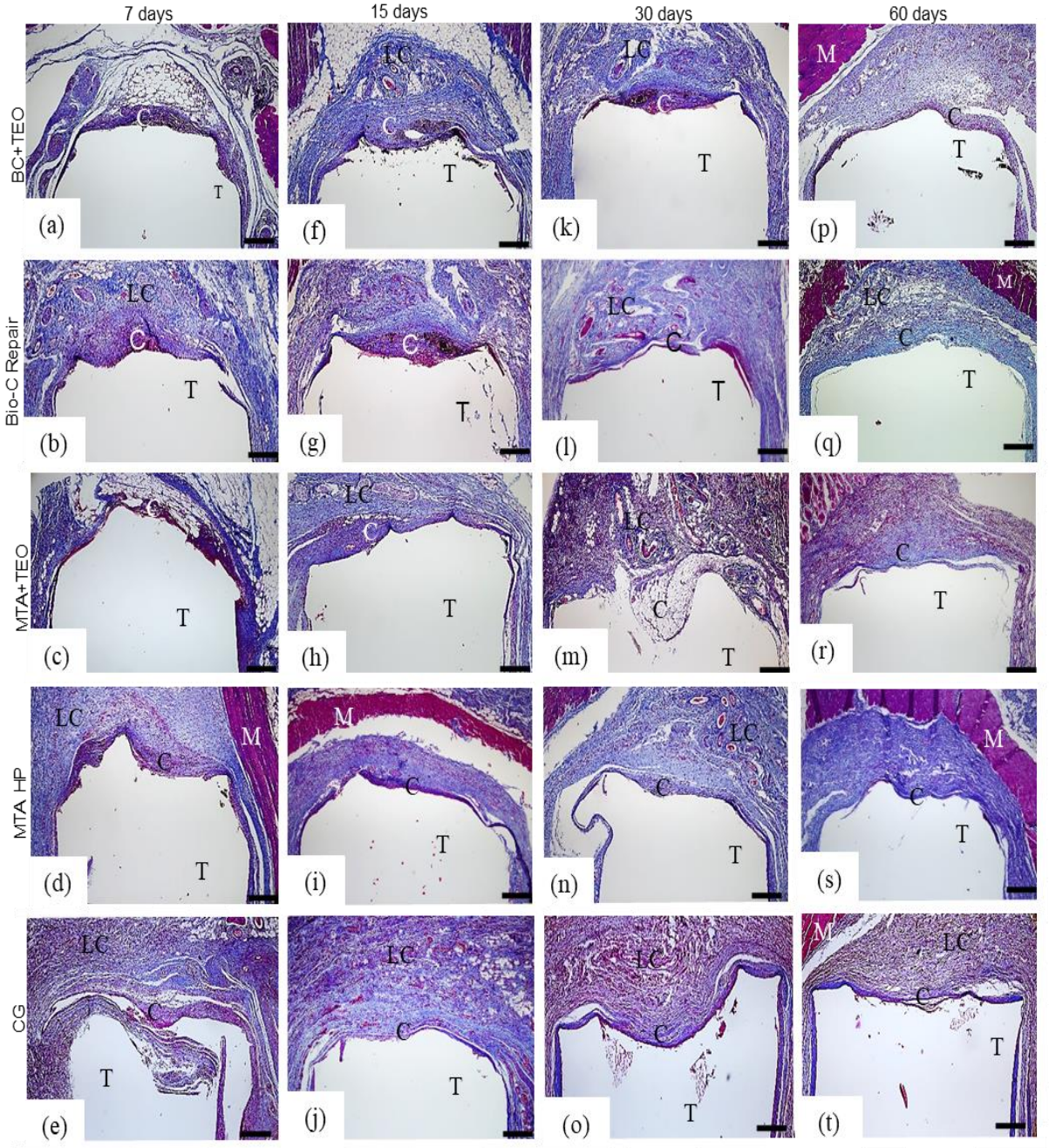

Figure 2: Light micrographs show a general view of capsules (C) adjacent to the opening of the tubes implanted (T). M, muscle tissue; LC, loose connective tissue. Masson's Trichrome. Scale bars: 900 µm.

Figure 3: HE sections.

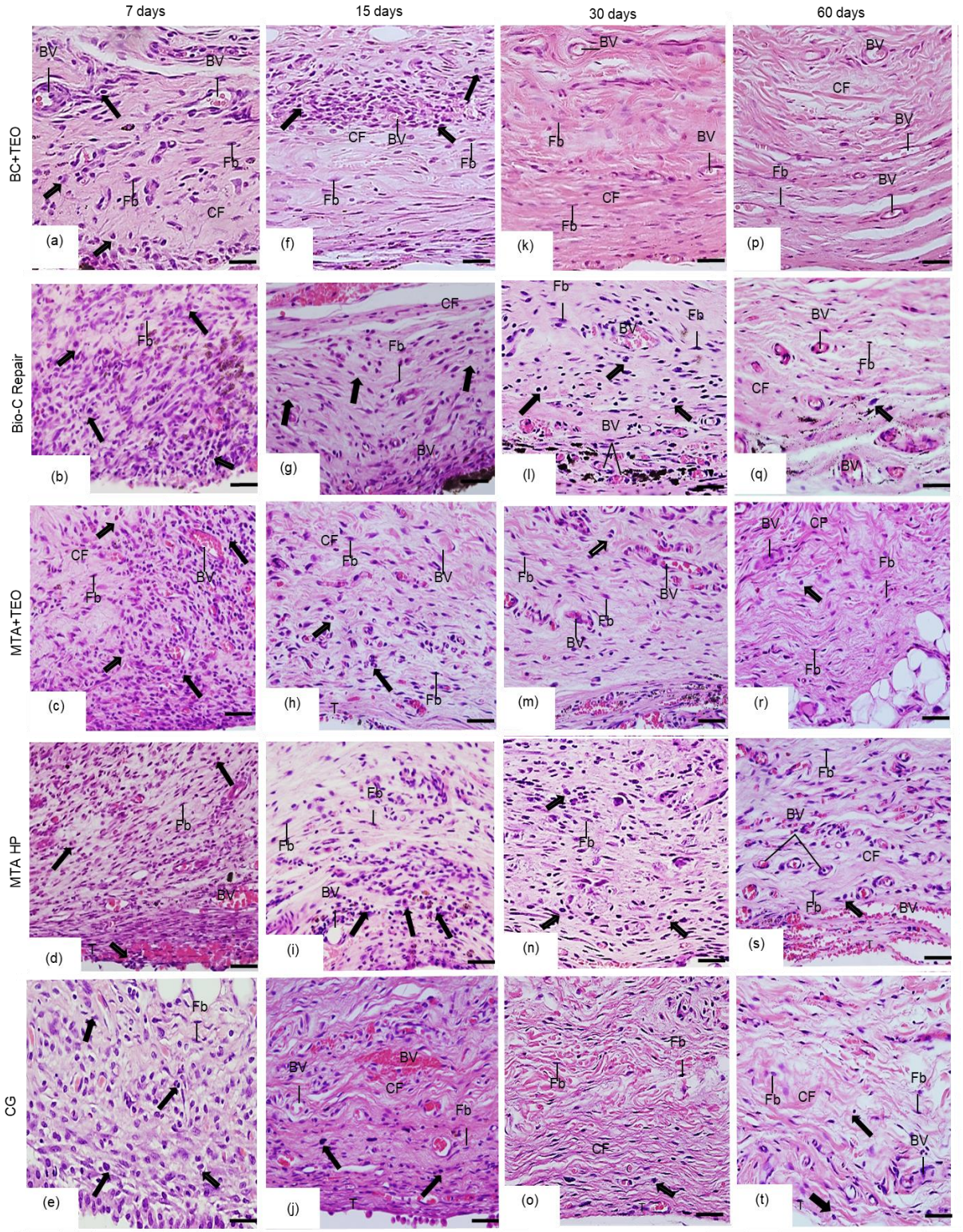

Figure 3: Light micrographs showing portions of sections of capsules adjacent to the polyethylene tubes (T) after 7 (a-e), 15 (f-j), 30 (k-o) and 60 days (p-t) of implantation. Arrows, inflammatory cells; Fb, fibroblasts; CF, collagen fibres; BV, blood vessels. Bars: 18 µm.

Birefringent collagen content

The analysis of picrosirius red-sections under polarized light revealed that the capsules around all implants exhibited collagen fibres in red/orange/green colours in all periods (Figs. 4a-4t). At 7 days BC+ TEO showed the highest values when compared to the other materials ($p < 0.05$). At 15 and 60 days, the capsules around the BC+TEO and MTA+ TEO materials contained a higher amount of collagen fibres than in Bio-C Repair and MTA HP specimens ($p < 0.05$) while no significant difference was observed between BIO-C and MTA HP specimens. At 30 days, significant differences in the collagen content were not seen amongst BC+TEO, BIO-C, MTA+TEO and MTA HP specimens. The highest percentage of birefringent collagen was observed in the capsules surrounding the CG specimens at all time points (Table 2).

Figure 4: Sections stained with picrosirius Red.

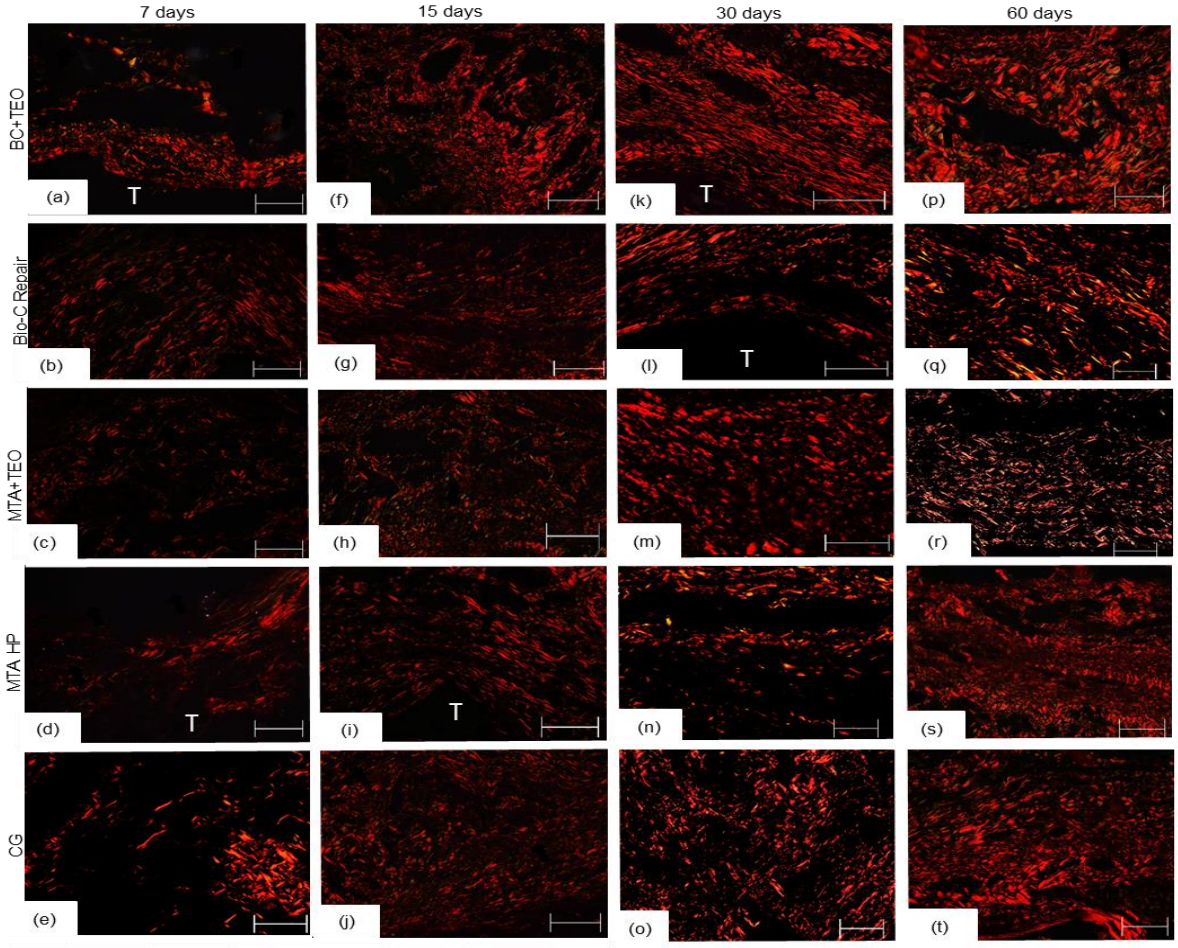

Figure 4: Light micrographs showing portions of sections of capsules adjacent to the polyethylene tubes (T) after 7 (a-e), 15 (f-j), 30 (k-o) and 60 days (p-t) days of implantation. Sections were subjected

to the picrosirius-red method and photographed under polarised light. Birefringent collagen fibers are mainly seen in red colour. Bars: 20 μm.

Immunohistochemical detection of osteocalcin

Few cells in the capsules around implanted materials exhibited cytoplasmic immunostaining (yellowish-brown colour) for osteocalcin. At 7, 15 and 30 days, OCN-immunolabelled cells were only observed in the capsules around BIO-C and MTA-HP specimens (Figs. 5b and 5d; Table 2). Immunoexpression of OCN was present in the capsules around all materials after 60 days, except in CG specimens (Figs. 5e-5j). In the sections used as negative control, OCN-immunolabelled cells were not observed (data not shown).

According to Table 2, no significant difference in the OCN immunoexpression was seen between BIO-C and MTA HP specimens at 7 days. However, the number of immunolabelled cells was significantly greater in the capsules around the MTA HP than in BIO-C specimens at 15, 30 and 60 days ($p < 0.0001$). Although at 60 days the capsules around all materials contained OCN-immunolabelled cells, a distinct pattern in the immunolabelling was observed in the different groups. The highest values were observed in the MTA HP while the lowest values were found in the BC+TEO specimens. Furthermore, significant differences were not observed between MTA+TEO and BIO-C specimens. Thus, the capsules around experimental materials exhibited reduced number of OCN-immunolabelled cells in comparison with BIO-C and MTA HP. In all time points, no immunolabelling was observed in the capsules of CG specimens.

Figure 5: Immunohistochemistry for osteocalcin detection.

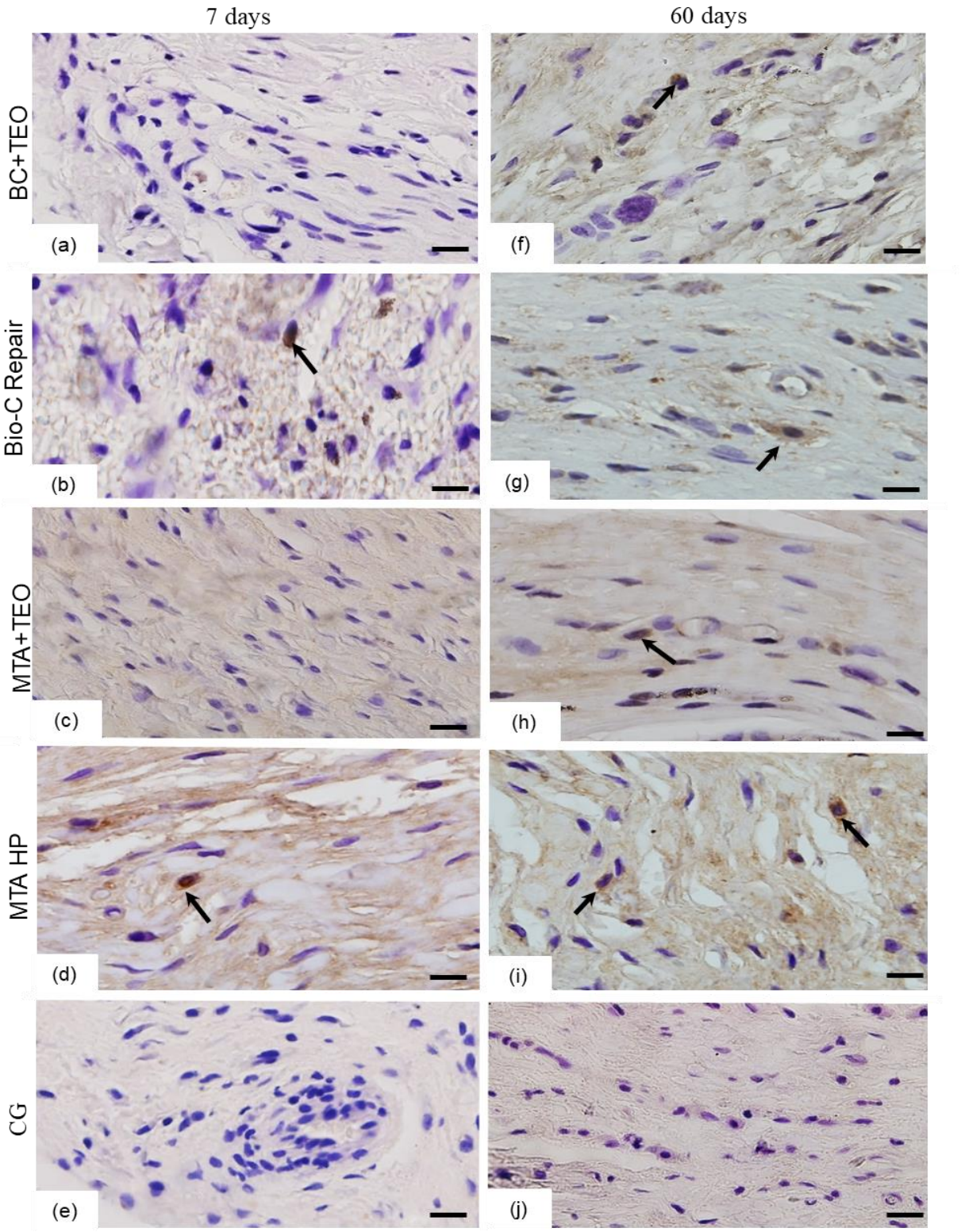

Figure 5: Light micrographs showing portions of capsules adjacent to the polyethylene tubes (T) after 7 (a-e), 15 (f-j), 30 (k-o) and 60 (p-t) days of implantation. Sections were submitted to immunohistochemistry for OCN detection and counterstained with haematoxylin. OCN-immunolabelled cells (arrows) are seen in the capsules. Bars: 18 µm.

Table 2 - The thickness of capsules (TC), number of inflammatory cells (IC) and of fibroblasts (Fb) per mm², number of osteocalcin-immunopositive cells per mm², and collagen content (CF) in the capsules were assessed around the Bio-C Repair + Thymes (BC+TEO), Bio-C Repair (BIO-C), MTA HP + Thymes (MTA+TEO), MTA HP (MTA HP), and Control Group (CG) at 7, 15, 30, and 60 days. Results are presented as mean values with corresponding standard deviations.

Periods	Analysis	BC+TEO	BIO-C	MTA+TEO	MTA HP	CG
7 Days	TC (µm)	202 ± 12$^{a;1}$	312 ± 26$^{b;1}$	212 ± 08^{a,1}	307 ± 22$^{b;1}$	149 ± 32$^{c;1}$
	IC/mm^2	885 ± 15$^{a;1}$	969 ± 11$^{b;1}$	814 ± 19^{a,1}	693 ± 27$^{c;1}$	248 ± 12$^{d;1}$
	Fb/mm^2	163 ± 12$^{a;1}$	131 ± 11$^{b;1}$	158 ± 12$^{a;1}$	110 ± 12$^{b;1}$	171 ± 08$^{c;1}$
	CF (%)	26 ± 6$^{a;1}$	22.8 ± 3$^{b;1}$	24 ± 3$^{b;1}$	24 ± 4$^{b;1}$	28.2 ± 3$^{a;1}$
	OCN	0.00 (0.0) $^{a;1}$	11.11(11.11)$^{b;1}$	0.00 (0.0)$^{a;1}$	11.11(11.11)$^{b;1}$	0.00(0.0)$^{a;1}$
15 Days	TC (µm)	196 ± 22$^{a;1}$	282 ± 11$^{b;2}$	198 ± 08$^{a;1}$	241 ± 20$^{b;2}$	189 ± 11$^{c;1}$
	IC/mm^2	624 ± 14$^{a;2}$	795 ± 12$^{b;2}$	725 ± 22$^{c;2}$	614 ± 12$^{a;2}$	236 ± 15$^{d;1}$
	Fb/mm^2	227 ± 6$^{a;2}$	182 ± 16$^{b;2}$	235 ± 12$^{a;2}$	203 ± 2 $^{b;2}$	246 ± 16 $^{c;2}$
	CF (%)	30 ±4$^{a;2}$	24 ± 2$^{b;1}$	31 ±3$^{a;2}$	25 ± 4$^{b;1}$	34 ± 5$^{c;2}$
	OCN	0.00 (0.0)$^{a;1}$	11.11 (11.11)$^{b;1}$	0.00 (0.0)^{a,1}	22.22(22.22) ^{c,2}	0.00 (0.0)$^{a;1}$
30 Days	TC (µm)	128 ± 7$^{a;2}$	209 ± 9$^{b;3}$	134 ± 14$^{a;2}$	212 ± 18$^{b;2}$	104 ± 4^{c,2}
	IC/mm^2	395 ± 15$^{a;3}$	382 ± 18$^{a;3}$	391 ± 20$^{a;3}$	379 ± 12$^{a;3}$	176 ± 25^{c,2}
	Fb/mm^2	306±9 $^{a;2}$	288 ± 9$^{b;3}$	311 ± 8$^{a;3}$	290 ± 10$^{b;3}$	331 ± 18$^{c;3}$
	CF (%)	32 ±6$^{a;1}$	26 ± 1$^{a;2}$	32 ±2$^{a;2}$	26 ± 3$^{a;1}$	34.6 ± 3$^{b;2}$
	OCN	0.00 (0.0) $^{a;1}$	22.22 (22.22)^{b,2}	0.00 (0.0)$^{a;1}$	44.44(33.34)$^{c;3}$	0.00 (0.0)$^{a;1}$
60 Days	TC (µm)	108 ± 4$^{a;3}$	148 ± 6$^{b;4}$	104 ± 12$^{a;3}$	129 ± 18$^{b;3}$	101 ± 12^{a,2}
	IC/mm^2	234 ± 13$^{a;4}$	242 ± 22$^{a;4}$	235 ± 12$^{a;4}$	232 ± 27$^{a;4}$	68 ± 11^{b,3}
	Fb/mm^2	453±12 $^{a;3}$	417 ± 17$^{b;4}$	441 ± 8$^{a;4}$	428 ± 6$^{b;4}$	534 ± 10$^{c;4}$
	CF (%)	35 ±3$^{a;2}$	29 ± 1$^{b;3}$	34 ±3$^{a;2}$	30.8 ± 1$^{b;2}$	36.2 ± 1^{a,2}
	OCN	11.11(11.11)$^{a;2}$	22.22 (22.22)$^{b;2}$	22.22(22.22)$^{b;2}$	55.56 (33.34)$^{c;4}$	0.00 (0.0)$^{d;1}$

The comparison between groups in the same period is indicated by superscript letters in the lines, same letters = no statistically significant difference.
The comparison between periods in the same group is indicated by superscript numbers in the columns; same numbers = no statistically significant difference. Tukey test ($p \leq 0.05$).
OCN: Values expressed as median and interquartile range. Analysis between groups in each period: Kruskal-Wallis followed by the Dunn test; analysis of each group over time: Friedman followed by the Nemenyi test ($p < 0.05$).

von Kossa reaction and analysis under polarised light

Sections subjected to the von Kossa histochemical method exhibited brown and/or yellow structures, i.e. von Kossa-positive structures in the capsules around all materials (Figs. 6a-6h). Unstained sections analyzed under polarised light revealed birefringent structures in regions of the capsules compatible with the von Kossa-positive structures (Figs. 6i-6p). Either von Kossa-positive or birefringent structures were not found in the CG capsules (data not shown).

Figure 6: von Kossa and birefringent structures in unstained sections.

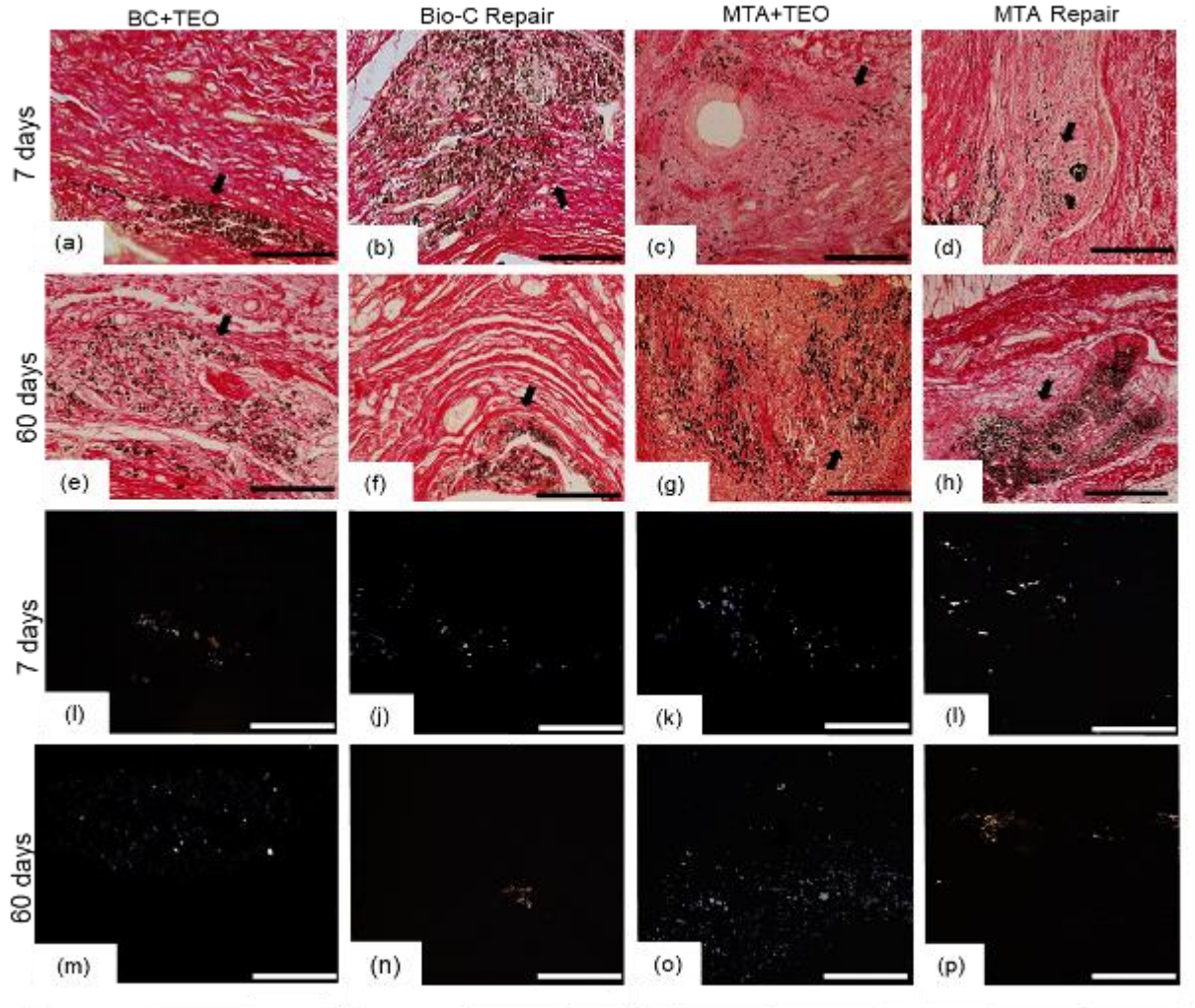

Figure 6: Photomicrographs of sections revealing segments of capsules subjected to the von Kossa reaction after 7 (a-d) and 60 days (h-i). Distinct von Kossa-positive structures (black-brown color) are evident in the capsule's specimens. Unstained sections, examined under polarized light, reveal birefringent structures in the capsules after 7 (e-g) and 60 (j-m) days. Scale bars: 36 µm.

Discussion

This study evaluated the biocompatibility and bioactivity of Bio-C Repair and MTA HP cements containing *Thyme Essential Oil* (TEO). These experimental materials induced a lower recruitment of inflammatory cells than BIO-C repair. Furthermore, the reduction in the inflammatory reaction accompanied by increase in the number of fibroblasts and in the collagen in the capsules around all the materials observed over time indicate that experimental materials are biocompatible. Although the addition of TEO did not harm the biocompatibility of BIO and MTA HP materials, the presence of immunoexpression of osteocalcin in the capsules around the BC+TEO and MTA+TEO specimens only at 60 days suggests that this anti-inflammatory oil may cause a delay in cellular differentiation. Thus, in the present study the null hypothesis was partially accepted.

Studies have shown that the addition of natural oils provides an increase in the antimicrobial effect without clearly compromising the physicochemical properties of dental materials. The addition of natural oils butia or copaiba to experimental resin-based endodontic cements enhanced the antibacterial activity without causing significant damage to their physicochemical properties (Reiznautt *et al.* 2023). 5% cinnamon essential oil incorporated into glass ionomer improved antimicrobial effects against *S. mutans* and *C. albicans,* in addition to stimulating the fluoride release without compromising its compressive strength (Sherief *et al.* 2020).

As expected, calcium silicate-based materials implanted in the subcutaneous connective tissue initially stimulate the recruitment of inflammatory cells, culminating in the formation of an inflammatory reaction in close juxtaposition to the materials due to the alkaline pH, Bio-C Repair demonstrated a pH around 7 (Oliveira *et al.* 2021), in turn, MTA repair provides an alkaline pH around 9 (Guimarães *et al.* 2018), this pH stimulates the recruitment of leukocytes. It is known that surgical procedure may cause an injury to the subcutaneous connective tissue (Viola *et al.* 2012, Alves-Silva *et al.* 2020) justifying, at least in part, the inflammatory reaction observed in the CG specimens. However, the capsules around the implanted materials contained approximately 2.7 to 3.9 folds more inflammatory cells than in CG specimens due to irritant potential of these materials.

In the present study, Bio-C Repair initially induced a marked inflammatory reaction compared to other bioceramic materials. The marked genotoxicity of Bio-C

Repair when added to the culture of NIH/3T3 mouse fibroblasts in comparison to MTA has been explained due to the presence of other components such as iron oxide, in addition to the high amount of calcium ions released by Bio-C Repair in the initial periods (Klein Júnior *et al.* 2021). Maru *et al. (*2023) they also demonstrated that Bio-C Repair released much more calcium (Ca) than MTA, influencing cell viability. When compared to MTA and Biodentine, Bio-C Repair presented the longest setting time and the greatest dimensional expansion, the prolonged effect of its substances may justify superior irritating potential (Campi *et al*.2023).

Our findings point to a potent effect anti-inflammatory of TEO, particularly, when this oil was added to the Bio-C Repair since this experimental material induced a lower recruitment of inflammatory cells than the BIO-C. It has been attributed to the thyme essential oil rich in carvacrol and thymol strong anti-inflammatory activity, antimicrobial effectiveness antioxidant activity, a broad-spectrum antibacterial activity against Gram-positive and Gram- (Ahmed *et al*. 2022).

However, both experimental materials allowed a gradual and significant reduction in the inflammatory cells culminating in the formation of thinner capsules than those around the BIO-C and MTA HP specimens. In fact, 30 days after implantation, thin capsules were only found around the experimental materials reinforcing the idea that this oil could reduce the irritant potential of these bioceramic materials and, therefore, does not interfere with biocompatibility of BIO-C and MTA HP materials. Besides biocompatibility presented by thyme oil added to the hydrogel membranes, this oil has also demonstrated great potential for effective wound treatment (Singh *et al*. 2022). A mild or moderate cytotoxic effect on fibroblasts 929 clone was only observed with elevate concentrations (at 1000 µg·mL 1) of thyme essential oil (Berecht *et al.* 2020).

In the present study, the TEO added to bioceramic materials induced the formation of capsules containing accentuated number of fibroblasts in comparison with pure bioceramic materials indicating, therefore, that this oil stimulated the proliferation of these cells. In fact, the capsules around experimental materials contained elevated content of collagen in comparison with BIO-C and MTA HP suggesting that these fibroblasts were responsible for production of extracellular matrix components, particularly, the collagen fibres.

The association of thyme with propolis revealed the promising nature of the pulp capping material. This assessment considered the antimicrobial properties and

cytotoxicity exhibited by the compounds under investigation. The thyme and propolis shows low cytotoxicity when added to culture of fibroblasts/ both at 24 and 72 hours (Esmaeilzadeh *et al.* (2023). The main compounds in thyme oil can reduce the levels of the cytokines IL-6 and TNFα and are even good candidates for use in preventing neuroinflammation and neurodegeneration (Horvát *et al.* 2021).

In rats that thyme oil and thymol neutralize the hepatotoxicity of doxorubicin (chemotherapy drug); thyme oil seemed more effective than thymol. This preventive effect may be mediated by increasing cellular antioxidant defenses and modulating inflammation and apoptosis (Ahmed *et al.* 2022)

The use of a cement with good biological and physical-chemical properties is essential for the success of endodontic treatment. The content of bioactive compounds in spice plants varies depending on the harvest time, type of processing, drying and storage, which can also considerably affect their therapeutic properties.

Currently, materials based on tricalcium silicate are the preferred choice for regeneration and repair procedures in endodontics, primarily due to their bioactivity. This bioactivity is, at least in part, ascribed to the hydration reaction of tricalcium and dicalcium silicates, which are the primary components of bioceramic materials. The interaction of di- and tricalcium silicates with water results in the formation of calcium silicate hydrate and calcium hydroxide (Camilleri 2020; Silva *et al.* 2021).

Calcium hydroxide undergoes dissociation, yielding Ca^{+2} and OH^{-}, causing an increase in the pH resulting in the alkaline microenvironment (Niu *et al*. 2014). Additionally, an excess of calcium in the extracellular fluid can lead to calcium precipitation, and in conjunction with phosphate from tissue fluids, may initiate apatite nucleation (Ding e*t al.* 2009). The process of calcium phosphate precipitation is regulated by various mediators, including alkaline phosphatase, bone sialoprotein, osteopontin, and osteocalcin (Delfino *et al*. 2021, Queiroz *et al.* 2023). Among these mediators, osteocalcin is a protein synthesized by cells of mineralized tissues and constitutes one of the main non-collagenous components of the bone matrix. When interacting with the calcium in hydroxyapatite, it has been suggested that this protein may regulate the nucleation of apatite crystals (Manolagas 2020, da Silva Sasso *et al.* 2023) as well as may have exert a role in the osteoblast differentiation (da Silva Sasso *et al.* 2023).

In the present study, cells immunostained with OCN were observed in the capsules of bioceramic materials, suggesting a bioactive potential of these materials

as described in other studies (Delfino *et al.* 2021, Queiroz *et al.* 2023, Inada *et al.* 2023). Here, BIO-C and MTA HP showed immunostaining in all periods. In contrast, the materials with the addition of essential oil induced the OCN-immunoexpression only after 60 days, although there is evidence suggesting that essential oils have an impactful bioactivity (Šojić *et al.* 2023). It has been suggested that the bioactive potential of thyme oil is directly related to its chemical composition, which can be influenced by the vegetative stage, seasonal variation in humidity, temperature, harvest, and post-harvest factors such as drying and storage. In the production of thyme essential oil, it is essential to guarantee the purity, efficacy, and safety of the final product, however, even with quality control, variations can be caused (Nascimento *et al.* 2020). Thus, it is possible that the delay in the immunoexpression of osteocalcin by cells of connective tissue from capsules around these experimental materials may be due to the partial loss of the proprieties of thyme oil. However, further studies are needed to clarify this issue.

In constrast, von Kossa-positive structures were noticed in the innermost portion of capsules around all materials, including experimental materials, in all time points. von Kossa reaction is a histochemical technique able to reveal calcium deposits in the tissues and/or organs (Viola *et al.* 2012, Delfino *et al.* 2021, Queiroz *et al.* 2023). Therefore, the presence of von Kossa-positive structures in the capsules juxtaposed to the implanted materials are indicative that these bioceramic materials release the calcium ions. The presence of von Kossa-positive structures in the capsules around BIO+TEO and MTA+TEO shows that thyme oil should not impede the calcium release by Bio-C and MTA HP repair materials.

Additionally, birefringent structures found in the capsules around all materials from unstained sections examined under polarised light, reinforce the concept that these structures may constitute amorphous calcite derived from calcium carbonate (Holland *et al.* 1999, Delfino *et al*. 2021, Queiroz *et al.* 2023). Bioceramic materials when hydrated give rise to calcium hydroxide whose dissociation provides calcium ions and hydroxyl (OH^-). Calcium ions react with carbonate dioxide present in the tissue fluids give rising to amorphous calcium carbonate (Khalil, Naaman & Camilleri, 2016, Camilleri, 2020). Considering that von Kossa and birefringent structures were seen either in the capsules around the experimental materials or BIO-C and MTA HP, it is conceivable to suggest that TEO did not interfere with calcium release.

As osteocalcin-immunolabelled cells, von Kossa-positive and birefringent structures were not observed in the capsules around the CG specimens, our findings taken together reinforce the concept that these materials present bioactive potential. It has been suggested that deposition of amorphous calcite may stimulate the mesenchymal cells to express phenotype of mineralized tissue-producing cells and, therefore, these materials could favour the repair of periodontal tissues, including alveolar bone and cementum. However, the interaction of TEO with BIO-C and MTA HP needs be further investigated, since these associations caused a delay in the immunoexpression of osteocalcin by cells of connective tissue, which could interfere with the mineralized tissues repair.

Conclusion

The addition of thyme oil to the Bio-C sealer reduced the recruitment of inflammatory cells indicating that this oil alleviated the inflammatory reaction caused by Bio-C repair. The marked reduction in the inflammatory reaction associated with evident increase in the number of fibroblasts and in the content of collagen in the capsules around experimental materials over time, support the idea that these materials are biocompatible. Besides biocompatibility, our results also suggested that experimental bioceramic materials present bioactive potential.

CONFLICT OF INTEREST

The authors have stated explicitly that there are no conflicts of interest in connection with this article.

References

Alves-Silva ECA, Tanomaru-Filho M, da Silva GF, Delfino MM, Cerri PS, Guerreiro-Tanomaru JM. (2020) Biocompatibility and bioactive potential of new calcium silicate–based endodontic sealers: Bio-C Sealer and Sealer Plus BC. *Journal of Endodontics* 46, 1470-1477.

Ahmed OM, Galaly SR, Mostafa MA, Eed EM, Ali TM, Fahmy AM, Zaky MY. (2022). Thyme oil and thymol counter doxorubicin-induced hepatotoxicity via modulation of inflammation, apoptosis, and oxidative stress. *Oxidative Medicine and Cellular Longevity*, *2022*.

Berechet MD, Gaidau C, Miletic A, Pilic B, Râpă M, Stanca M, Lazea-Stoyanova A. (2020). Bioactive properties of nanofibres based on concentrated collagen hydrolysate loaded with thyme and oregano essential oils. *Materials 13* (7), 1618.

Camilleri, J. (2020) Classification of hydraulic cements used in dentistry. *Frontiers in Dental Medicine*, 1, 9.

Campi LB, Rodrigues EM, Torres FFE, Reis JMDSN, Guerreiro-Tanomaru JM, Tanomaru-Filho M. (2023). Physicochemical properties, cytotoxicity, and bioactivity of a ready-to-use bioceramic repair material. *Brazilian Dental Journal* 34, 29-38.

da Silva Sasso GR, Florencio-Silva R, de Pizzol-Júnior JP, Gil CD, Simões MDJ, Sasso-Cerri, E, Cerri PS. (2023). Additional Insights Into the Role of Osteocalcin in Osteoblast Differentiation and in the Early Steps of Developing Alveolar Process of Rat Molars. *Journal of Histochemistry & Cytochemistry* 71 (12), 689-708.

Delfino MM, de Abreu Jampani JL, Lopes CS, Guerreiro-Tanomaru JM, Tanomaru-Filho M, Sasso-Cerri E, *et al.* (2021) Comparison of Bio-C Pulpo and MTA repair HP with White MTA: effect on liver parameters and evaluation of biocompatibility and bioactivity in rats. *International Endodontic Journal* 54, 1597–1513.

Ding SJ, Shie MY, Wang, CY. (2009) Novel fast-setting Calcium silicate bone cements with high bioactivity and enhanced osteogenesis in vitro. *Journal of Materials Chemistry* 19, 1183–1190.

Esmaeilzadeh M, Moradkhani S, Daneshyar F, Arabestani MR, Asl SS, Tayebi S, Farhadian, M. (2023). Antimicrobial and cytotoxic properties of calcium-enriched mixture cement, Iranian propolis, and propolis with herbal extracts in primary dental pulp stem cells. *Restorative Dentistry & Endodontics* 48(1).

Holland R, de Souza V, Nery MJ, Otoboni Filho JA, Bernabé PFE, Dezan Jr, E. (1999). Reaction of dogs' teeth to root canal filling with mineral trioxide aggregate or a glass ionomer sealer. *Journal of Endodontics* 25, 728-730.

Horváth G, Horváth A, Reichert G, Böszörményi A, Sipos K, Pandur E. (2021). Three chemotypes of thyme (Thymus vulgaris L.) essential oil and their main compounds affect differently the IL-6 and TNFα cytokine secretions of BV-2 microglia by modulating the NF-κB and C/EBPβ signalling pathways. *BMC Complementary Medicine and Therapies 21*(1), 1-14.

Jafri H, Ahmad I. (2020). Thymus vulgaris essential oil and thymol inhibit biofilms and interact synergistically with antifungal drugs against drug resistant strains of Candida albicans and Candida tropicalis. *Journal de Mycologie Medicale 30*(1), 100911.

Khalil I, Naaman A, Camilleri J. (2016). Properties of tricalcium silicate sealers. *Journal of Endodontics* 42(10), 1529-1535.

Klein-Junior CA, Zimmer R, Dobler T, Oliveira V, Marinowic DR, Özkömür A, Reston EG. (2021) Cytotoxicity assessment of Bio-C Repair ion^{+}: A new calcium silicate-based cement. *Journal of Dental Research, Dental Clinics, Dental Prospects* 15, 152.

Lima SPR, Santos GLD, Ferelle A, Ramos SP, Pessan JP, Dezan-Garbelini CC. (2020) Clinical and radiographic evaluation of a new stain-free tricalcium silicate cement in pulpotomies. *Brazilian Oral Research* 34, e102.

Lozano-Guillén A, López-García S, Rodríguez-Lozano FJ, Sanz JL, Lozano A, Llena C, Forner L. (2022) Comparative cytocompatibility of the new calcium silicate-based cement NeoPutty versus NeoMTA Plus and MTA on human dental pulp cells: an in vitro study. *Clinical Oral Investigations* 26, 7219-7228.

Inada RNH, Queiroz MB, Lopes CS, Silva ECA, Torres FFE, da Silva GF *et al.* (2023) Biocompatibility, bioactive potential, porosity, and interface analysis calcium silicate repair cement in a dent in tube model. *Clinical Oral Investigations* 1-15.

International Organization for Standardization. (2016). ISO 10993-6 Biological evaluation of medical devices. Part 6: Tests for local effects after implantation. Geneva: ISO.

Manolagas, S. C. (2020) Osteocalcin promotes bone mineralization but is not a hormone. *PLoS Genetics*, 16, e1008714.

Maru V, Madkaikar M, Gada A, Pakhmode V, Padawe D, Bapat S. (2023). Response of stem cells derived from human exfoliated deciduous teeth to Bio-C Repair and Mineral Trioxide Aggregate Repair HP: Cytotoxicity and gene expression assessment. *Dental Research Journal*, 20.

Nagendrababu V, Kishen A, Murray PE, Nekoofar MH, de Figueiredo JAP, Priya E, Dummer PMH. (2021) PRIASE 2021 guidelines for reporting animal studies in endodontology: a consensus-based development. *International Endodontic Journal* 54, 848-857.

Nascimento L, Barbosa de Moraes AA, Santana da Costa K., Pereira Galúcio JM, Taube PS, Leal Costa CM, Guerreiro de Faria LJ. (2020). Bioactive natural compounds and antioxidant activity of essential oils from spice plants: new findings and potential applications. *Biomolecules 10*(7), 988.

Niu LN, Jiao K, Zhang W, Camilleri J, Bergeron BE, Feng HL, Tay FR. (2014) A review of the bioactivity of hydraulic calcium silicate cements. *Journal of Dentistry* 42, 517-533.

Parirokh M, & Torabinejad M. (2010). Mineral trioxide aggregate: a comprehensive literature review—part I: chemical, physical, and antibacterial properties. *Journal of Endodontics* 36(1), 16-27.

Queiroz MB, Inada RN, Jampani JLDA, Guerreiro-Tanomaru JM, Sasso-Cerri E, Tanomaru-Filho M, Cerri PS. (2023) Biocompatibility and bioactive potential of an experimental tricalcium silicate-based cement in comparison with Bio-C repair and MTA Repair HP materials. *International Endodontic Journal* 56, 259-277.

Reiznautt CM, Ribeiro JS, Kreps E, da Rosa WL, de Lacerda H, Peralta SL, Lund RG. (2021). Development and properties of endodontic resin sealers with natural oils. *Journal of Dentistry,* 104, 103538.

Ruiz-Linares, M., Ferrer-Luque, C. M., Arias-Moliz, T., de Castro, P., Aguado, B., & Baca, P. (2014). Antimicrobial activity of alexidine, chlorhexidine and cetrimide against Streptococcus mutans biofilm. *Annals of Clinical Microbiology and Antimicrobials 13*, 1-6.

Silva GF, Tanomaru-Filho M, Bernardi MI, Guerreiro-Tanomaru JM, Cerri PS. (2015). Niobium pentoxide as radiopacifying agent of calcium silicate-based material: evaluation of physicochemical and biological properties. *Clinical Oral investigations* 19, 2015-2025.

Silva GF, Guerreiro-Tanomaru JM, Da Fonseca TS, Bernardi MIB, Sasso-Cerri E, Tanomaru-Filho M, Cerri PS. (2017). Zirconium oxide and niobium oxide used as radiopacifiers in a calcium silicate-based material stimulate fibroblast proliferation and collagen formation. *International Endodontic Journal* 50, e95-e108.

Silva ECA, Tanomaru-Filho M, Silva GF, Lopes CS, Cerri OS, Guerreiro-Tanomaru JM. (2021) Evaluation of the biological properties of two experimental calcium silicate sealers: an in vivo study in rats. *International Endodontic Journal*, 54, 100–111.

Sherief DI, Fathi MS, Abou El Fadl RK. (2021). Antimicrobial properties, compressive strength, and fluoride release capacity of essential oil-modified glass ionomer cements an in vitro study. *Clinical Oral Investigations,* 25, 1879-1888.

Schött G, Liesegang S, Gaunitz F, Gleß A, Basche S, Hannig C, Speer K. (2017). The chemical composition of the pharmacologically active Thymus species, its

antibacterial activity against Streptococcus mutans and the antiadherent effects of T. vulgaris on the bacterial colonization of the in-situ pellicle. *Fitoterapia*, *121*, 118-128.

Singh P, Verma C, Mukhopadhyay S, Gupta A, Gupta B. (2022). Preparation of thyme oil loaded κ-carrageenan-polyethylene glycol hydrogel membranes as wound care system. *International Journal of Pharmaceutics*, *618*, 121661.

Šojić B, Milošević S, Savanović D, Zeković Z, Tomović V, & Pavlić B. (2023). Isolation, bioactive potential, and application of essential oils and terpenoid-rich extracts as effective antioxidant and antimicrobial agents in meat and meat products. *Molecules*, *28*(5), 2293.

Viola NV, Guerreiro-Tanomaru JM, da Silva GF, Sasso-Cerri E, Tanomaru-Filho M. & Cerri PS. (2012) Biocompatibility of experimental MTA sealer implanted in the rat subcutaneous: quantitative and immunohistochemical evaluation. *Journal Biomedical Materials Research Part B, Applied Biomaterials*, 100, 1773-1781.

Yaltirik M, Ozbas H, Bilgic B, Issever H. (2004) Reactions of connective tissue to mineral trioxide aggregate and amalgam. *Journal of Endodontics* 30, 95–99.

Zhang R, Chen M, Lu Y, Guo X, Qiao F, Wu L. (2015). Antibacterial and residual antimicrobial activities against enterococcus faecalis biofilm: A comparison between EDTA, chlorhexidine, cetrimide, MTAD and QMix. *Scientific Reports,* 5(1), 12944.

4 DISCUSSÃO

Os materiais à base de silicato de cálcio implantados no tecido conjuntivo subcutâneo inicialmente induzem o recrutamento de células inflamatórias, com o grau de reação inflamatória associado à composição química e propriedades físicas dos materiais[10,11].

O NPutty demonstrou maior recrutamento de células inflamatórias que BC e MTA HP, possivelmente devido a substâncias orgânicas presentes em seu componente líquido. De forma similar, o material NeoFlo demonstrou maior recrutamento de células inflamatórias em comparação com o BC e o AHP, resultando em uma reação inflamatória moderada que persistiu por até 60 dias após o implante. No entanto, tanto NPutty quanto o NeoFlo demonstraram capacidade de estimular a expressão de OCN e promover a deposição de fosfato/cálcio, indicando potencial bioativo.

Embora o NeoFlo e o Bio-C Repair apresentem silicato tricálcico e dicálcico como principais componentes, suas composições diferem em outros aspectos. O NeoFlo possui sulfato de cálcio, grossita e tantalita, além de um agente espessante cuja composição não é especificada pelo fabricante, enquanto o BC contém óxido de cálcio, óxido de ferro, dióxido de silício e óxido de zircônio como radiopacificador. Essas diferenças na composição química podem influenciar as reações teciduais.

O tempo de presa do NeoFlo (1344 minutos)[6], mais longo em comparação com o BC (220 minutos)[19], e pode contribuir para a intensidade da resposta inflamatória induzida por esses cimentos. Apesar de uma redução gradual no número de células inflamatórias ao redor do NeoFlo ao longo do tempo, foi observada uma reação inflamatória persistente em 60 dias, enquanto o BC apresentou uma reação inflamatória leve nesse período.

A composição química dos materiais à base de silicato de cálcio pode influenciar suas propriedades e reações teciduais. Estudos mostraram que cimentos à base de aluminato tricálcico e óxido de tântalo também apresentam biocompatibilidade e potencial bioativo em diferentes contextos[2,20]. Apesar do atraso no rearranjo do tecido conjuntivo ao redor do NPutty, houve uma regressão significativa na reação inflamatória ao longo do tempo, sugerindo que o material causou danos iniciais, mas permitiu a recuperação gradual do tecido.

Foi demonstrado que os cimentos endodônticos à base de silicato de cálcio estão envolvidos na diferenciação osteoblástica[21]. A osteocalcina (OCN) é uma glicoproteína pequena, expressa preferencialmente pelos osteoblastos, principalmente nos estágios finais de sua diferenciação, e consequentemente sua presença pode ser considerada como um indicador da capacidade formar tecido mineralizado[10,11,21]. OCN liga-se fortemente ao cálcio e, portanto, essa proteína não colágena parece estar envolvida na regulação da mineralização da matriz.

Células imunomarcadas com OCN foram observadas nas cápsulas dos cimentos NeoFlo e BC, onde BC apresentou os maiores valores aos 60 dias. O cimento BC pode contribuir no processo de mineralização dos tecidos periapicais, pois demonstra potencial bioativo[10]. Aos 60 dias a imunoexpressão de OCN para NPutty foi reduzida sugerindo que o atraso na regressão da reação inflamatória e no reparo do tecido conjuntivo pode interferir na bioatividade dos materiais biocerâmicos.

Os materiais à base de silicato tricálcico são utilizados em procedimentos de regeneração e reparo endodôntico devido à sua bioatividade, promovendo a formação de silicato de cálcio hidratado e hidróxido de cálcio, que alcalinizam o microambiente e estimulam a nucleação de apatita[4,10,11,22].

Além da imunoexpressão de OCN, as cápsulas ao redor desses cimentos também exibiram estruturas positivas para von Kossa, indicando depósitos de sal (cálcio e/ou fosfato)[22]. Nas amostras AHP foram observadas estruturas birrefringentes apenas na superfície mais interna das cápsulas, concordando com outros estudos que demonstraram menor liberação de íons cálcio para AH Plus do que aquela promovida por selantes biocerâmicos[10,11]. Os resultados obtidos de von Kossa combinados com estruturas birrefringentes sugerem um potencial bioativo do NeoFlo, NPutty, BC e MTA HP. O processo de reação dos íons cálcio e dióxido de carbono leva à formação de calcita, estrutura amorfa e birrefringente que é considerada um parâmetro sugestivo do potencial bioativo de um material endodôntico[10,11,22].

Um material bioativo cria um ambiente compatível com a osteogênese e, em alguns casos, compatível com tecidos moles, desenvolvendo uma interface de ligação natural entre materiais vivos e não vivos[23].

A CTR é um surfactante catiônico conhecido por sua atividade antibacteriana, que pode ser adicionado aos cimentos endodônticos para melhorar sua eficácia

antibacteriana[14]. Apesar da intensa reação inflamatória inicial, os cimentos com adição de CTR mostraram redução significativa no número de células inflamatórias ao longo do tempo, indicando biocompatibilidade. No entanto, a adição de CTR ao cimento BioRoot™ RCS causou uma lesão tecidual mais grave em comparação com o NeoSealer Flo, sugerindo que a escolha do melhor cimento pode depender do grau de infecção do canal radicular.

A diferença na composição química dos cimentos pode explicar os padrões diferentes de reação tecidual observados. Enquanto o BioRoot™ RCS é à base de silicato de cálcio[24], o NeoSealer Flo contém sulfato de cálcio, grossita e tantalita[6], o que pode influenciar a liberação de íons e o pH do microambiente. Apesar da reação inflamatória, a liberação de íons pelos cimentos biocerâmicos pode criar um ambiente propício para a diferenciação de células mesenquimais em células produtoras de tecido mineralizado. A redução da reação inflamatória foi acompanhada por um aumento gradual no conteúdo de fibroblastos e colágeno ao longo do tempo, indicando, portanto, que esses cimentos são biocompatíveis. Estruturas birrefringentes e imunoexpressão de OCN sugerem potencial bioativo de NeoFlo e BROOT puros, bem como destes cimentos com adição de 1% de cetrimida.

Os materiais com TEO induziram um menor recrutamento de células inflamatórias em comparação com o Bio-C Repair puro. Apesar da adição de TEO não prejudicar a biocompatibilidade dos materiais, a presença deste óleo pode atrasar a diferenciação celular, como indicado pela imunoexpressão de osteocalcina observada apenas aos 60 dias.

A literatura tem demonstrado que a adição de óleos naturais pode aumentar a atividade antimicrobiana dos materiais odontológicos sem comprometer suas propriedades físico-químicas[25,26]. No entanto, o Bio-C Repair demonstrou inicialmente uma reação inflamatória mais acentuada devido à liberação de íons cálcio e outros componentes.

O óleo de tomilho, rico em carvacrol e timol, possui forte atividade anti-inflamatória e antimicrobiana, o que pode reduzir o recrutamento de células inflamatórias. Além disso, a presença de TEO estimulou a proliferação de fibroblastos e a produção de colágeno, sugerindo um efeito benéfico na cicatrização. Embora a adição de óleo essencial de tomilho tenha induzido a imunoexpressão de osteocalcina apenas após 60 dias, a presença de estruturas positivas para von

Kossa nas cápsulas ao redor dos materiais com óleo sugere que este não interfere na liberação de cálcio.

5 CONCLUSÃO

De acordo com os resultados obtidos no presente estudo, conclui-se:

O NeoFlo mostrou menor biocompatibilidade do que o cimento Bio-C Sealer e maior recrutamento de células inflamatórias quando comparado ao AH Plus. Além disso, tanto o NeoFlo quanto o BC foram capazes de estimular a imunoexpressão de OCN nas cápsulas, bem como permitir a deposição de calcita amorfa, sugerindo um potencial bioativo;

Considerando os resultados em conjunto, indica-se que o NeoPutty é biocompatível, embora o potencial irritante deste material biocerâmico no tecido conjuntivo seja maior do que o do Bio C Repair e do MTA HP. Além disso, a imunoexpressão da osteocalcina pelas células do tecido conjuntivo, assim como as estruturas positivas para von Kossa e os depósitos birrefringentes, são parâmetros sugestivos de que o NeoPutty apresenta potencial bioativo;

A adição de cetrimida aos cimentos biocerâmicos NeoSealer e BioRoot RCS induziu um maior recrutamento de células inflamatórias. No entanto, a redução na reação inflamatória foi acompanhada por um aumento gradual nos fibroblastos e no teor de colágeno ao longo do tempo, indicando, portanto, que esses cimentos são biocompatíveis. Estruturas birefringentes e imunoexpressão de OCN sugerem o potencial bioativo do NeoFlo puro e do BROOT, bem como desses selantes com adição de 1% de cetrimida.;

A adição de óleo de tomilho ao cimento Bio-C reduziu o recrutamento de células inflamatórias, indicando que este óleo atenuou a reação inflamatória causada pelo Bio-C Repair. A significativa redução na reação inflamatória, associada ao aumento evidente no número de fibroblastos e no teor de colágeno nas cápsulas ao redor dos materiais experimentais ao longo do tempo, apoia a ideia de que esses materiais são biocompatíveis. Além da biocompatibilidade, nossos resultados também sugeriram que os materiais biocerâmicos experimentais apresentam potencial bioativo.

REFERÊNCIAS*

1. Sun Q, Meng M, Steed JN, Sidow SJ, Bergeron BE, Niu LN, Tay FR et al. Manoeuvrability and biocompatibility of endodontic tricalcium silicate-based putties. J Dent. 2021; 104: 103530.

2. Lozano-Guillén A, López-García S, Rodríguez-Lozano F J, Sanz JL, Lozano A, Llena C et al. Comparative cytocompatibility of the new calcium silicate-based cement NeoPutty versus NeoMTA Plus and MTA on human dental pulp cells: an in vitro study. Clin Oral Investig. 2022: 26(12): 7219–28.

3. KleinJunior CA, Zimmer R, Dobler T, Oliveira V, Marinowic DR, Özkömür, A et al. Cytotoxicity assessment of Bio-C Repair Íon+: A new calcium silicate-based cement. J Dent Res Dent Clin Dent Prospects. 2021; 15(3): 152-6.

4. Queiroz MB, Inada RN, Jampani JLDA, Guerreiro-Tanomaru JM, Sasso-Cerri, E, Tanomaru-Filho M et al. Biocompatibility and bioactive potential of an experimental tricalcium silicate-based cement in comparison with Bio-C repair and MTA Repair HP materials. Int Endod J. 2022; 56(2): 259-77.

5. Vazquez-Garcia F, Tanomaru-Filho M, Chávez-Andrade GM, Bosso-Martelo R, Basso-Bernardi MI, Guerreiro-Tanomaru JM. Effect of silver nanoparticles on physicochemical and antibacterial properties of calcium silicate cements. Braz Dent J. 2016; 27(5): 508-14.

6. Zamparini F, Prati C, Taddei P, Spinelli A, Di Foggia M, Gandolfi MG. Chemical-physical properties and bioactivity of new premixed calcium silicate-bioceramic root canal sealers. Int J Mol Sci. 2022; 23(22): 13914.

7. Alshaikh NA, Perveen K. Susceptibility of fluconazole-resistant Candida albicans to thyme essential oil. Microorganisms. 2021; 9(12): 24-54.

8. Horváth G, Horváth A, Reichert G, Böszörményi A, Sipos K, Pandur E. (2021). Three chemotypes of thyme (Thymus vulgaris L.) essential oil and their main compounds affect differently the IL-6 and TNFα cytokine secretions of BV-2 microglia by modulating the NF-κB and C/EBPβ signalling pathways. BMC Complementary Medicine and Therapies 21(1), 1-14.

9. Jung S, Libricht, V, Sielker S, Hanisch MR, Schäfer E, Dammaschke T. Evaluation of the biocompatibility of root canal sealers on human periodontal ligament cells ex vivo. Odontology. 2019; 107(1): 54-63.

10. Alves-Silva EC, Tanomaru-Filho M, da Silva GF, Delfino MM, Cerri PS, Guerreiro-Tanomaru JM. Biocompatibility and bioactive potential of new calcium silicate–based endodontic sealers: Bio-C sealer and sealer plus BC. J Endod. 2020; 46(10): 1470-7.

* De acordo com o Guia de Trabalhos Acadêmicos da FOAr, adaptado das Normas Vancouver. Disponível no site da Biblioteca: http://www.foar.unesp.br/#biblioteca/manual.

11. Silva ECA, Tanomaru-Filho M, Silva GF, Lopes CS, Cerri PS, Guerreiro Tanomaru JM. Evaluation of the biological properties of two experimental calcium silicate sealers: an in vivo study in rats. Int Endod J. 2021; 54(1): 100-11.

12. Colombo M, Poggio C, Dagna A, Meravini MV, Riva P, Trovati F et al. Biological, and physico-chemical properties of new root canal sealers. J Clin Exp Dent. 2018; 10(2): e120.

13. Ruiz-Linares M, Ferrer-Luque CM, Arias-Moliz T, de Castro P, Aguado B, Baca P. Antimicrobial activity of alexidine, chlorhexidine and cetrimide against Streptococcus mutans biofilm. Ann Clin Microbiol Antimicrob. 2014; 13: 1-6.

14. Zhang R., Chen M, Lu Y, Guo X, Qiao F, Wu L. Antibacterial and residual antimicrobial activities against Enterococcus faecalis biofilm: a comparison between EDTA, chlorhexidine, cetrimide, MTAD and QMix. Sci Rep. 2015; 5: 1-5.

15. Delfino MM, Jampani JLDA, Lopes CS, Guerreiro-Tanomaru JM, Tanomaru-Filho M, Sasso-Cerri E et al. The participation of fibroblast growth factor-1 and interleukin-10 in connective tissue repair following subcutaneous implantation of bioceramic materials in rats. Int Endod J. 2023; 56(3): 385-401.

16. Saraiva JA, Da Fonseca TS, Da Silva GF, Sasso-Cerri E, Guerreiro-Tanomaru JM, Tanomaru-Filho M et al.Reduced interleukin-6 immunoexpression and birefringent collagen formation indicate that MTA Plus and MTA Fillapex are biocompatible. Biomed Mater. 2018; 13(3): 035002.

17. Yaltirik M, Ozbas H, Bilgic B, Issever H. Reactions of connective tissue to mineral trioxide aggregate and amalgam. J Endod. 2004; 30(2): 95-9.

18. de Pizzol Júnior JP, Sasso-Cerri E, Cerri, PS. Matrix metalloproteinase-1 and acid phosphatase in the degradation of the lamina propria of eruptive pathway of rat molars. Cells. 2018; 7(11): 206.

19. Zordan-Bronzel CL, Torres FFE, Tanomaru-Filho M, Chávez-Andrade GM, Bosso-Martelo R, Guerreiro-Tanomaru JM. Evaluation of physicochemical properties of a new calcium silicate–based sealer, Bio-C Sealer. J Endod. 2019; 45(10): 1248-1252.

20. Silva GF, Guerreiro-Tanomaru JM, da Fonseca TS, Bernardi MIB, Sasso-Cerri E, Tanomaru-Filho M, et al. Zirconium oxide and niobium oxide used as radio pacifiers in a calcium silicate-based material stimulate fibroblast proliferation and collagen formation. Int Endod J. 2017; 50 Suppl 2: e95–e108.

21. Viana Viola N, Guerreiro-Tanomaru J, Ferreira da Silva G, Sasso-Cerri E, Tanomaru-Filho M, Cerri PS. Biocompatibility of an experimental MTA sealer implanted in the rat subcutaneous: quantitative and immunohistochemical evaluation. Journal of Biomedical Materials Research Part B: Applied Biomaterials. 2012; 100(7): 1773-1781.

22. Silva GF, Tanomaru-Filho M, Bernardi MI, Guerreiro-Tanomaru JM, Cerri, PS. Niobium pentoxide as radiopacifying agent of calcium silicate-based material: evaluation of physicochemical and biological properties. Clin Oral Investig. 2015; 19: 2015-2025.

23. Niu LN, Jiao K, Zhang W, Camilleri J, Bergeron BE, Feng HL, Tay FR. (2014) A review of the bioactivity of hydraulic calcium silicate cements. J Dentistry. 2014; 42: 517-533

24. Dimitrova-Nakov S, Uzunoglu E, Ardila-Osorio H, Baudry A, Richard G, Kellermann O, Goldberg M. In vitro bioactivity of Bioroot™ RCS, via A4 mouse pulpal stem cells. Dental Materials. 2015; 31(11): 1290-1297.

25. Esmaeilzadeh M, Moradkhani S, Daneshyar F, Arabestani MR, Asl SS, Tayebi S et al. Antimicrobial and cytotoxic properties of calcium-enriched mixture cement, Iranian propolis, and propolis with herbal extracts in primary dental pulp stem cells. Restor Dent Endod. 2022 Dec 1; 48(1):e2

26. Horváth G, Horváth A, Reichert G, Böszörményi A, Sipos K, Pandur E. Three chemotypes of thyme (Thymus vulgaris L.) essential oil and their main compounds affect differently the IL-6 and TNFα cytokine secretions of BV-2 microglia by modulating the NF-κB and C/EBPβ signalling pathways. BMC Complementary Medicine and Therapies. 2021; 21(1): 1-14.

APÊNDICE A – METODOLOGIA DETALHADA

Animais

Os experimentos foram conduzidos de acordo com as leis nacionais que regulamentam o uso de animais em pesquisa (CONCEA 26/2016). O protocolo da pesquisa foi aprovado pelo Comitê de Ética no Uso de Animais (CEUA) da Faculdade de Odontologia de Araraquara – FOAr/UNESP (Processo nº 19/2021 – ANEXO A).

Foram utilizados 100 ratos adultos Holtzman (*Rattus norvegicus albinus*) com peso entre 220-250 g que foram mantidos em gaiolas de polietileno forradas com maravalha. A maravalha foi trocada no mínimo três vezes por semana, juntamente com a lavagem das gaiolas e bebedouros. Os ratos foram mantidos em salas do biotério da FOAr com controle do ciclo de sob luz (12 horas de luz), da temperatura (23 ± 2ºC) e umidade (55 ± 10%), com água e alimento fornecidos *ad Libitum*. Os ratos foram distribuídos equitativamente em grupos, de acordo com os subprojetos. Subprojeto1: NeoSealer Flo, Bioc-C Sealer, AH Plus e grupo controle. Subprojeto 2**:** Neoputty, Bio-C Repair, MTA HP e grupo controle. Subprojeto 3: NeoSealer, NeoSealer Flo + Cetramina, BioRoot ™ RCS, BioRoot ™ RCS + Cetramina e grupo controle. Subprojeto 4: MTA Repair, MTA Repair + *Thime Essential Oil* (TEO), Bio-C Repair, Bio-C Repair + *Thime Essential Oil* (TEO) e grupo controle. Os animais foram anestesiados com 80 mg/kg de cloridrato de ketamina e 8 mg/kg de cloridrato de xilazina que foi administrado com seringa e agulha de insulina por via intraperitoneal. Após tricotomia na região do dorso, a pele foi desinfectada com solução de iodo a 5%. Em seguida, com uma lâmina de bisturi foi realizada uma incisão no sentido crânio-caudal com 1 cm de extensão e com uma tesoura de ponta rombra os tecidos foram divulcionados, criando uma bolsa no subcutâneo. Posteriormente, os tubos de polietileno, de aproximadamente 10 mm de comprimento e 1,6 mm de diâmetro, foram preenchidos com os respectivos materiais. No grupo controle, os tubos de polietileno foram mantidos vazios.

Foram utilizados 288 tubos de polietileno, Cada grupo período/material apresentou o n=6, previamente esterelizados com óxido de etileno.

Os tubos de polietileno foram implantados no tecido conjuntivo do subcutâneo, em forma de rodízio de quadrante (Figura A1). O local da pele incisada

foi suturado com pontos simples. Após 7, 15, 30 e 60 dias de implantação, os animais foram eutanasiados com sobredose dos anestésicos, parte da pele do dorso de cada rato foi removida, estirada sobre uma placa de parafina e separado os implantes de acordo com os grupos. O implante de cada tubo foi aderido a um papel de filtro, inserido num cassete histológico com a identificação do grupo e período e imersos em formaldeído a 4% pelo período de 48 horas.

Figura A1- Procedimento cirúrgico

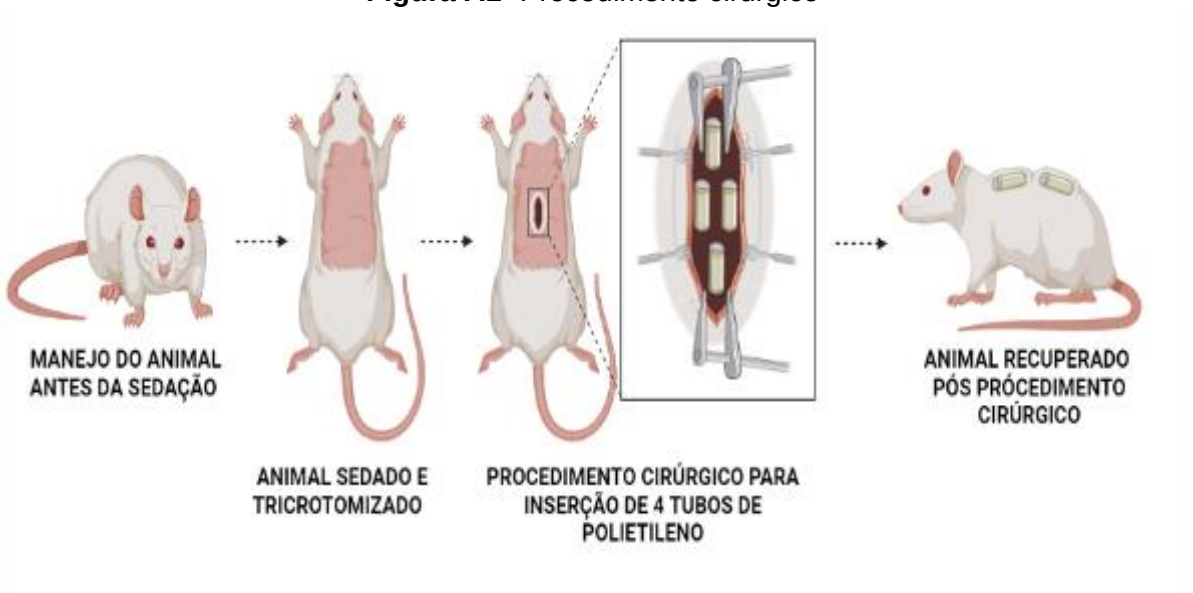

Figura A1: Etapas do procedimento cirúrgico, iniciado com o manejo do animal (1) que após sedação foi realizado a tricotomia de parte da região dorsal (2). Após a assepsia, uma incisão paralela ao plano sagital foi realizada e os tecidos foram divulcionados com uma tesoura de ponta rombra (3) para criação de uma bolsa no subcutâneo dorsal do rato para colocação dos 4 tubos de polietileno (4). Após a sutura, os animais foram acompanhados para verificar o retorno da sedação.

Fonte: Elaboração própria.

Processamento histológico

A fixação dos tecidos circunjacentes aos tubos de polietileno implantados foi realizada com solução de formaldeído a 4% tamponado com fosfato de sódio 0,1 M com pH 7,2, durante 48 horas. Após fixação, as peças foram desidratadas com soluções crescentes de etanol, diafanizadas, embebidas em parafina líquida (60ºC) e incluídas em parafina, de maneira a permitir a obtenção de cortes longitudinais dos implantes. Com um micrótomo rotativo (Leica, modelo RM2125 RST, Heidelberg, Alemanha) e navalhas descartáveis de aço inoxidável foram obtidos cortes com 6 µm de espessura. Alguns cortes foram corados com hematoxilina & eosina (HE)

para a análise morfológica, estimativa do número de células inflamatórias e de fibroblastos nas cápsulas. Cortes foram também aderidos a lâminas de vidro previamente tratadas com silano a 4%, para realização da reação imuno-histoquímica para detecção de osteocalcina (Figura A2).

Figura A2- Demonstração do processamento histológico

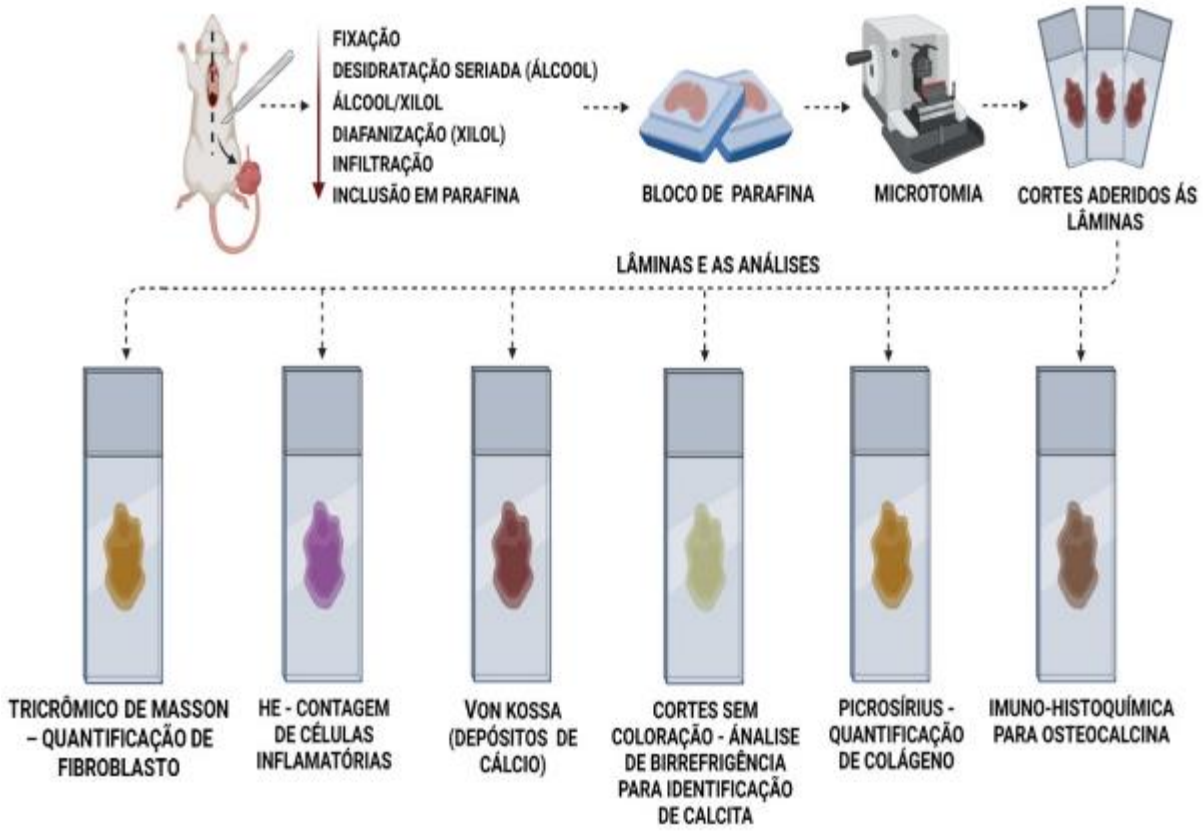

Figura A2: Remoção dos tubos de polietileno com os tecidos adjacentes. O processamento histológico foi iniciado através da fixação por 48 horas, desidratação com soluções de álcool a 70%, 90% e álcool absoluto. Diafinização com xilol, e infiltração e inclusão em parafina para obtenção dos blocos de parafina. Os blocos obtidos foram cortados em microtómo para obtenção de cortes em 20 lâminas. Após a obtenção dos cortes aderidos às lâminas, esses foram submetidos a diferentes metodologias para a realização das análises: quantificação de células inflamatória e de fibroblastos, mensuração do conteúdo de colágenos nos cortes submetidos ao picrosírius-red, detecção de calcita (von Kossa e análise de cortes não corados ao microscópio de polarização) e detecção imuno-histoquímica de osteocalcina.

Fonte: Elaboração própria.

Espessura das cápsulas

A espessura (em µm) das cápsulas adjacentes aos tubos implantados foi mensurada. Usando uma câmera (DP-71, Olympus – Japão) acoplada ao microscópio de luz (Olympus, BX-51, Japão) foram capturadas três imagens de cortes não seriados corados com HE de cada espécime. As imagens foram capturadas com a objetiva de 4x. Usando o programa de análise de imagens (Image-Pro Express 6.0, Olympus, Tóquio, Japão), a espessura das cápsulas foi estimada na porção média a partir de sua superfície adjacente ao material até o seu limite com os tecidos adjacentes. Após a obtenção dos valores, foi calculado o valor médio a partir das medidas obtidas dos três cortes para cada espécime. Esta mensuração foi obtida em todos os espécimes (n=6 por grupo) e em todos os períodos. As cápsulas foram caracterizadas como espessas, quando exibia espessura acima de 150 µm e delgadas/finas, com até 150 µm de espessura.

Densidade numérica de células inflamatórias

O número de células inflamatória (CI) foi computado usando o programa Image-Pro Express 6.0 Olympus. As imagens foram capturadas usando câmera digital acoplada ao microscópio de luz e objetiva de 40x. Em cada corte, foi capturada uma área padrão de 0,09 mm^2 da cápsula adjacente à abertura dos tubos implantados. O número de CI (neutrófilos, linfócitos, plasmócitos e macrófagos) foi computado considerando as características morfológicas. O número de CI e de fibroblastos foi obtido a partir de 3 cortes de cada implante, totalizando uma área de 0,27 mm^2 por implante. Em cada área, o número de células inflamatórias calculado, sendo obtido o número de células inflamatórias por mm^2 de cada amostra. Ao final, obteve-se o valor médio por grupo e período.

Após a obtenção do número de células inflamatórias, a intensidade da reação inflamatória foi classificada de acordo com os seguintes parâmetros: reação inflamatória leve (cápsula contendo até 25 CI/campo), reação inflamatória moderada (cápsula contendo de 26 a 125 CI/campo) e grave/intensa reação inflamatória (cápsula contendo mais de 125 CI/campo).

Densidade numérica de fibroblastos

A quantidade de fibroblastos por mm² nas cápsulas adjacentes aos implantes foi determinada por meio de cortes corados com tricrômico de Masson. O número dessas células foi estimado a partir de três cortes não seriados de cada implante, mantendo-se um intervalo mínimo de 100 µm entre os cortes. Utilizando uma câmera (DP-71, Olympus – Japão) acoplada ao microscópio de luz (Olympus, modelo BX-51) com a objetiva de 40x (aumento final de 695x), foram capturadas imagens do tecido adjacente aos materiais implantados. Posteriormente, com auxílio de um programa de análise de imagens (Image-Pro Express 6.0, Olympus – Japão), realizou-se a contagem dos fibroblastos em cada corte, em uma área de teste de aproximadamente 0,09 mm² da cápsula.

Os fibroblastos foram identificados com base em sua morfologia, considerando seu formato fusiforme ou elíptico. O total de fibroblastos em cada espécime (obtido a partir das áreas dos três cortes/implante) foi dividido pela área total (0,27 mm²), resultando em um valor de fibroblastos/mm². Ao final, foi calculada a média para cada grupo em cada período. A análise foi conduzida por um examinador calibrado e "cego" aos grupos e períodos.

Reação imuno-histoquímica para detecção de osteocalcina

Após desparafinização e hidratação, os cortes foram imersos em tampão citrato de sódio 0,001 M com pH 6,0 e submetidos ao aquecimento no micro-ondas (96-98ºC) por 15 minutos. Após o resfriamento, as lâminas foram lavadas em tampão PBS 0,01 M (pH 7,2) e, em seguida, imersas em solução aquosa de peróxido de hidrogênio a 5%. Os cortes foram lavados novamente e, então, incubados com albumina do soro bovino a 2% (Sigma-Aldrich Co., Saint Louis, Missouri, USA) e incubadas com anticorpo primário anti-osteocalcina produzido em coelho (1: 150; Sigma-Aldrich Co., Saint Louis, Missouri, EUA) por 16 horas a 4ºC em câmara umidificada. Subsequentemente as lavagens em PBS, as seções foram incubadas com polímero conjugado com HRP (EnVision + Dual Link System-HRP, Dako Inc., Carpinteria, CA, EUA; código: K4061) por 1 h à temperatura ambiente. Após as lavagens com tampão, a atividade da peroxidase foi revelada pelo cromogênio da 3,3'-diaminobenzidina (ImmPACTTM DAB Vector, Burlingame, CA,

Estados Unidos da América). As seções foram contrastadas com a hematoxilina de Carazzi. Como controle negativo, as seções foram incubadas com soro não imune em vez de anticorpo primário. O número de células imunopositivas foi calculado com auxílio de um programa de análise de imagens (Image-Pro Express 6.0, Olympus, Tóquio, Japão). Assim, o número de células imunopositivas/mm^2 de cápsula foi obtido para cada implante (Figura A3).

Figura A3- Diagrama ilustrativo da reação imuno-histoquímica para detecção de osteocalcina

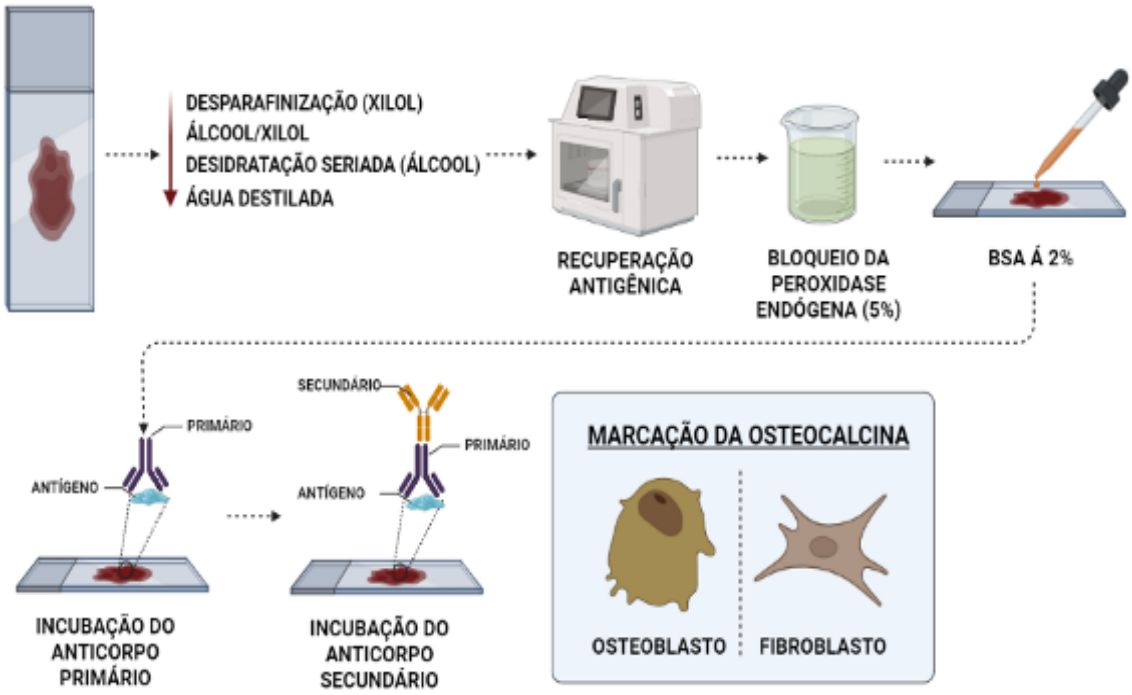

Figura A3 - A reação de imuno-histoquímica foi realizada com a desparafinização e desidratação das lâminas, com posterior recuperação antigênica realizada em micro-ondas por 25 minutos, bloqueio da peroxidase endógena com peróxido de hidrogênio a 5%. Incubação por vinte minutos com albumina de soro bovino e posterior incubação com anticorpo primário. Após 16 horas as lâminas foram incubadas com anticorpo secundário. A marcação positiva é realizada nas células osteoblásticas e fibroblásticas.

Fonte: Elaboração própria.

Estimativa do conteúdo de colágeno birrefringente

Para avaliar a quantidade de colágeno birrefringente, três cortes não seriados por espécime foram corados com solução de picrosirius red e analisados sob luz polarizada (BX51, Olympus). A quantidade de colágeno birrefringente foi calculada usando um software de análise de imagem (ImageJ; National Institutes of Health;

Bethesda, EUA). O colágeno birrefringente foi estimado considerando as definições padronizadas de matiz: vermelho/laranja (2-23 e 230-256), amarelo (39-51) e verde (52-128). A quantidade de colágeno birrefringente foi calculada e expressa como a porcentagem do número de pixels ocupados pelo colágeno birrefringente (Figura A4).

Figura A4 - Demonstração da análise de contéudo de colágeno

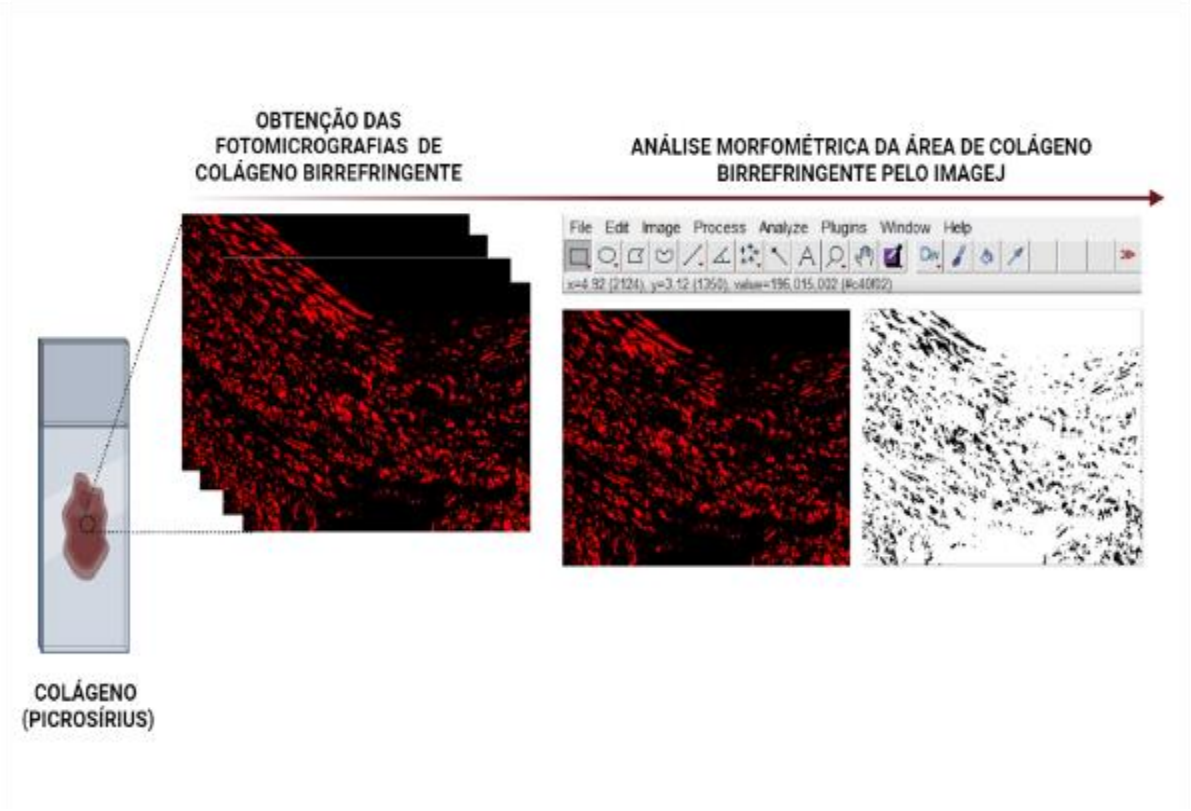

A análise do contéudo de colágeno foi realizada com o auxílio do programa de análise de imagens (Image-J), a fotomicrografia foi aberta e, após calibração a porcentagem ocupada pelos matizes (vermelho/alaranjado, amarelo e verde) foi calculada a partir do número de pixels em cada faixa de matiz.

Fonte: Arquivo pessoal da autora.

Técnica de von Kossa

Cortes das cápsulas ao redor dos implantes no subcutâneo foram submetidos à técnica de von Kossa, para detectar precipitação de fosfato no tecido adjacente ao material. Após desparafinização e hidratação, os cortes foram imersos na solução de nitrato de prata a 5%, durante 1 hora, sob a ação de uma lâmpada incandescente (100 Watts). As lâminas foram lavadas em água destilada por 3 min e em seguida,

imersas em solução de hipossulfito de sódio a 5% por 5 min. Em seguida, os cortes foram novamente lavados em água destilada por 5 min e então corados pelo picrosírius-red e montados em meio resinoso.

Análise sob luz polarizada

Considerando que os cristais de calcita exibem birrefringência quando submetidos à luz polarizada, cortes próximos àqueles submetidos ao von Kossa foram desparafinizados, desidratados e montados. Os cortes sem coloração foram analisados ao microscópio de luz equipado com filtros de polarização (Olympus, BX51).

Análise estatística

Os dados foram avaliados por ANOVA two-way seguido do teste de Tukey, com nível de significância de 5%. Os dados da osteocalcina foram submetidos ao teste de Kruskal-Wallis e ao teste *post hoc* de Dunn e Friedman e Nemenyi para análise ao longo do tempo.

ANEXO A – CERTIFICADO COMITÊ DE ÉTICA

UNIVERSIDADE ESTADUAL PAULISTA
Faculdade de Odontologia
Campus de Araraquara

Comissão de Ética no Uso de Animais - CEUA

CERTIFICADO

Certificamos que o protocolo nº 19/2021 referente à pesquisa ***"AVALIAÇÃO DA BIOCOMPATIBILIDADE E POTENCIAL BIOATIVO DE MATERIAIS BIOCERÂMICOS ENDODÔNTICOS REPARADORES E OBTURADORES"*** sob a responsabilidade da **Profª Drª Juliane Maria Guerreiro Tanomaru** está de acordo com os Princípios Éticos em Experimentação Animal adotado pela legislação brasileira atualmente em vigor, tendo sido aprovado pela Comissão de Ética no Uso de Animais (CEUA) da Faculdade de Odontologia de Araraquara-UNESP.

CERTIFICATE

We certify that the protocol 19/2021 referring to the research ***"EVALUATION OF BIOCOMPATIBILITY AND BIOACTIVE POTENTIAL OF BIOCERAMIC REPAIR AND FILLING ENDODONTIC MATERIALS"*** under responsibility of **Profª Drª Juliane Maria Guerreiro Tanomaru** in agreement with the nowadays specific Brazilian laws and was approved by the Araraquara Dental School-UNESP Ethical Committee for Animal Research (CEUA).

Araraquara, 21 de junho de 2023.

unesp

Assinado de forma digital por Débora Simões de Almeida Colombari:12207983847
Dados: 2023.06.21 11:16:34 -03'00'

Prof. Dr. DÉBORA SIMÕES DE ALMEIDA COLOMBARI
Coordenadora da CEUA/FOAr/UNESP

Araraquara, 27 de março de 2024 .

Evelin Carine Alves Silva